Geol. Mag. **155** (3), 2018, pp. 586–629. © Cambridge University Press 2016
doi:10.1017/S0016756816000893

Age and correlation of the transgressive *Gonioclymenia* Limestone (Famennian, Tafilalt, eastern Anti-Atlas, Morocco)

SVEN HARTENFELS* & RALPH THOMAS BECKER

Institut für Geologie und Paläontologie, Westfälische Wilhelms-Universität Münster, Corrensstr. 24, D-48149 Münster, Germany

(*Received* 8 March 2016; *accepted* 31 August 2016; *first published online* 21 November 2016)

Abstract – The widely quarried and commercially exploited *Gonioclymenia* Limestone of the western and southern Tafilalt Platform (Anti-Atlas, SE Morocco) represents a transgressive but strongly condensed and shallowing upwards unit that overlies conformably or unconformably Famennian to Lower Devonian deposits. It is characterized by abundant, giant-sized *Gonioclymenia speciosa*, which characterizes the Famennian V-B, and rare *Leviclymenia ramula* sp. nov. Associated conodont faunas fall in the *Bispathodus costatus* Subzone of the *B. aculeatus aculeatus* (= Middle *expansa*) Zone. A rare outcrop at Jebel Ihrs West proved that *Kalloclymenia* and conodont faunas of the *B. ultimus ultimus* (= Upper *expansa*) Zone occur in a separate, overlying unit of the lower part of Famennian VI. Consequently, joint occurrences of *Gonioclymenia* and *Kalloclymenia* on large limestone slabs that are on offer in rock shops are artificial assemblages; there is no evidence for a regional co-occurrence of both genera. This is supported by correlation into thicker sections of the adjacent Maider and Tafilalt Basins. The Tafilalt *Gonioclymenia* Transgression may represent the regional expression of a eustatic pulse in the *B. costatus* Subzone that is known on the Ardennes Shelf as the transgressive Epinette Event. The conodont faunas yielded *Neopolygnathus fibula* sp. nov., *Pseudopolygnathus primus tafilensis* ssp. nov., new morphotypes of *B. spinulicostatus* and *Pseudopolygnathus primus primus*, the oldest *Siphonodella (Eosiphonodella)* and variable 'siphonodelloids' that are currently left in open nomenclature.

Keywords: Upper Devonian, conodonts, ammonoids, biostratigraphy, carbonate microfacies, sea-level change, North Africa.

1. Introduction

The Devonian of southern Morocco is world-famous for its rich fossils that are widely commercially exploited and sold in rock shops of many countries. Apart from its trilobites, polished middle to uppermost Famennian ammonoids are intensively traded (Fig. 1a, b). Large-sized to giant *Gonioclymenia speciosa* are sold as individuals or several specimens are mounted on large limestone slabs. These derive from a peculiar condensed and massive cephalopod limestone, the upper Famennian *Gonioclymenia* Limestone. It is exploited in km-long trenches dug through the desert or in small subsurface mines of the Tafilalt (eastern Anti-Atlas). The heavy mining has more or less destroyed all outcrops (Fig. 2a, e, f). Only in rare cases of vertical bedding can small stretches of the bed, even with numerous giant specimens on its upper surface (Fig. 2g, h), still be seen in the field.

The first record of this marker unit goes back to Hollard (1960), who observed in the area S of Jebel Amelane that a massive red limestone with *Sphenoclymenia* (probably = *Gonioclymenia*) lies with an angular unconformity above the upper Frasnian, or, laterally, even on limestones with upper Givetian pharciceratids (still assigned to the lower Frasnian at the time of Hollard's publication). A similar transgression of a condensed limestone with *Gonioclymenia* was reported from El Fecht in the western Maider, which belongs to the separate Maider Platform (palaeogeography of Wendt, 1988*b*). Hollard (1967) noted the enormous size (up to 40 cm) of the clymeniids.

In their pioneer work on the Upper Devonian sedimentation of the Tafilalt, Wendt, Aigner & Neugebauer (1984) commented on the widespread prominent bed with *Gonioclymenia*, with specimens up to 60 cm in diameter, and assigned it to the Famennian V ß. This dating was based on the outdated ammonoid zonal terminology of Wedekind (1914). They emphasized that the unconformity below reflects an episode of non-deposition, not necessarily a Famennian tectonic phase with subaerial exposure of parts of the Tafilalt, as claimed by Hollard (1960). This interpretation was repeated in Wendt (1988*a*), with new age assignments based on conodonts. Details or faunal lists, however, were not given. For the extremely condensed succession S of Jebel Amelane, Wendt (1988*a*) showed in his figure 4 an erosional omission surface, with reworked Frasnian clasts, of the Lower *expansa* (= *Bispathodus stabilis stabilis*) Zone, a second, iron-stained omission surface between wackestones of the Lower and Middle *expansa* zones (= *B. aculeatus aculeatus*

*Address for correspondence: shartenf@uni-muenster.de

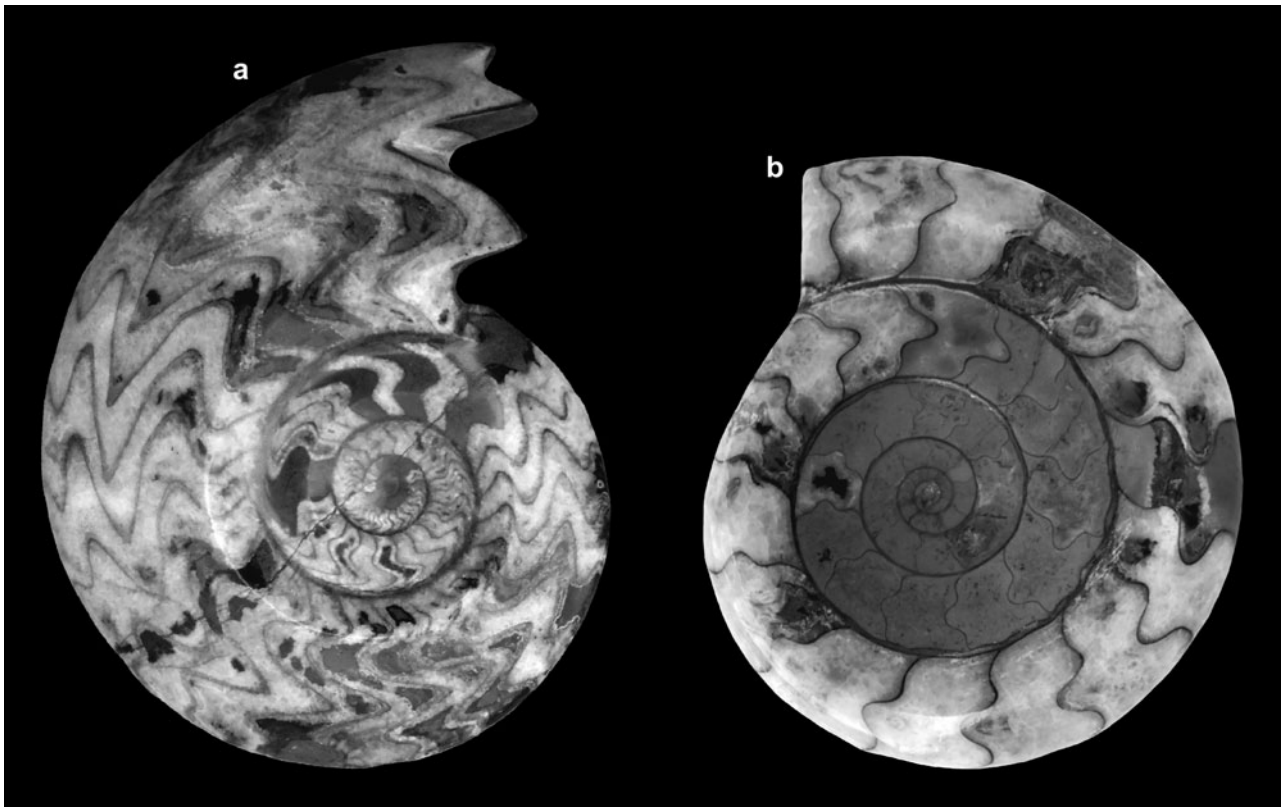

Figure 1. Examples of upper/uppermost Famennian polished clymeniids from the Tafilalt purchased from Erfoud rock shops. (a) *Gonioclymenia speciosa* (Münster, 1831), ×0.5; (b) *Kalloclymenia subarmata* (Münster, 1832), ×1.

Zone), followed by nodular limestone with the giant clymeniids assigned to the Upper *expansa* Zone (= *B. ultimus ultimus* Zone). Subsequently, Wendt (1988*b*) remarked that the up to 50 cm thick, prominent marker bed with giant clymeniids occurs all over the Tafilalt Platform and even in adjacent marginal areas of the Tafilalt Basin. His claims of an association of *Gonioclymenia* with *Platyclymenia* are at odds with the global record of both genera and have not been substantiated (Korn, 1999; Korn, Klug & Reisdorf, 2000; Becker *et al*. 2002; Hartenfels, 2011). A significant upper Famennian transgression that flooded episodically emergent areas of the Maider and Tafilalt platforms was confirmed. In the subsequent regional sea-level curve of Wendt & Belka (1991, fig. 16), this main transgression was placed within the Lower *expansa* Zone, without discussing their previous different phases of the successive Lower to Upper *expansa* zones.

Korn, Klug & Reisdorf (2000) correlated a range of lateral sections in the Amessoui Syncline of the southern Tafilalt and depicted the *Gonioclymenia* Limestone as a 30–40 cm thick, rather uniform cephalopod packstone and significant marker, which overlies locally different older Famennian rocks. It was noted that the abundant, large-sized gonioclymeniids belong to *Gonio. speciosa*. They assigned the marker level to a *Kosmoclymenia lamellosa* Fauna with a still unclear correlation with the German zonation, since the zonal index species of the German *Clymenia* Stufe (Upper Devonian = UD V) were not found in Morocco (see discussion in Korn, 1999, p. 153). Some large *Gonioclymenia* slabs on sale in Erfoud or Rissani rock shops show a direct association of large *Gonio. speciosa* with subordinate, somewhat smaller and more evolute *Kalloclymenia subarmata*. The occurrence of both taxa in the extensive *Gonioclymenia* trenches at Jebel Ihrs West, the western continuation of Jebel Amelane, was confirmed during joint field work with the late M. R. House in March 1994. *Kalloclymenia* was found in place at the top of the reddish limestone. Very solid blocks of the mining debris yielded in addition mostly incomplete *Cly. laevigata*, *Kiaclymenia laevis*, *Cymaclymenia* sp., *Erfoudites rherisensis* and *Mimimitoceras* sp. Based on the alleged co-occurrence of *Kalloclymenia* with the typical Dasbergian genus *Clymenia* in Cornwall (Selwood, 1960), and on the association with *Gonio. corpulenta* in the famous Kiya succession of NW Kazakhstan (Simakov *et al.* 1983; updates in Nikolaeva & Bogoslovskiy, 2005; Nikolaeva, 2007), Becker *et al.* (2002) introduced a *Kallo. subarmata* Zone (UD V-C) for the Tafilalt, characterized by a *Gonioclymenia–Kalloclymenia* association. However, they noted that this interval was only known from the very condensed Tafilalt succession, whilst the thicker, more basinal Famennian ammonoid sequences of the region gave no indication for an overlap of both genera.

Ginter, Hairapetian & Klug (2002) described shark teeth from upper Famennian sections of the Amessoui Syncline (southern Tafilalt; Fig. 3). They noted the presence of *B. ziegleri* (= *B. ultimus ultimus*

https://doi.org/10.1017/S0016756816000893 Published online by Cambridge University Press

Morphotype 1) in the *Gonioclymenia* Limestone of Oum el Jerane, which was consequently assigned to the Upper *expansa* (= *B. ultimus ultimus*) Zone. It was recognized that the conodont age was in conflict with the ammonoid–conodont correlation elsewhere, but preference was given to the conodont dating. Samples from Tizi Nersas to the W were said to contain virtually identical conodont faunas but their details were not revealed. Kaiser (2005) found no marker conodonts of the *B. ultimus ultimus* Zone in a sample from the *Gonioclymenia* Limestone (her Bed 2) at Jebel Ouaoufilal, at the eastern end of the Amessoui Syncline. Hartenfels & Becker (2009) and Hartenfels (2011) also analysed upper Famennian conodont faunas of the Amessoui Syncline, but did not report conodonts from the *Gonioclymenia* Limestone.

To summarize the evidence of past research, it is clear that the *Gonioclymenia* Limestone records an important episode of transgression and subsequent condensation in the upper Famennian of the Tafilalt. However, the controversial data concerning its precise timing prevent a meaningful international correlation and interpretation in the light of eustatic changes or regional synsedimentary tectonics. They also leave significant uncertainties concerning the precise ammonoid–conodont correlation, with implications for the regional and international ammonoid zonation. The data reported here provide a clear distinction between different and successive *Gonioclymenia* and *Kalloclymenia* limestones. Faunas allow a revision of the regional conodont and ammonoid zonations, their correlation, and recognition of a eustatic deepening pulse in the upper part of the *B. aculeatus aculeatus* Zone (= higher *B. costatus* Subzone or higher Middle *expansa* Zone).

2. Material and methods

We applied two approaches to resolve the stratigraphic contradictions by (a) using individual *Gonioclymenia* and *Kalloclymenia* specimens with attached matrix from various localities as conodont samples, and (b) sampling a new upper Famennian section that was exposed for a brief interval in one of the extensive *Gonioclymenia* trenches at Jebel Ihrs West (Fig. 2a–c). Between 2011 and 2013, three field campaigns provided more than 16 conodont samples of the *Gonioclymenia* interval. As is common practice in stratigraphic conodont studies, only the Pa element taxonomy has been utilized, because many Famennian multi-element reconstructions are still doubtful. Each sample was dissolved using a 10 % solution of formic acid and the residues were separated by diluted sodium polytungstate ($[Na_6(H_2W_{12}O_{40})\cdot H_2O]$ 2.76–2.78 g ml^{-1}). The samples yield a variable number of conodonts, ranging from a minimum of zero to a maximum of 849 platform elements per kg. All Pa elements have been identified and counted.

Our conodont biofacies analysis builds on the model of Sandberg (1976) as well as subsequent modifications by Ziegler & Sandberg (1984, 1990) and Dreesen, Sandberg & Ziegler (1986). Since it is long known that different species groups within platform genera show different facies distributions, we expand the classical concept by documenting frequencies of the following groups separately: *Palmatolepis perlobata* Group, *Pa. gracilis* Group, single and double rowed bispathodids. The *Pa. gracilis* Group seems to represent a distinctive genus in multi-element taxonomy (*Tripodellus*, cf. Dzik, 2006).

Abreviations and repository

Conodonts: *B.* = *Bispathodus*, *Biz.* = *Bizignathus*, *Br.* = *Branmehla*, *Clyd.* = *Clydagnathus*, *D.* = *Dasbergina*, *Eo.* = *Eosiphonodella*, *M.* = *Mehlina*, *Neo.* = *Neopolygnathus*, *Pa.* = *Palmatolepis*, *Po.* = *Polygnathus*, *Ps.* = *Pseudopolygnathus*, *S.* = *Siphonodella*, *Sc.* = *Scaphignathus*; ammonoids: *Cly.* = *Clymenia*, *Costa.* = *Costaclymenia*, *Cyma.* = *Cymaclymenia*, *Erf.* = *Erfoudites*, *Gonio.* = *Gonioclymenia*, *K.* = *Kiaclymenia*, *Kallo.* = *Kalloclymenia*, *Kosmo.* = *Kosmoclymenia*, *Levi.* = *Leviclymenia*, *Medio.* = *Medioclymenia*, *Muess.* = *Muessenbiaergia*, *Nano.* = *Nanoclymenia*, *Parawo.* = *Parawocklumeria*, *Pl.* = *Platyclymenia*, *Post.* = *Postclymenia*, *Protacto.* = *Protactoclymenia*, *Rect.* = *Rectimitoceras*, *Sp.* = *Sporadoceras*, *Spheno.* = *Sphenoclymenia*. The used ammonoid zonal key follows Becker *et al.* (2002).

Apart from the types of *Gonio. hoevelensis* (nos 388-54 and 588-53, Geowissenschaftliches Zentrum of the Georg-August-University of Göttingen) and a Tafilalt *Kallo. subarmata* (MB.C.3553, Museum für Naturkunde Berlin), all figured specimens (nos B9A.4-1 to B9A.4-84 for conodonts, nos B6C.42-1 to B6C.43-3 for ammonoids) are deposited in the Geomuseum Münster (GMM) of the Westfälische Wilhelms-University.

3. *Gonioclymenia* Limestone localities and samples (Fig. 3)

Our investigation revealed a restricted distribution of the true *Gonioclymenia* Limestone that follows the condensed parts of the hemipelagic Tafilalt Platform in the upper Famennian palaeogeographic map of Wendt (1988*b*, fig. 6). The extent of the marker unit is mirrored in the field by the km-long commercial trenches (Fig. 2f). A western occurrence from the S of the Jebel Amelane and Jebel Ihrs West ridges (Fig. 2a) continues much less distinctively to the NE of Rissani and the Rich Haroun/Seheb el Rhassal region. There is no typical development at Bou Tchrafine, the Jebel Erfoud or in the Rheris Basin further to the N, nor in the Achguig-Ouidane Chebbi and Mfis areas that fall in the eastern transition to the Tafilalt Basin. The marker unit is also missing in the Bou Maiz Syncline (e.g. near Ottara; Fig. 2d), which partly belongs to the western slope of the Tafilalt Platform towards the Maider Basin (cf. Lubeseder *et al.* 2010). The southern outcrop belt of the Amessoui Syncline (Fig. 2e, f) shows

https://doi.org/10.1017/S0016756816000893 Published online by Cambridge University Press

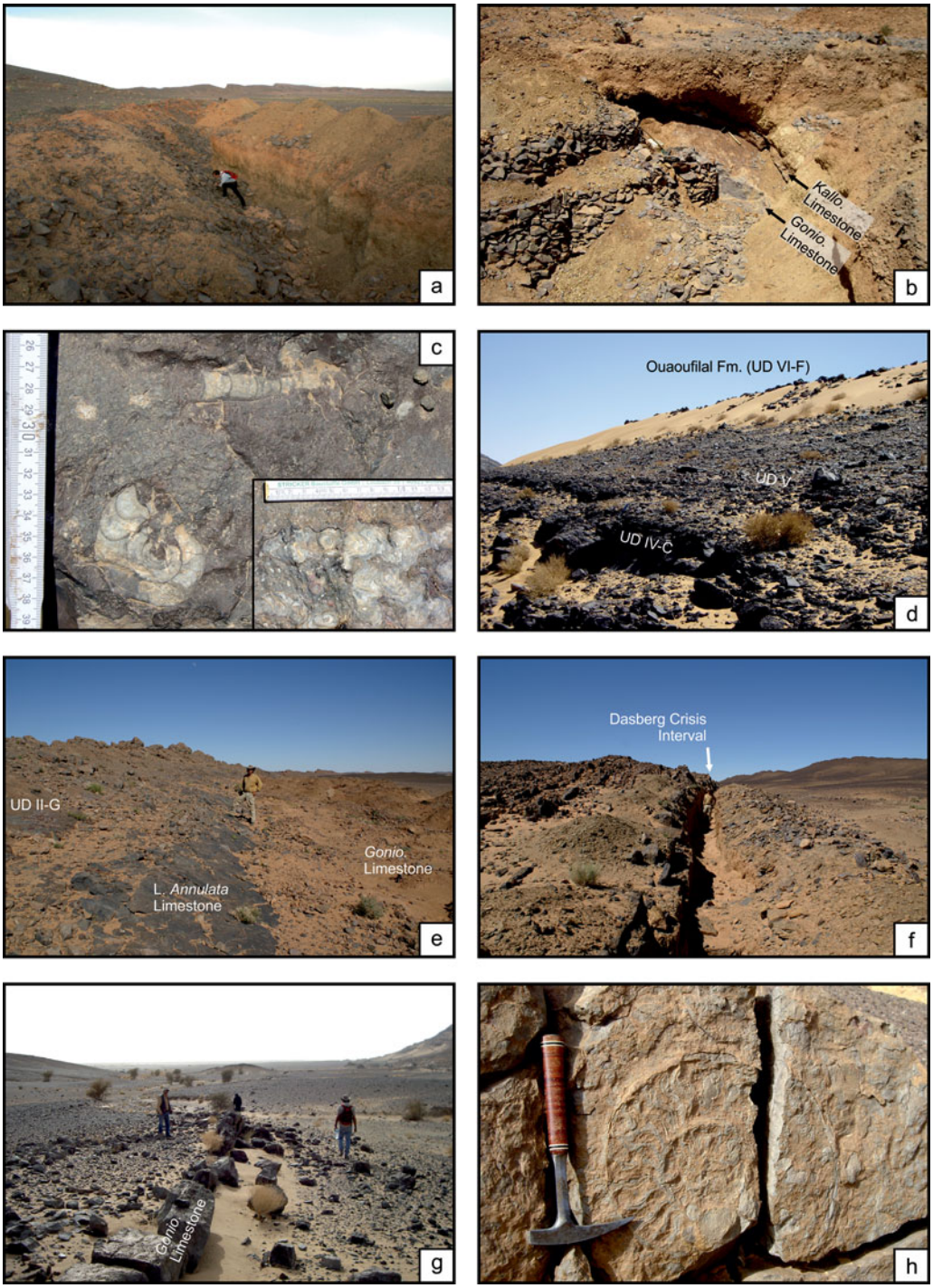

Figure 2. (Colour online) Tafilalt field photos. (a) Extensive trenches of the *Gonioclymenia* Limestone at the western end of Jebel Ihrs (western Tafilalt); (b) temporary exposure of the upper/uppermost Famennian succession with the *Gonioclymenia* and *Kalloclymenia* limestones at Jebel Ihrs West (spring 2011); (c) corroded and hematite-impregnated, reddish top of the *Costaclymenia* Limestone at Jebel Ihrs West (Bed 2), with *Costaclymenia* sp., large orthocones, and crinoid roots (insert); (d) position of *Gonio. speciosa* level within reddish nodule beds above the UD IV-C marker limestone at Ottara East (Bou Maiz Syncline, central Tafilalt); (e) trenched *Gonioclymenia* Limestone directly overlying the basal upper Famennian Lower *Annulata* Limestone (UD IV-A) at Takhbtit West (northern limb of Amessoui Syncline, southern Tafilalt); (f) deep, km-long *Gonioclymenia* Trench at Oum el Jerane (southern limb of Amessoui Syncline); (g) vertical outcrop of the locally massive *Gonioclymenia* Limestone above basal upper Emsian marls (Daleje Shale Equivalents) at a hill S of Jebel Kfiroun; (h) giant-sized (up to 40 cm in diameter) *Gonio. speciosa* on the upper surface of the *Gonioclymenia* Limestone at Jebel Kfiroun South.

interruptions, e.g. between Tizi Nersas and Oum el Jerane (Korn, Klug & Reisdorf, 2000). It does not reach its NE part (El Khraouia; Hartenfels *et al.* 2013), where the platform deposits turn into argillaceous, basinal deposits that continue towards Hassi Nebech, Tazoult Nehra and the Erg Kseir (cf. middle Famennian cross-section of Wendt, Aigner & Neugebauer, 1984, fig. 8). South of the Amessoui Syncline, at the Jebel el Mrier, all of the

https://doi.org/10.1017/S0016756816000893 Published online by Cambridge University Press

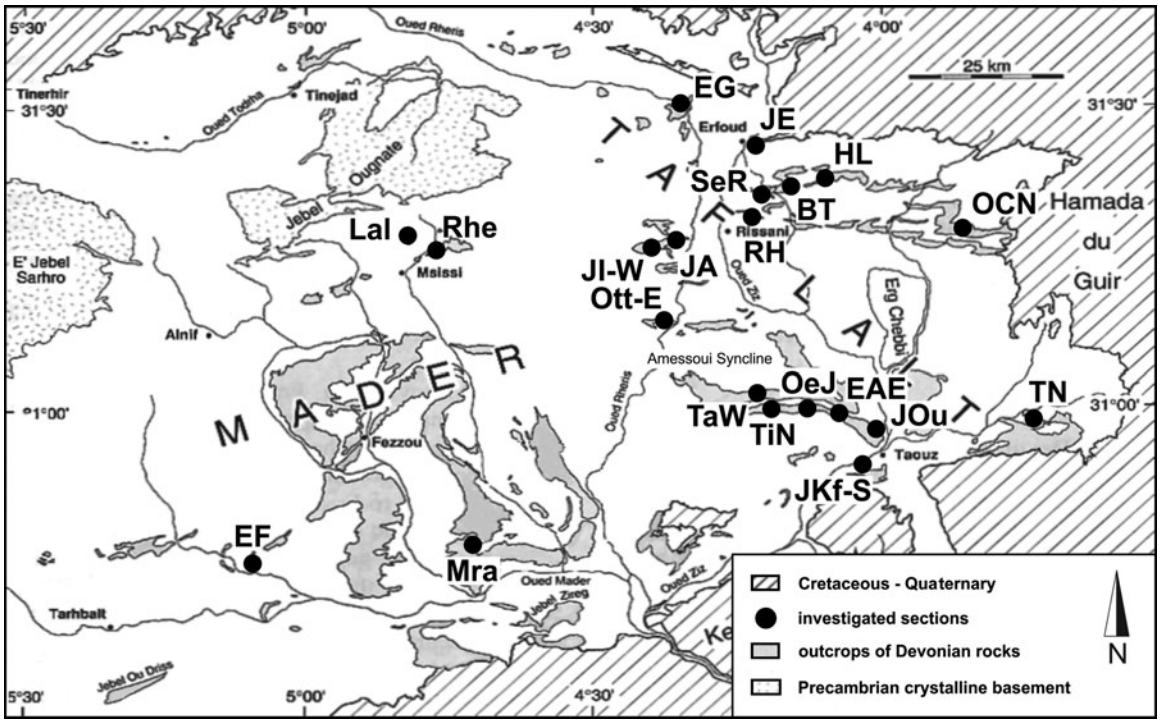

Figure 3. Position of sampled *Gonioclymenia* and uppermost Famennian conodont localities in the Tafilalt and Maider; EG = El Gara, JE = Jebel Erfoud, HL = Hamar Lagdad East, BT = Bou Tchrafine, SeR = Seheb el Rhassal, RH = Rich Haroun, OCN = Ouidane Chebbi Northwest, JA = Jebel Amelane, JI-W = Jebel Ihrs West, Ott-E = Ottara East, TaW = Takhbtit West, TiN = Tizi Nersas, OeJ = Oum el Jerane, EAE = El Atrous East, JOu = Jebel Ouaoufilal, TN = Tazoult Nehra, JKf-S = Jebel Kfiroun South, Mra = Mrakib, EF = El Fecht, Rhe = Jebel Rheris West, Lal = Lalla Mimouna.

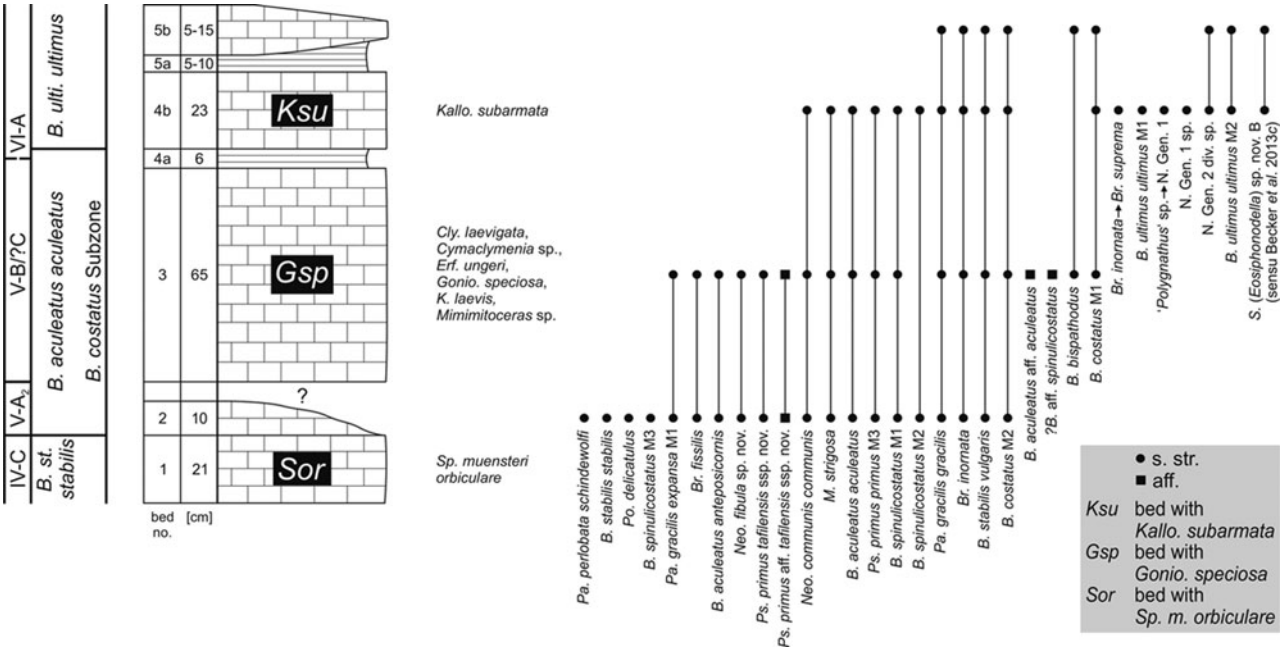

Figure 4. Section Jebel Ihrs West: bed numbers, thicknesses, ammonoid and conodont ranges and zonation (ammonoid zonal key after Becker *et al*. 2002 and Becker, El Hassani & Tahiri, 2013).

Upper Devonian is missing due to an unconformity below Upper Tournaisian/Lower Viséan strata. But remnants of the *Gonioclymenia* Limestone are beautifully exposed closer to Taouz, S of the Jebel Kfiroun (Fig. 2g, h), where it onlaps the Lower Devonian (basal upper Emsian; Aboussalam, Becker & Bultynck, 2015).

3.a. Jebel Ihrs West (Figs 2a–c, 4–7)

In spring 2011 the re-opening of a *Gonioclymenia* trench at the western end of Jebel Ihrs (GPS coordinates: 31° 15′ 35.3″ N, 004° 25′ 20.3″ W, map sheet 244 Tafilalt-Taouz) provided the temporary opportunity to sample a section through the condensed

https://doi.org/10.1017/S0016756816000893 Published online by Cambridge University Press

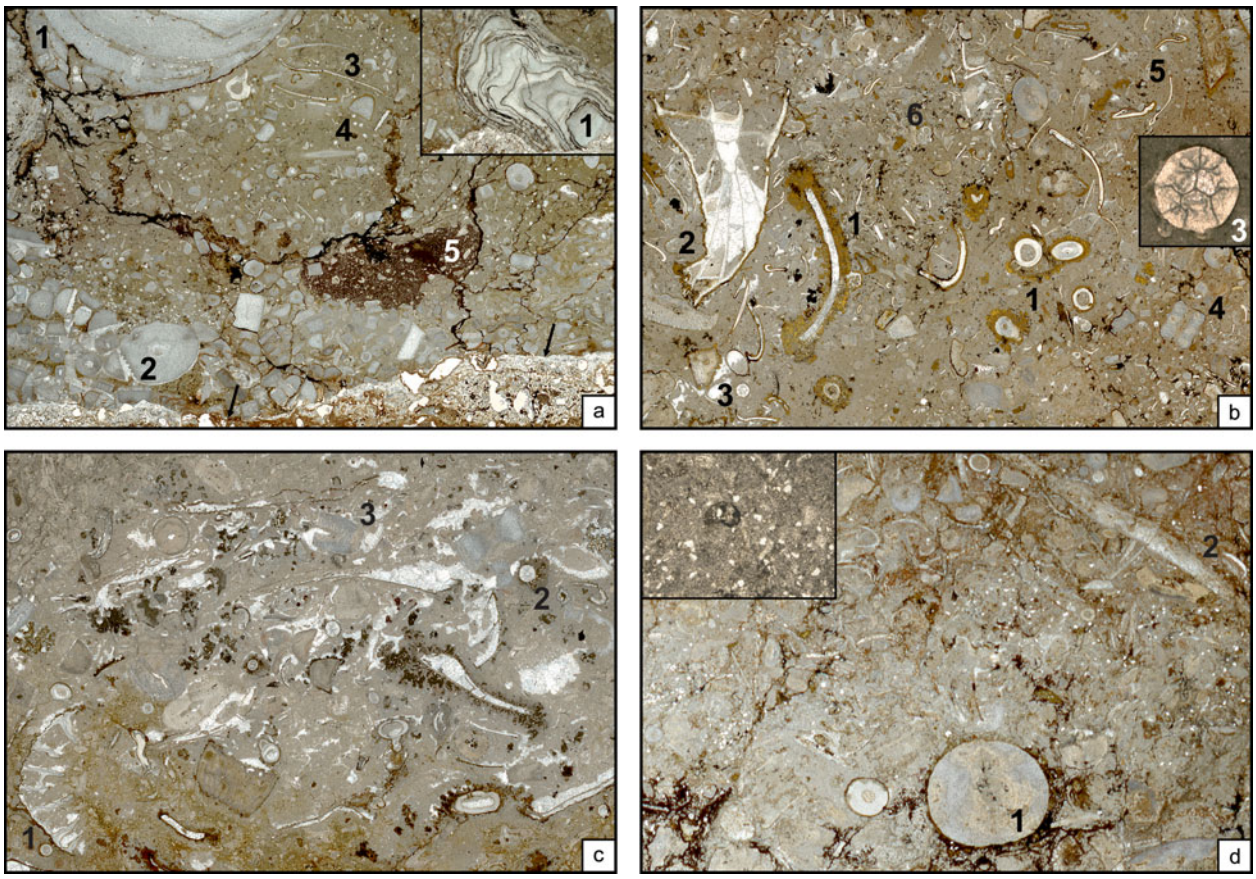

Figure 5. (Colour online) Microfacies of upper/uppermost Famennian marker beds at Jebel Ihrs West. (a) *Costaclymenia* Bed (Bed 2, lower *B. costatus* Subzone), fining upwards sequence within a crinoidal (2) packstone with shell filaments (3), ostracods (4) and bioturbation (5) above an irregular hardground surface as evidence of submarine karstification (black arrows, figure width *c.* 30 mm). *In situ* crinoidal holdfasts (1) show irregular and branched shapes due to repeated encrustation (insert, figure width *c.* 32 mm); (b) *Gonioclymenia* Limestone (Bed 3, upper B. *costatus* Subzone), macrofossil-rich, oncolithic packstone with golden brown *Frutexites* encrustations (1), fragmented shells, crinoid remains (4), ostracods, solitary deep water rugose corals (2), trilobites (5), rare heterocorals (3, insert, 0.8 mm diameter) and minute gastropods (6); figure width *c.* 24 mm; (c) *Kalloclymenia* Limestone (Bed 4b, lower *B. ultimus ultimus* Zone), macrofossil-rich microbial packstone with crinoids (3), numerous sparite-filled fenestrae, fragmented ammonoids, ostracods, thin-shelled bivalves, rare trilobites, solitary rugose corals (1), heterocorals (2), bioclasts encrusted by brownish-black *Frutexites*-lamina, extremely rare oncolites, and angular quartz (silt) grains; figure width *c.* 27 mm; (d) Bed 5b (higher *B. ultimus ultimus* Zone), silty (see insert, figure width *c.* 2.5 mm) crinoidal (1) packstone with *Frutexites* encrustations, ostracods, shell filaments (2), rare trilobites, and bioturbation; figure width *c.* 14 mm).

upper/uppermost Famennian (Figs 2b, 4). The upper part of Famennian IV consists of massive, reddish cephalopod limestone (Bed 1) with marker species of UD IV-C, such as *Sp. muensteri orbiculare* and large *Protacto. ventriosa* (Becker *et al.* 2002).

Costaclymenia Bed (Bed 2)

Encrusted on top of the underlying bed with *Sp. muensteri orbiculare* is a unit (Bed 2) with many crinoidal holdfasts in life position (Fig. 5a, insert), similar to those illustrated from older Famennian beds of the Jebel Bou Ifarherioun and Jebel Mech Irdane (Wendt, Aigner & Neugebauer, 1984; Wendt, 1988*a*). They show irregular and branched shapes (Fig. 2c, insert), formed by repeated encrustation. Bed 2 consists of several depositional units. An irregular hardground surface with cavities is developed in the basal part (Fig. 5a, arrows) and formed the fundament for thin hematitic crusts. Above this hiatus surface, coarse crinoidal packstones follow. Fining upward gradings suggests storm sedimentation, which is supported by the fragmentation and only sub-rounded outline of crinoid ossicle pieces. Marginal microborings, probably by cyanobacteria, indicate an influx from a nearby shallow setting but there are no typical neritic faunas. The assemblage of Bed 2 contains ostracods, fragmented bivalves, rare small-sized gastropods, and ammonoids. Bioturbation is evident in the matrix-rich upper part. Reddish-brown to sporadically yellow-golden microstromatolites encrusted skeletal remains and caused cauliflower structures. They resemble *Frutexites* (Böhm & Brachert, 1993) and were previously described by Préat, El Hassani & Mamet (2008) and Hartenfels (2011) from the higher Famennian of the Maider and Tafilalt. In general, laminated iron encrustations are regionally widespread in the Tafilalt (Wendt, Aigner & Neugebauer, 1984; Becker, 1993, fig. 53; Becker *et al.* 2000; Jakubowicz, Belka & Berkowski, 2014) and indicate extremely slow depositional rates. Préat, El Hassani & Mamet (2008) postulated that such crusts originated under

https://doi.org/10.1017/S0016756816000893 Published online by Cambridge University Press

supraregional conodont zonation	*B. costatus* Subzone		*B. ultimus ultimus* Zone		number of Pa elements/taxon
Tafilalt regional conodont zonation	*B. costatus* Subzone		*B. ultimus ultimus* Zone		
sample/bed no.	2	3	4b	5b	
dissolved carbonate [g]	1324.3	2321	1514.3	363.1	
number of Pa elements	413	447	210	13	
taxa/bed	20	20	15	9	
conodont biofacies [%]					
Pa. perlobata Group	0.5				
Pa. gracilis Group	37.1	34.2	2.9	7.7	
Polygnathus	0.2		0.5		
Neopolygnathus	22.8	24.6	4.8		
Bispathodus (single row taxa)	12.6	18.1	4.3	15.4	
Bispathodus (multiple row taxa)	6.8	4.5	44.8	38.5	
Branmehla/*Mehlina*	15.7	13.7	38.6	15.4	
Pseudopolygnathus	4.4	4.9	0.5		
N. Gen. 1 & 2/*S.* (*Eosiphonodella*)			3.8	23.1	
Pa. perlobata schindewolfi	2				2
B. stabilis stabilis	7				7
Po. delicatulus	1				1
B. spinulicostatus M3	1				1
Pa. gracilis expansa M1	13	1			14
Br. fissilis	4	3			7
B. aculeatus anteposicornis	2	5			7
Neo. fibula sp. nov.	1	2			3
Ps . primus tafilensis ssp. nov.	4	8			12
Ps. primus aff. *tafilensis* ssp. nov.	1	3			4
Neo. communis communis	93	108	10		211
M. strigosa	29	23	1		53
B. aculeatus aculeatus	22	45	18		85
Ps. primus primus M3	13	10	1		24
B. spinulicostatus M1	2	20	18		40
B. spinulicostatus M2	1	-	3		4
Pa. gracilis gracilis	140	152	6	1	299
Br. inornata	32	35	75	2	144
B. stabilis vulgaris	45	18	9	2	74
B. costatus M2	1	7	43	1	52
B. aculeatus aff. *aculeatus*		3			3
?B. aff. *spinulicostatus*		1			1
B. bispathodus		2	-	1	3
B. costatus M1		1	5	2	8
Br. inornata → *Br. suprema*			5		5
B. ultimus ultimus M1			3		3
'*Polygnathus*' sp. → N. Gen. 1			1		1
N. Gen. 1 sp.			1		1
N. Gen. 2 div. sp.			5	2	7
B. ultimus ultimus M2			4	1	5
S. (*Eosiphonodella*) sp. nov. B (sensu Becker*et al.* 2013*c*)			2	1	3

Figure 6. Conodont record and biofacies at Jebel Ihrs West, beds 2 to 5b.

dysaerobic conditions, which interpretation, however, was questioned by Koptíková *et al.* (2010) and Hartenfels (2011), due to co-occurring normal benthic faunas. Grain margin solution, particularly between crinoid remains, is the result of diagenesis. Pseudopeloids occur only within ammonoid shells, where they were protected from diagenetic compression (cf. Hartenfels, 2011). The micritic matrix outside may have lost its original pseudopeloid structure by diagenesis. In summary, Bed 2 accumulated adjacent to a storm-swept crinoidal shoal (upper carbonate ramp). The hardground in the lower parts reflects an interval of regression and

https://doi.org/10.1017/S0016756816000893 Published online by Cambridge University Press

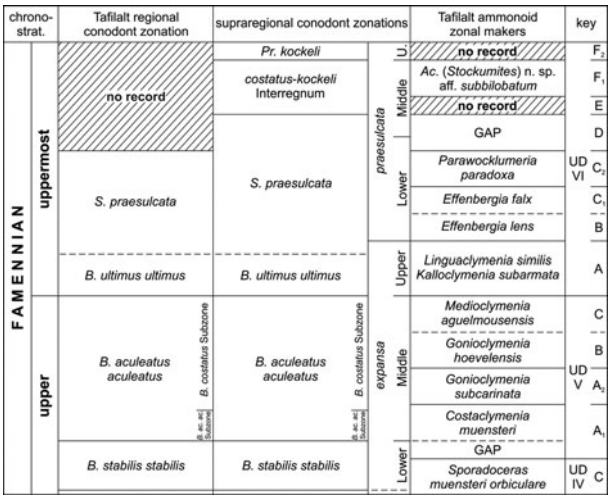

Figure 7. Correlation of upper/uppermost Famennian Tafilalt and supraregional conodont as well as ammonoid biostratigraphy.

non-deposition. A second hardground is developed on the top surface, where corroded clymeniids and crinoid holdfasts (Fig. 2c, insert) suggest submarine carstification during long-lasting non-deposition.

Costaclymenia sp. (Fig. 2c) indicate the lower Dasbergian (of German substage terminology) or UD V-A. The rich conodont fauna (Fig. 6) include rare, slender pseudopolygnathids (*Ps. primus tafilensis* ssp. nov. and *Ps. primus* aff. *tafilensis* ssp. nov.) and a single *B. costatus* Morphotype 2, the index species of the *B. costatus* Subzone of the *B. aculeatus aculeatus* Zone (Fig. 7; Hartenfels, 2011). Consequently, the Dasberg Event Beds of the basal *B. aculeatus aculeatus* Zone (and Subzone), which are widespread in other Tafilalt sections (Hartenfels & Becker, 2009), are missing locally in the highly condensed sequence, possibly at the hardground level. There is a dominance of *Pa. gracilis gracilis* and *Neo. communis communis*, followed in terms of abundance by simple bispathodids and spathognathodids (*Branmehla* and *Mehlina*). This faunal composition agrees with a moderately deep shelf setting (see conodont biofacies model of Sandberg, 1976).

Gonioclymenia Limestone *(Bed 3)*

The transition from Bed 2 to the *Gonioclymenia* Limestone (Bed 3) was not exposed in the trench. It is likely that most or all of the *Gonio. subcarinata* Zone (UD V-A_2) is locally missing. Bed 3 is up to 65 cm thick and consists of grey to reddish crinoidal limestone (Fig. 4). In thin-sections (Fig. 5b), it is developed as a bioturbated, macrofossil-rich float- packstone with a minor content of small-sized, angular quartz grains. The fauna is dominated by ammonoids (*Gonio. speciosa*; Fig. 8a), broken, reworked crinoid remains, trilobites and corals. There are small-sized oncolites/ooids, which were probably washed in by storms. Oncolites were previously documented in the region by Wendt (1988*a*, fig. 4) from the *B. aculeatus aculeatus* Zone of a condensed section 2 km south of the Amelane road pass. As in Bed 2, there is no typical neritic or even euphotic

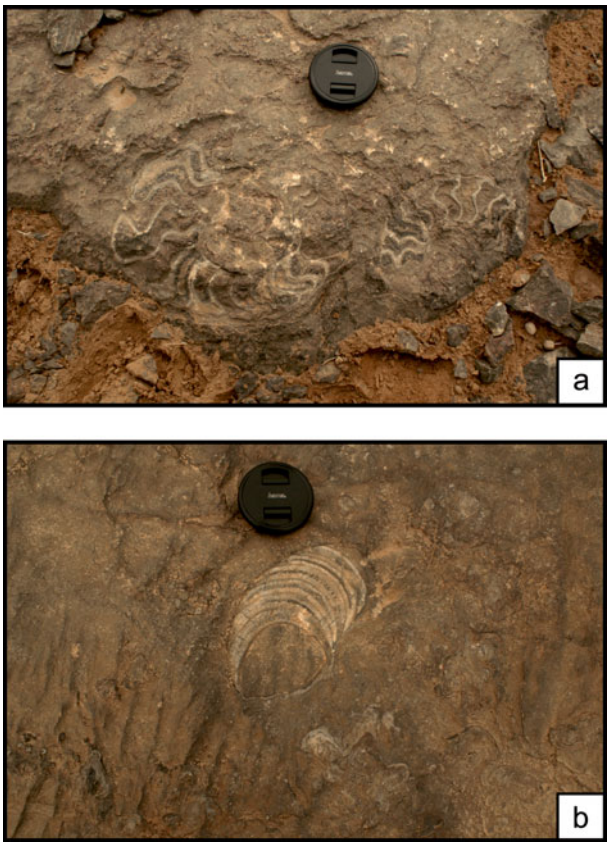

Figure 8. (Colour online) Corroded top surface of the *Gonioclymenia* Limestone, indicating a long interval of non-deposition and submarine carstification, exposed widely at the western end of Jebel Ihrs. (a) Surface with deeply corroded *Gonioclymenia speciosa* (Münster, 1831); (b) corroded section of a large oncoceratid.

fauna. In contrast, orthoconic cephalopods, ostracods, remains of thin-shelled bivalves, trilobites, gastropods and deep-water, solitary rugose corals are common in thin-section. A bulk of the skeletal elements is fractured and broken. As a special feature there are heterocorals (Fig. 5b, insert). Based on records from the Rhenish Slate Mountains and Tafilalt, Weyer (1995, 1997) and Piecha (2004*a*) showed that they are typical for dysphotic Famennian cephalopod limestones, but rare in aphotic environments. They occur widely in the upper Famennian of the Tafilalt Platform, including the hypoxic Dasberg Event Beds of the Amessoui Syncline (Hartenfels, 2011). Abundant laminated iron crusts enclosed both skeletal grains and early consolidated burrows. Evidence for diagenesis is given by grain margin solution. The micritic matrix consists of compacted pseudopeloids. Deposition took place below the normal wave base but was affected by storm waves, which explains the high percentage of fragmented benthic remains. Microborings of bioclasts, the silt content and the ooids/oncoids are evidence for reworking and an influx from an adjacent up-ramp environment that reached the photic zone. In the wide, undulating outcrop towards the western end of Jebel Ihrs, the top of Bed 3 shows eroded and corroded gonioclymeniids (Fig. 8a) and oncoceratid nautiloids

https://doi.org/10.1017/S0016756816000893 Published online by Cambridge University Press

supraregional conodont zonation	*B. costatus* Subzone	*B. ultimus ultimus* Zone		number of Pa elements/taxon
Tafilalt regional conodont zonation	*B. costatus* Subzone	*B. ultimus ultimus* Zone		
sample/bed no.	*Gonio. subcarinata*	*Kallo. subarmata*	*Kalloclymenia* sp.	
dissolved carbonate [g]	604.6	1504.2	777.5	
number of Pa elements	327	849	615	
taxa/bed	22	21	20	
conodont biofacies [%]				
Pa. perlobata Group	0.9			
Pa. gracilis Group	39.1	26.5	11.2	
Polygnathus	0.3	1.4	3.6	
Neopolygnathus	4.3	9.3	5.5	
Bispathodus (single row taxa)	27.8	1.8	4.2	
Bispathodus (multiple row taxa)	9.5	52.9	61.8	
Branmehla/Mehlina	15.9	4.6	10.1	
Pseudopolygnathus	2.1	2.6	1.1	
N. Gen. 1 & 2/*S.* (*Eosiphonodella*)		0.9	2.4	
Pa. perlobata schindewolfi	2			2
Pa. perlobata helmsi	1			1
Pa. gracilis sigmoidalis	1			1
B. stabilis bituberculatus	2			2
B. stabilis stabilis	26			26
Po. delicatulus	1			1
M. strigosa	3	2		5
B. spinulicostatus M3	1	4		5
Ps . primus tafilensis ssp. nov.	1	2		3
B. primus aff. *primus*	1	1		2
Neo. communis communis	14	64	34	112
Pa. gracilis gracilis	118	225	66	409
Br. inornata	38	37	57	132
B. stabilis vulgaris	63	15	26	104
Pa. gracilis expansa M1	9	-	3	12
Br. fissilis	11	-	1	12
B. aculeatus aculeatus	16	164	109	289
Ps. primus primus M3	5	18	7	30
B. aculeatus anteposicornis	2	2	2	6
B. spinulicostatus M1	5	90	23	118
B. costatus M2	7	112	161	280
Ps. controversus M2		1		1
Neo. fibula sp. nov.		15		15
aff. N. Gen. 2 sp.		1		1
S. (*Eosiphonodella*) sp. nov. B (sensu Becker*et al.* 2013*c*)		1		1
B. spinulicostatus M2		12	20	32
B. costatus M1		1	32	33
B. ultimus ultimus M2		1	8	9
B. ultimus ultimus M1		63	18	81
'*Polygnathus*' div. sp. → N. Gen. 1		12	22	34
N. Gen. 2 div. sp.		6	8	14
B. bispathodus			7	7
Br. inornata → *Br. suprema*			4	4
N. Gen. 1 div. sp.			7	7

Figure 9. Conodont record and biofacies of loose slabs with *Gonioclymenia* or *Kalloclymenia* from Jebel Ihrs West.

(Fig. 8b). This suggests a next interval of submarine carstification during long-lasting non-deposition due to increased turbulence and regression. This explains the local lack of ammonoids typical for UD V-C (*Medioclymenia*).

As for Bed 2, the rich conodont fauna of Bed 3 (Figs 6, 9) is dominated by *Pa. gracilis gracilis* and *Neo. communis communis*; *B. aculeatus aculeatus* is moderately common. Slender pseudopolygnathids as well as *B. costatus* Morphotype 2 continue from below as rare forms; *B. costatus* Morphotype 1 is also present. A similar association, but with rare *Pa. perlobata schindewolfi*, *Pa. perlobata helmsi*, *B. stabilis bituberculatus*, *Ps. primus tafilensis* ssp. nov. and *Ps. primus* aff. *primus*, with fewer *Neo. communis communis* and a higher content of *B. stabilis vulgaris*, was recovered by the dissolution of a limestone slab with a *Gonio. subcarinata* (Fig. 9). Therefore, both the loose and the *in situ* sample of the *Gonioclymenia* Limestone fall in the (higher) *B. costatus* Subzone.

https://doi.org/10.1017/S0016756816000893 Published online by Cambridge University Press

Kalloclymenia Limestone *(Bed 4b)*

Separated by *c.* 6 cm deeply weathered marl/shale (Bed 4a, Fig. 4), a second quarried, massive, slightly more reddish limestone (Bed 4b) is 23 cm thick and contains *Kalloclymenia* sp. Therefore, it is here called *Kalloclymenia* Limestone. The fauna is dominated by crinoids and ammonoids, but both are mostly broken. In thin-section (Fig. 5c) there are associated ostracods, fragmented bivalves, rare trilobites, rugose deep water corals, heterocorals and burrows. Again, brownish-black, laminated, *Frutexites*-type structures enclose many skeletal grains, which attests continuing slow sedimentation rates. As in Bed 3, there are some angular, small-sized quartz grains and, extremely rare, oncolites. However, as a significant difference, there are also numerous, irregular, sparite-filled, small-scale fenestral fabrics in the middle part (cf. Tebbutt, Conley & Boyd, 1965). Such structures are commonly interpreted as filled biogenic/microbial textures and have previously been described from the Tafilalt (Wendt, Aigner & Neugebauer, 1984). Wolf (1965) introduced the term 'open-space structures' for variously sized cavities in carbonate rocks, filled with calcite and/or internal sediment (Flügel, 2004). The whole bed shows an advanced microsparitization. According to Folk (1959), microsparite refers to a calcite matrix with rather uniform crystal size (5–10 μm) and equal shape. The recrystallization took place during late diagenesis, affected by surface water (Folk, 1974; Longman, 1977). The *Gonioclymenia* and *Kalloclymenia* limestones are separated by an interval of non-deposition (UD V-C), re- and transgression. The microbialithic microfacies of the latter suggests a moderately agitated, slightly shallower deposition within the dysphotic zone.

The conodont fauna of Bed 4b (Figs 6, 9) differs from the *Gonioclymenia* Limestone by the presence of *B. ultimus ultimus* Morphotype 1 and Morphotype 2 and by transitional forms between *Br. inornata* and *Br. suprema*. There are also several species of two different genera ('siphonodelloids'), which are related to early *Siphonodella*. These were called N. Gen. 1 and N. Gen. 2 in Becker *et al*. (2013*c*). They differ from typical *S. (Eosiphonodella)* in the shape and morphology of their basal cavities. They are left in open nomenclature because of parallel ongoing taxonomic investigations by H. Tragelehn. Rare *S.* (*Eosiphonodella*) sp. nov. B (*sensu* Becker *et al.* 2013*c*) could be taken as evidence for the *praesulcata* Zone, but in the absence of the zonal index species Bed 4b is still kept in the *B. ultimus ultimus* Zone. Like the microfacies, the conodont biofacies has changed to some extent from Bed 3, now with a strong dominance of *Br. inornata*. *Bispathodus costatus* Morphotype 2 is also very common in Bed 4b, followed by *B. aculeatus aculeatus* and *B. spinulicostatus* Morphotype 1. *Palmatolepis perlobata schindewolfi* has disappeared; on a global scale it is not known to have overlapped with *B. ultimus ultimus* (Kaiser *et al*. 2009). This branmehlid (double rowed)–bispathodid assemblage seems to represent a new, moderately shallow (dysphotic) outer shelf conodont biofacies type.

Two loose slabs, one with *Kallo. subarmata*, one with *Kalloclymenia* sp., have similar conodont assemblages to Bed 4b (Fig. 9), but with more *Pa. gracilis gracilis*, *B. aculeatus aculeatus* and *B. ultimus ultimus* Morphotype 1. Their palmatolepid–bispathodid biofacies is more typical for pelagic cephalopod limestones (see Sandberg, 1976). Rare *B. spinulicostatus* Morphotype 3, *B. ultimus ultimus* Morphotype 2, *Neo. fibula* sp. nov., *Ps. primus tafilensis* ssp. nov. and *Ps. primus* aff. *primus* represent accessory taxa. Furthermore, N. Gen. 1 div. sp., N. Gen. 2 div. sp. and a yet different 'siphonodelloid' ('aff. N. Gen. 2 sp.') co-occur with a single specimen of *S.* (*Eosiphonodella*) sp. nov. B (*sensu* Becker *et al.* 2013*c*). Therefore, all our *Kalloclymenia* limestone samples fall in the same interval.

Topmost Famennian (Bed 5b)

Separated by a thin, 5–10 cm thick marl/shale (Bed 5a, Fig. 4), a reddish, lenticular limestone with variable thickness between 5 and 15 cm terminates the local Famennian succession. Bed 5b is a coarse crinoidal packstone with some very fine quartz detritus (Fig. 5d). Skeletal remains derive from ostracods, bivalves, rare trilobites and burrows of uncertain origin. Reddish-brown microstromatolites encrusted skeletal remains, especially crinoids. Constant reworking during storm events is indicated by fragmentation whilst microborings confirm a shallow outer shelf setting. Grain margin solution, particularly between crinoid remains, is common. Similarly to the *Kalloclymenia* Limestone, Bed 5b shows a distinctive microsparitization. It was deposited on or directly adjacent to a storm-swept crinoidal shoal, but without an influx of skeletal grains from the photic zone. The scarcity of pelagic fauna is distinctive. So far there are no ammonoids and there is only a sparse conodont fauna (Figs 4, 6) with, amongst others, both morphotypes of *B. costatus*, *B. ultimus ultimus* Morphotype 2 and, again, N. Gen. 2 div. sp. as well as *S.* (*Eosiphonodella*) sp. nov. B (*sensu* Becker *et al.* 2013*c*). The restricted fauna resembles the worsening of environmental conditions recorded in the contemporaneous crinoidal limestone platform of the northern Maider (Becker *et al*. 2013*c*). By comparison with sections of the central (Jebel Erfoud; Fig. 10) and eastern Tafilalt Platform (Ouidane Chebbi; Hartenfels, 2011) and northern Maider (western Jebel Rheris to Lalla Mimouna), the uppermost Famennian of Jebel Ihrs is extremely condensed and incomplete.

3.b. Jebel Erfoud (Figs 3, 10)

A summary of the investigation history of the Jebel Erfoud (GPS coordinates: 31° 25′ 49.6″ N, 004° 13′ 05.6″ W, map sheet 244 Tafilalt-Taouz) is given in Hartenfels (2011), who studied in detail the succession from the base of the middle Famennian to the Dasberg Event beds. Above, there are only very sparse conodont data for Famennian V/VI in Alberti (1970,

https://doi.org/10.1017/S0016756816000893 Published online by Cambridge University Press

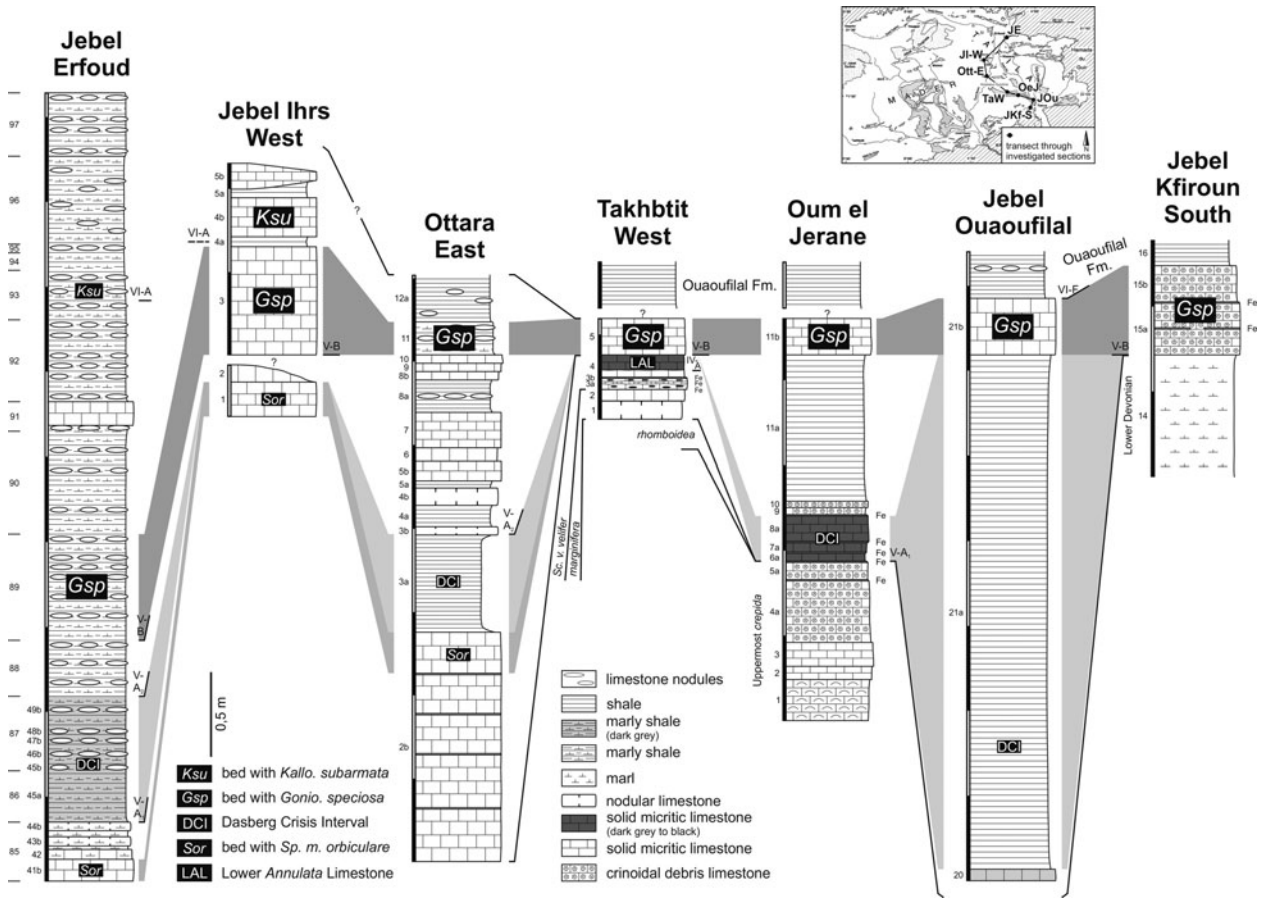

Figure 10. Correlation of the *Gonioclymenia* Limestone section at Jebel Ihrs West with thicker or strongly condensed and incomplete successions with *Gonio. speciosa*, along a curved transect through the Tafilalt Platform (see inserted map).

section 'Bordj East at Erfoud'). His written section log, unfortunately, cannot be compared with the log with ammonoid ranges in Korn (1999, 'Bordj d´Erfoud') or with our succession. Locally there is no typical development of the *Gonioclymenia* Limestone (Fig. 10). But a nodule level within Bed 89, which is not very distinctive from under- and overlying nodular beds, yielded the marker species *Gonio. speciosa* in association with kosmo- and cymaclymeniids. Fragmentary *Kallo. subarmata* commence above an interval without gonioclymeniids, probably the top of Famennian V, in layers of small, greenish-grey limestone nodules (Bed 93; compare the onset of *Kalloclymenia* above an interval of very small nodules in Korn, 1999). Linguaclymeniids, the alternative index group for the Wocklumian (UD VI; Becker, Kaiser & Aretz, 2016) enter just above, followed latest in Bed 98 by the *Muess. bisulcata* Group, the index forms of UD VI-A_2, and higher by *Effenbergia lens* (Korn, 1999: Bed 42), the index species of UD VI-B.

supraregional conodont zonation	*B. costatus* Sub.
Tafilalt regional conodont zonation	*B. costatus* Sub.
sample/bed no.	5
dissolved carbonate (g)	414.9
number of Pa elements	21
taxa/bed	5
conodont biofacies (%)	
Pa. gracilis Group	24
Neopolygnathus	19
Bispathodus (multiple row taxa)	48
Branmehla/Mehlina	10
Neo. communis communis	4
Pa. gracilis gracilis	5
M. strigosa	1
Br. inornata	1
B. aculeatus aculeatus	10

Figure 11. Conodont record and biofacies of the *Gonioclymenia* Limestone at Takhbtit West.

3.c. Ottara East (Figs 2d, 3, 10)

As at Jebel Erfoud, a massive marker limestone is not developed at Ottara East in the Bou Maiz Syncline of the western-central Tafilalt (map sheet 244 Tafilalt-Taouz, 500 m to the east of section s2 of Lubeseder *et al.* 2010). The *Gonioclymenia* level is locally a fossiliferous, reddish, shale/marl interval with red carbonate nodules yielding *Cyma. striata* and *Gonio. speciosa* (Fig. 2d). Higher strata are mostly covered by debris of the topmost Famennian (Hangenberg Crisis Interval) Ouaoufilal (= Aoufital) Formation.

https://doi.org/10.1017/S0016756816000893 Published online by Cambridge University Press

supraregional conodont zonation	*B. costatus* Sub.
Tafilalt regional conodont zonation	*B. costatus* Sub.
sample/bed no.	11b
dissolved carbonate (g)	1801.3
number of Pa elements	294
taxa/bed	15
conodont biofacies (%)	
Pa. perlobata Group	0.3
Pa. gracilis Group	24.8
Polygnathus	4.1
Neopolygnathus	18.7
Bispathodus (single row taxa)	18.7
Bispathodus (multiple row taxa)	18
Branmehla/Mehlina	14
Pseudopolygnathus	1.4
Pa. gracilis gracilis	73
Pa. perlobata schindewolfi	1
B. aculeatus aculeatus	47
B. aculeatus aff. *aculeatus*	1
B. aculeatus anteposicornis	4
M. strigosa	22
B. stabilis vulgaris	43
Neo. communis communis	55
Po. delicatulus	12
Ps. primus primus M3	3
Br. inornata	17
B. stabilis stabilis	12
Br. fissilis	2
B. costatus M2	1
Ps. primus tafilensis ssp. nov.	1

Figure 12. Conodont record and biofacies of a loose *Gonioclymenia* slab from Oum el Jerane.

3.d. Takhbtit West (Figs 2e, 3, 10, 11)

This section on the northern limb of the Amessoui Syncline (GPS coordinates: 31° 00′ 44.5″ N, 004° 10′ 15.7″ W, map sheet 244 Tafilalt-Taouz) was first illustrated by Korn, Klug & Reisdorf (2000) and re-studied by Hartenfels (2011). Very intensive fossil mining has destroyed all natural outcrop of the *Gonioclymenia* Limestone (Fig. 2e). A dissolved *Gonio. speciosa* produced a sparse conodont fauna dominated by *B. aculeatus aculeatus* (Fig. 11) and with approximately equally common *Pa. gracilis gracilis* and *Neo. communis communis*. There is no record of *Kalloclymenia* or any other UD VI ammonoids from Takhbtit West.

3.e. Oum el Jerane (Figs 2f, 3, 10, 12)

The condensed Famennian of Oum el Jerane on the southern Amessoui Syncline (GPS coordinates: 30° 59′ 39.3″ N, 004° 08′ 18.7″ W, map sheet 244 Tafilalt-Taouz) has been investigated by Korn, Klug & Reisdorf (2000), Ginter, Hairapetian & Klug (2002), Hartenfels & Becker (2009), Hartenfels (2011) and Becker *et al.* (2013*b*). The deeply trenched *Gonioclymenia*

supraregional conodont zonation	*B. costatus* Sub.
Tafilalt regional conodont zonation	*B. costatus* Sub.
sample/bed no.	21b
dissolved carbonate (g)	248.9
number of Pa elements	4
taxa/bed	1
conodont biofacies (%)	
Bispathodus (multiple row taxa)	100
B. aculeatus aculeatus	4

Figure 13. Conodont record and biofacies of a loose *Gonioclymenia* slab from Jebel Ouaoufilal.

Limestone (Fig. 2f) is separated from the underlying three-fold, thin-bedded, extremely fossiliferous black limestones of the transgressive Dasberg Crisis Interval (UD V-A_1, beds 6a–8a: *Costaclymenia* – previously *Endosiphonites* – Limestones; compare Hartenfels, 2011 and Becker *et al.* 2013*b*) by a sequence of reddish-brown, iron-rich crinoidal debris limestones and subsequent greenish, unfossiliferous shale. The conodont assemblage of the *Gonioclymenia* Limestone is dominated by *Pa. gracilis gracilis*, *Neo. communis communis*, *B. aculeatus aculeatus* and *B. stabilis vulgaris* (Fig. 12), which resembles Takhbtit West. Based on a single *B. costatus* Morphotype 2 this palmatolepid–bispathodid–neopolygnathid assemblage falls in the *B. costatus* Subzone of the *B. aculeatus aculeatus* Zone, as at Jebel Ihrs. Above, the top of UD-V and the main part of the uppermost Famennian (UD VI) is missing due to an unconformity below the siliciclastic Aoufital Formation (Becker *et al.* 2013*b*).

3.f. Jebel Ouaoufilal (Figs 3, 10, 13)

The Famennian of Jebel Ouaoufilal in the southeastern part of the Amessoui Syncline (GPS coordinates: 30° 57′ 31.2″ N, 004° 02′ 22.6″ W, map sheet 244 Tafilalt-Taouz; Aoufital on the topographic sheet Taouz-Ouest) has been studied by Korn, Klug & Reisdorf (2000), Becker *et al.* (2002), Kaiser (2005), Hartenfels & Becker (2009), Hartenfels (2011) and Kaiser *et al.* (2011). It is especially famous for its rich and diverse goethitic ammonoids of the Dasberg Event beds (*Costa. muensteri* Zone, UD V-A_1). The *Gonioclymenia* Limestone appears to follow above an unconformity that encompasses the *Gonio. subcarinata* Zone (UD V-A_2). Due to the intensive quarrying the direct shale–limestone contact has not been observed. The dissolution of a *Gonio. speciosa* from the mining debris yielded a sparse, monospecific fauna with four *B. aculeatus aculeatus* (Fig. 13). Kaiser (2005) obtained a richer assemblage, with rare *B. aculeatus aculeatus*, *B. aculeatus anteposicornis* and *B. stabilis stabilis* (= *stabilis* Morphotype 2), in association with more common *Br. inornata*, *M. strigosa*, *Pa. gracilis gracilis* and *Neo. communis communis*. There is no evidence for *B. ultimus ultimus*; therefore, the *Gonio. speciosa* Limestone fauna is placed in the (higher) *B. aculeatus*

https://doi.org/10.1017/S0016756816000893 Published online by Cambridge University Press

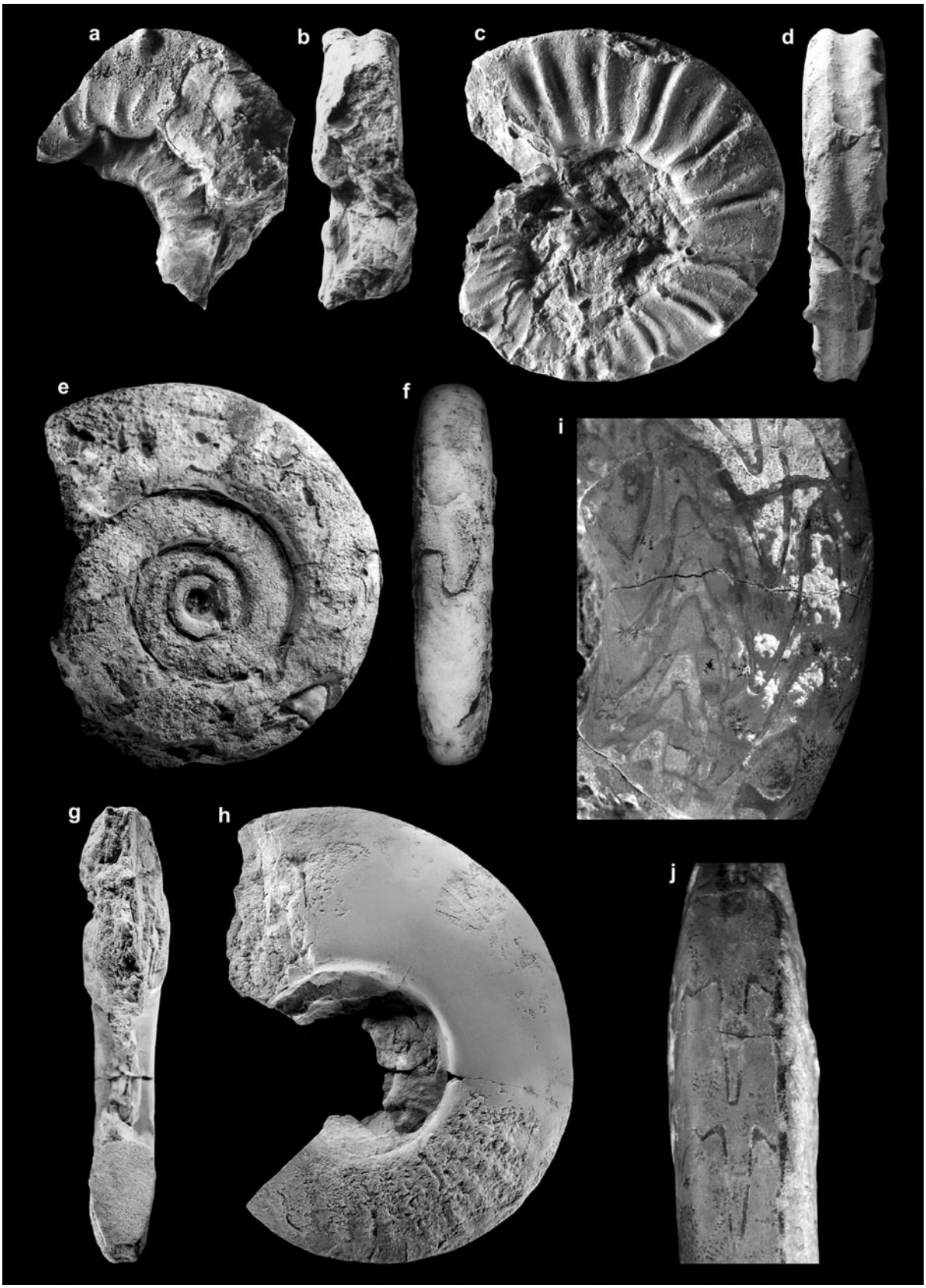

Figure 14. Upper/uppermost Famennian Gonioclymeniidae. (a, b) Lectotype of *Gonioclymenia hoevelensis* Wedekind, 1914, preserved part, lateral and ventral views, Hövel, Rhenish Massif, Göttingen collection, no. 388-54, partial re-illustration of Wedekind (1914: pl. 6, fig. 2a), ×1; (c, d) paralectotype of *Gonioclymenia hoevelensis* Wedekind, 1914, lateral (re-illustration of Wedekind, 1914: pl. 5, fig. 7) and new ventral views, Hövel, Rhenish Massif, Göttingen collection, no. 588-53, ×1; (e, f) *Kalloclymenia subarmata* (Münster, 1832), MB.C.3553, M'karig, Bed 18, basal *B. ultimus ultimus* Zone, re-illustration from Becker *et al*. (2002: pl. 5, figs 1–2), ×0.55; (g–j) *Leviclymenia ramula* sp. nov., holotype, GMM B6.C.42-3, loose from *Gonioclymenia* Limestone at Jebel Ouaoufilal, *B. costatus* Subzone, ×0.55 (g, h), ×1.18 (i, j).

https://doi.org/10.1017/S0016756816000893 Published online by Cambridge University Press

aculeatus Zone. As an unexpected novelty, the fossil miners discarded an incomplete specimen of *Levi. ramula* sp. nov. (Fig. 14g–j), the first Moroccan representative of a genus that was so far only known from the upper Famennian of the southern Urals (Bogoslovskiy, 1981; Korn & Klug, 2002). Its upper surface is encrusted by numerous thecae of *Cladochonus*, a deep-water tabulate coral. They suggest that the clymeniid shell formed a small benthic island before burial. *Kalloclymenia* or other ammonoids of the pre-Hangenberg Event uppermost Famennian (Wocklumian, UD VI-A/D) are not known from the locality. Deeply weathered equivalents of the Hangenberg Blackshale can be observed just adjacent to the *Gonioclymenia* Limestone (Kaiser *et al*. 2011).

3.g. Jebel Kfiroun South (Figs 2g, h, 3, 10, 15)

At Jebel Kfiroun South, 3 km SW of Taouz (GPS coordinates: 30° 53′ 06.4″ N, 004° 02′ 20.0″ W, map sheet 244 Tafilalt-Taouz; see Aboussalam, Becker & Bultynck, 2015), the *Gonioclymenia* level is beautifully exposed as a massive, 56 cm thick, greenish-grey to brownish-grey, vertical marker limestone (Fig. 2g) with crinoidal debris and numerous giant-sized *Gonio. speciosa* (up to 40 cm in diameter) on the upper surface (Fig. 2h). The bed consists of a sequence of individual depositional events, notably with two levels of reworked red iron crusts and nodules. These suggest recurring phases of extreme condensation and subsequent storms. Whilst a sample from the base of the bed was barren, the top yielded a relatively rich conodont fauna, again dominated by *B. aculeatus aculeatus* (Fig. 15). The occurrence of *B. costatus* Morphotype 2 and the absence of *B. ultimus ultimus* indicate the regional *B. costatus* Subzone.

3.h. Seheb el Rhassal (Figs 3, 16)

The middle/upper Famennian succession of Seheb el Rhassal (GPS coordinates: 31° 21′ 19.2″ N, 004° 11′ 14.2″ W, map sheet 244 Tafilalt-Taouz), the SW continuation of the more famous Bou Tchrafine, has not yet been published. It is also subject to very intensive quarrying, mostly of beds with *Maeneceras* and platyclymeniids (UD II-G and UD IV). It is the source for rather well-preserved, giant *Protacto. giganta*, *Protacto. ventriosa*, and *Pl. ibnsinai* of Famennian IV, which are sometimes sold unpolished. During several visits, there was no outcrop of the obviously directly overlying *Gonioclymenia* Limestone. A conodont fauna extracted from a dissolved, loose *Gonio. speciosa* is dominated by *Pa. gracilis gracilis*, followed in abundance by *Neo. communis communis* and *B. aculeatus aculeatus* (Fig. 16). The ammonoids suggest an identical age to that at the two previous localities. Furthermore, the conodont biofacies is the same. Again, *Kalloclymenia* and all UD VI strata are locally missing in an unconformity.

supraregional conodont zonation	*B. costatus* Sub.
Tafilalt regional conodont zonation	*B. costatus* Sub.
sample/bed no.	15b
dissolved carbonate (g)	1069.6
number of Pa elements	39
taxa/bed	11
conodont biofacies (%)	
Pa. gracilis Group	5.1
Polygnathus	12.8
Neopolygnathus	2.6
Bispathodus (single row taxa)	10.3
Bispathodus (multiple row taxa)	48.7
Branmehla/Mehlina	18
Pseudopolygnathus	2.6
Po. semicostatus central M	1
Neo. communis communis	1
Pa. gracilis gracilis	2
M. strigosa	3
Br. inornata	4
B. stabilis vulgaris	4
Po. delicatulus	4
B. aculeatus aculeatus	16
B. aculeatus anteposicornis	1
Ps. primus primus M3	1
B. costatus M2	2

Figure 15. Conodont record and biofacies of the *Gonioclymenia* Limestone at Jebel Kfiroun South.

3.i. Ouidane Chebbi Northwest (Fig. 3)

In the eastern Tafilalt, the Famennian of the Ouidane Chebbi area was investigated by Belka *et al.* (1999), Korn (1999), Becker *et al.* (2002), Kaiser (2005), Hartenfels & Becker (2009) and Hartenfels (2011). At section Ouidane Chebbis Northwest (GPS coordinates: 31° 14′ 57.4″ N, 003° 50′ 00.2″ W, map sheet 244 Tafilalt-Taouz), the *Gonioclymenia* marker bed is developed as a 21 cm thick, brownish-grey, solid cephalopod limestone (Bed 24b; Hartenfels, 2011, fig. 42) with well-preserved *Gonio. subcarinata*, *Gonio. speciosa*, *Erfoudites* sp., *Kosmo. lamellosa*, *Muess. diversa*, *Rect. lineare* and *Rect.* aff. *lineare*. This rich pelagic macrofauna contrasts with a very sparse conodont fauna (a single *Pa. gracilis gracilis*), which illustrates well the ecologically independent distribution of both fossil groups. *Kalloclymenia* enters above, within a rather uniform, not very fossiliferous and cyclic succession (Hartenfels, 2011, Bed 33b). Kaiser (2005) provided a conodont record across the UD V/VI transition for an adjacent section further to the east and, several km beyond, for section Mkarig (see also Kaiser *et al*. 2011).

3.j. Bou Tchrafine (Fig. 3)

The higher upper Famennian (UD IV-V) of Bou Tchrafine has been briefly described by Becker & House (2000, with geographic coordinates). Above the

https://doi.org/10.1017/S0016756816000893 Published online by Cambridge University Press

supraregional conodont zonation	*B. costatus* Subzone		number of Pa elements/taxon
Tafilalt regional conodont zonation	*B. costatus* Subzone		
sample/bed no.	*Gonioclymenia* sp.	*Gonio. speciosa*	
dissolved carbonate (g)	789.6	665.3	
number of Pa elements	10	149	
taxa/bed	3	10	
conodont biofacies (%)			
Pa. gracilis Group	80	53	
Neopolygnathus		20.1	
Bispathodus (single row taxa)		5.4	
Bispathodus (multiple row taxa)	10	13.4	
Branmehla/Mehlina	10	6	
Pseudopolygnathus		2	
Pa. gracilis gracilis	8	79	87
B. aculeatus aculeatus	1	18	19
M. strigosa	1	2	3
Neo. communis communis		30	30
B. stabilis vulgaris		7	7
Br. inornata		7	7
B. stabilis stabilis		1	1
B. spinulicostatus M1		2	2
Ps. primus primus M3		1	1
Ps. primus tafilensis ssp. nov.		2	2

Figure 16. Conodont record and biofacies of loose *Gonioclymenia* slabs from Seheb el Rhassal.

Dasberg Event Beds, locally a green, unfossiliferous shale unit, there is an ammonoid-rich, very condensed succession (beds Z–Zb). Since most of the fauna was collected from scree, the ammonoid succession of UD V is only roughly established. There is no solid *Gonioclymenia* marker bed but *Gonio. speciosa* fragments occur abundantly in loose nodules assigned to 'Bed Za', followed by a loose collection ('Bed Zb') without *Gonioclymenia* but with frequent *Medio. aguelmousensis* that show that early whorls are spinose. This feature was not noted in the original description of Korn & Klug (2002) and caused a false record of *Gonio. hoevelensis* in Becker & House (2000). A spot conodont sample taken in 2012 showed that the succession ranges above the UD V-C with *Mediocymenia*, into the basal uppermost Famennian. *Bispathodus ultimus ultimus* Morphotype 1 is accompanied by both morphotypes of *B. costatus*, *B. bispathodus*, *B. jugosus*, *B. aculeatus aculeatus*, *B. spinulicostatus* Morphotype 1, *Br. inornata*, *Br. fissilis*, *Neo. communis communis*, and *Pa. gracilis gracilis*. Various 'siphonodellids' provide a correlation with the *Kalloclymenia* Limestone and there is no *S. (Eo.) praesulcata*. Loose *Muess. sublaevis* and *Linguaclymenia* sp. nov. are in agreement with an UD VI-A_1 age for the youngest exposed limestones.

3.k. Hamar Laghdad East (Fig. 3)

The upper Famennian section described by Becker *et al.* (2002) was found to be mostly covered in spring 2015. As at Bou Tchrafine to the west and Ouidane Chebbi to the east there is no *Gonioclymenia* marker bed, but *Gonio. speciosa* and *Medio. aguelmousensis* (originally recorded as *Spheno. brevispina*) occur within a *c.* 2 m thick nodular succession at the local top of the Devonian.

4. Upper/uppermost Famennian conodont zonation of the Tafilalt (Figs 7, 17)

The regional Famennian conodont zonation of the Tafilalt was introduced by Hartenfels (2011) and Becker, El Hassani & Tahiri (2013). Spalletta *et al.* (2015*a*, *b*) proposed a new global zonation scheme, which can be easily correlated.

4.a. *B. aculeatus aculeatus* Zone

4.a.1. B. aculeatus aculeatus *Subzone*

Definition. Lower boundary: Entry of *B. aculeatus aculeatus*. Upper boundary: Entry of either morphotype of *B. costatus*.

Other markers. Entry of *B. aculeatus anteposicornis* and *Clyd. plumulus*; both are rare forms, with locally delayed entries, and therefore of limited stratigraphic use. Oldest specimens of both coexist at Oum el Jerane (basal bed of *Costaclymenia* Limestone, Dasberg Crisis Interval) with the first *B. aculeatus aculeatus*. *Bispathodus spinulicostatus* Morphotype 1 (Jebel

https://doi.org/10.1017/S0016756816000893 Published online by Cambridge University Press

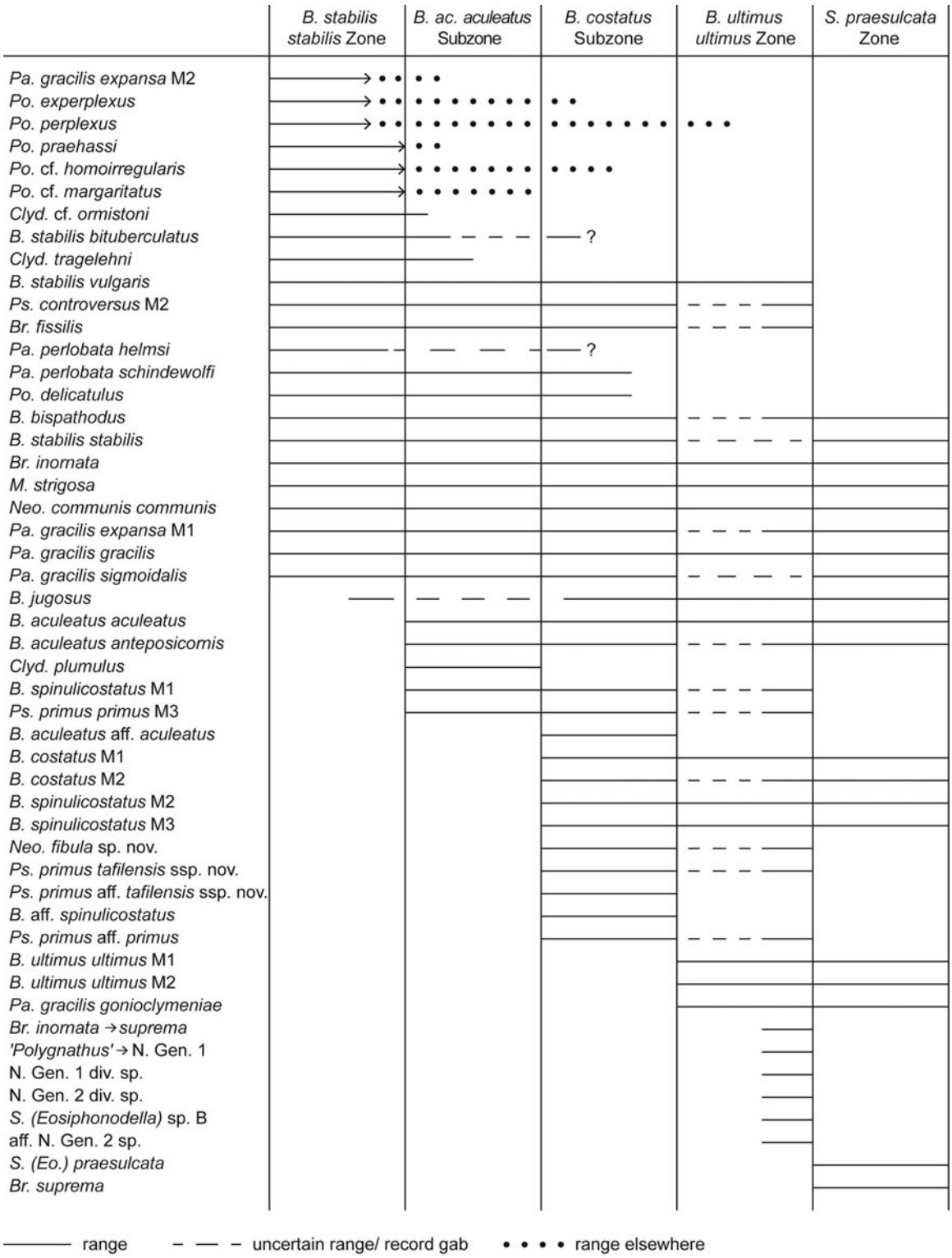

Figure 17. Range chart of all recorded conodonts from the *B. stabilis stabilis* to *S. (Eo.) praesulcata* zones of the Tafilalt.

Erfoud, Bed 45b; Oum el Jerane, Bed 6a) and *Ps. primus primus* Morphotype 3 (Oum el Jerane, Bed 6a) enter on the Tafilalt Platform at the base of the subzone or just above (cf. Hartenfels, 2011).

Associated taxa. The oldest *B. aculeatus aculeatus* coexisted in the Tafilalt for a short term with *Clyd. ormistoni* (Jebel Erfoud, Bed 46b; Oum el Jerane, Bed 6a; Hartenfels, 2011), *B. stabilis bituberculatus* (= *stabilis* Morphotype 3, Oum el Jerane, Bed 8a) and *Clyd. tragelehni* (Oum el Jerane, Bed 9; Fig. 17). The following taxa range through the subzone: *B. bispathodus*, *B. stabilis stabilis* (= *stabilis* Morphotype 2), *B. stabilis vulgaris* (= *stabilis* Morphotype 1), *Br. fissilis*, *Br. inornata*, *M. strigosa*, *Neo. communis communis*, *Pa. gracilis expansa* Morphotype 1, *Pa. gracilis gracilis*, *Pa. gracilis sigmoidalis*, *Pa. perlobata schindewolfi*, *Po. delicatulus* and *Ps. controversus* Morphotype 2.

https://doi.org/10.1017/S0016756816000893 Published online by Cambridge University Press

Some taxa, which range elsewhere into the *B. aculeatus aculeatus* (Sub)zone, disappear earlier in the Tafilalt, high in or at the end of the preceding *B. stabilis stabilis* Zone. These are *Pa. gracilis expansa* Morphotype 2 (see higher range in Hartenfels, 2011), *Po. experplexus* (allegedly ranging into the lower *costatus* Subzone (Sandberg & Ziegler, 1979, but without giving any precise evidence); co-occurrence with the oldest *Po. znepolensis* in the Carnic Alps (Perri & Spalletta, 1991)), *Po. perplexus* (ranging in the Carnic Alps as a very rare form into the *B.ultimus ultimus* Zone; Perri & Spalletta, 1998), *Po*. cf. *homoirregularis* (record of Kaiser, 2005; see range of the typical form into the lower *B. costatus* Subzone in the Carnic Alps (Spalletta, Perri & Pondrelli, 1998), and Thailand (Savage, 2013)), and *Po*. cf. *margaritatus* (record of Kaiser, 2005; see imprecise upper range in Schäfer, 1976). By contrast with German sections, there are also no Tafilalt records at this level of *Bizignathus*, *Dasbergina*, *Pa. perlobata postera*, subspecies of *Pa. rugosa*, *Po. extralobatus*, *Po. hassi*, *Po. marginvolutus*, *Po. restrictus*, *Po. rhabdotus*, *Po. znepolensis*, *Ps. marburgensis marburgensis* or *Ps. micropunctatus*. There is also a lack of early *B. jugosus*. This gives a much reduced biodiversity, which is also true for the ammonoid faunas, and which may reflect the more southern palaeolatitude.

At M'Karig (Bed 12), Kaiser (2005) recorded two specimens, unfortunately without illustration, of *Neo. carina* (= *Po. communis carina*). Normally this is a Lower Carboniferous species; it may refer to a homoeomorphic form (see systematic palaeontology).

Conodont–ammonoid correlation. In the Tafilalt the base of the *B. aculeatus aculeatus* Subzone correlates with the *Costa. muensteri*-Zone (UD V-A_1). This is based on *Costaclymenia* records from Hassi Nebech (Bed M1a), Jebel Erfoud (Bed 46b), Ouidane Chebbi Northwest (Bed 18a), Jebel Ouaoufilal (Bed 21a) and Oum el Jerane (beds 6a–8a) (Fig. 10; Hartenfels, 2011).

4.a.2. B. costatus Subzone

Definition. Lower boundary: Entry of either morphotype of *B. costatus*. Upper boundary: Entry of *B. ultimus ultimus* Morphotypes 1 or 2.

Discussion. A slightly earlier entry of Morphotype 1 than of Morphotype 2, as is common in central Europe (Hartenfels, 2011), could not be verified in southern Morocco. Previous regional records of *B. costatus* were from the UD V-B of M'Karig (Kaiser, 2005) or from the highest part of the *B. ultimus ultimus* Zone (Kaiser, 2005: Ouidane Chebbi, Bed 17c).

Other markers. *Bispathopdus aculeatus* aff. *aculeatus*, *B. spinulicostatus* Morphotypes 2–3, *?B*. aff. *spinulicostatus*, *Neo. fibula* sp. nov., *Ps. primus tafilensis* ssp. nov., *Ps. primus* aff. *tafilensis* ssp. nov. and *Ps. primus* aff. *primus* first occur within this subzone but are not common enough for a consistent and reliable use as index taxa.

Associated taxa. A dissolved *Gonioclymenia* from Jebel Ihrs yielded *B. stabilis bituberculatus* (= *stabilis* Morphotype 3) and *Pa. perlobata helmsi*, which implies range extensions. Reworking is unlikely but not completely ruled out. Sandberg & Ziegler (1979) did not record an overlap of *Pa. perlobata helmsi* and *B. costatus*. There is evidence that *Pa. perlobata schindewolfi* and *Po. delicatulus* range until high in the subzone (compare Ji & Ziegler, 1993 and Kaiser *et al.* 2006). The following taxa go through (Fig. 17): *B. bispathodus*, *B. stabilis stabilis* (= *stabilis* Morphotype 2), *B. stabilis vulgaris* (= *stabilis* Morphotype 1), *B. jugosus* (records of Kaiser, 2005), *B. aculeatus aculeatus*, *B. aculeatus anteposicornis*, *B. spinulicostatus* Morphotype 1, *Br. fissilis*, *Br. inornata*, *M. strigosa*, *Neo. communis communis*, *Pa. graxilis expansa* Morphotype 1, *Pa. gracilis gracilis*, *Pa. gracilis sigmoidalis*, *Ps. controversus* Morphotype 2 and *Ps. primus primus* Morphotype 3.

Conodont–ammonoid correlation. The base of the *B. costatus* Subzone correlates roughly with the *Gonio. subcarinata* Zone (UD V-A_2). Above, the subzone certainly comprises the *Gonio. hoevelensis* Zone (UD V-B), with the giant *Gonio. speciosa* as an alternative index species (Figs 1a, 2h), and, at the top, the new regional *Medio. aguelmousensis* Zone of Becker, El Hassani & Tahiri (2013; previously recorded as level of *Spheno. intermedia* (Becker *et al*. 2002) UD V-C; conodont faunas, but without *B. costatus*, from Ouidane Chebbi, beds 10a–11f, in Kaiser, Fig. 8). In the Algerian continuation of the Tafilalt Devonian (Ben Zireg region), there are similar joint *Gonioclymenia–B. costatus* occurrences (Weyant & Pareyn, 1975). For the lower part of the *B. costatus* Subzone there are more precise data for the *Progonioclymenia–Gonioclymenia* assemblage (UD V-A_2) of the condensed Malpasso succession of the Carnic Alps (Korn, 1998: Bed 5c; Perri & Spalletta, 1998: conodont sample ML 7; Hartenfels & Becker, 2009: Bed 7b/c). In the Rhenish Massif, the corresponding *Cly. laevigata* (or *Progonioclymenia acuticostata*) Zone was reported to begin slightly below the first *B. costatus* (Korn & Luppold, 1987: data from Effenberg). This agrees with recent data from Thuringia (Bartzsch & Weyer, 2012; Kononova & Weyer, 2014), where both *Clymenia* (Bed 1.1) and *Gonioclymenia* (Bed 3.2) enter several shale–limestone cycles below *B. costatus* (Bed 8). Accordingly, *B. costatus* was only found in an upper unit with *Gonioclymenia–Kosmoclymenia* faunas of the Cantabrian Mountains (Sanz-López *et al*. 1999: Unit 5b).

4.b. *B. ultimus ultimus* Zone

Definition. Lower boundary: Entry of *B. ultimus ultimus* Morphotypes 1 or 2. Upper boundary: Entry of *S. (Eo.) praesulcata* s.l. (see Tragelehn, 2010).

https://doi.org/10.1017/S0016756816000893 Published online by Cambridge University Press

Discussion. The *B. ultimus ultimus* Zone was previously recognized in the Tafilalt by Ginter, Hairapetian & Klug (2002: Oum el Jerane, sample 4, *B. ziegleri* = *B. ultimus ultimus* Morphotype 1), Kaiser (2005: M'Karig, Ouidane Chebbi) and Kaiser *et al*. (2011).

Other markers. In many other regions throughout the world the entry of *Pa. gracilis gonioclymeniae* is a reliable alternative marker (e.g. Ji & Ziegler, 1993; Kaiser *et al.* 2009). Alberti (1970) listed this taxon from several levels at Jebel Erfoud but its precise position in refined section logs (Korn, 1999; Fig. 10) is not yet clear. It is absent from our *Kalloclymenia* Limestone samples and from the faunas of Kaiser (2005). *Pseudopolygnathus marburgensis trigonicus* is a third reliable zonal marker but completely lacking from the Tafilalt. The entry of *Br. suprema* is less reliable (Ziegler & Sandberg, 1984; new data from Franconia by H. Tragelehn & S. Hartenfels), and in the Tafilalt it was only rarely recorded from the next higher zone (Kaiser, 2005: M'Karig). An intermediate form between *Br. inornata* and *Br. suprema* from Jebel Ihrs was previously described by Hartenfels (2011) from Kahlleite East in Thuringia, where it co-occurs with *Pa. gracilis gonioclymeniae*.

As briefly discussed by Becker, Kaiser & Aretz (2016), any record of a *S. (Eosiphonodella)* could be used to place samples in the next younger *S. (Eo.) praesulcata* Zone. However, in accord with Tragelehn (2010) our faunas from the *Kalloclymenia* Limestone and similar faunas reported from crinoidal limestones of Lalla Mimouna (Becker *et al.* 2013*c*) are probably slightly older, from the lower range of *Kalloclymenia* and the oldest *Linguaclymenia*. Conodont faunas may contain very rare new *S. (Eosiphonodella)* species, but no *S. (Eo.) praesulcata* (s.l., see Kaiser & Corradini, 2011), and more common different 'siphonodelloids' (N. Gen. 1 and 2 *sensu* Becker *et al*. 2013*c*, aff. N. Gen. 2, and intermediates between *Polygnathus* and N. Gen. 1; including possibly the record of *Po. symmetricus* from M'karig in Kaiser (2005)). Due to ongoing detailed taxonomic studies by H. Tragelehn, we leave all taxa of this group in open nomenclature. A precise stratigraphical placing in the Tafilalt is hampered by the fact that there is no *B. ultimus ultimus* – 'siphonodelloid' – *S. (Eo.) praesulcata* succession; the available 'siphonodelloid faunas' come from shallow biofacies (Jebel Ihrs, Lalla Mimouna) or isolated spot samples (Bou Tchrafine). A wide range of 'siphonodelloids' was documented by Kononova & Weyer (2014: as species of *Polygnathus?*) from just above the entry of *Kalloclymenia* and *Br. suprema* and from well below the entry of *Effenbergia* lens. This lends further support for a range of this group within the *B. ultimus ultimus* Zone; unfortunately, *S. (Eo.) praesulcata* has not yet been recognized in the Thuringian succession.

Associated taxa. Based on records in Kaiser (2005), the following (sub)species and morphotypes occur in the Tafilalt: *B. jugosus*, *B. stabilis vulgaris* (= *stabilis* Morphotype 1), *B. aculeatus aculeatus*, *B. costatus* Morphotype 1, *B. spinulicostatus*, *Br. inornata*, *M. strigosa*, *Neo. communis communis* and *Pa. gracilis gracilis*. Our samples with 'siphonodelloids' and rare, new *S. (Eosiphonodella)*, possibly from high within the *B. ultimus ultimus* Zone, add *B. aculeatus anteposicornis*, *B. bispathodus*, *B. costatus* Morphotype 2, *B. spinulicostatus* Morphotype 1, *Br. fissilis*, *Pa. gracilis expansa* Morphotype 1, *Neo. fibula* sp. nov., *Ps. primus primus* Morphotype 3, *Ps. primus tafilensis* ssp. nov. and *Ps. primus* aff. *primus*. Regional Lazarus Taxa are *B. stabilis stabilis* (= *stabilis* Morphotype 2) and *Pa. gracilis sigmoidalis*.

Conodont–ammonoid correlation. In the Tafilalt, the base of the *B. ultimus ultimus* Zone is directly correlated with the onset of the *Kallo. subarmata* Zone at M'karig (Kaiser, 2005: Bed 18; see also Kaiser *et al*. 2011; fig. 13.3a–b, re-illustrated from Becker *et al*. 2002: pl. 5, figs 1–2). In the Rhenish Massif, the *Spheno. brevispina* Zone, which includes *Kallo. subarmata* as an alternative or better index form at the base (Becker, Kaiser & Aretz, 2016), begins with *Pa. gracilis gonioclymeniae* (Korn & Luppold, 1987: Dasberg section), whilst *B. ultimus ultimus* is locally absent. In Thuringia (Saalfeld area), Kononova & Weyer (2014) mentioned a co-occurrence of first *B. ultimus ultimus* with *Gonioclymenia*, before the entry of *Kalloclymenia*. Unfortunately, there is no detailed description or illustration of these oldest specimens. Furthermore, *B. spinulicostatus*, a species which is very similar to *B. ultimus ultimus* Morphotype 1 (= *B. ziegleri*; cf. Ziegler, Sandberg & Austin, 1974, p. 103) was not considered. The oldest *Kalloclymenia* (Bed 20.4) is from above the oldest bispathodids of the *ultimus* Group, which require further study, and from below the first *Pa. gracilis gonioclymeniae* (Bed 21.3, cf. Kononova & Weyer, 2014).

4.c. *Siphonodella praesulcata* Zone

Definition. Lower boundary: Entry of *S. (Eo.) praesulcata* s.l. (see Tragelehn, 2010). Upper boundary: Extinction of *B. costatus* (base of the *costatus–kockeli* Interregnum).

Other markers. None.

Discussion. The regional knowledge of this zone is based on Kaiser (2005). Based on the restricted number of samples, the regional spectrum of species is not yet fully established. This leads to a wrong picture of strongly reduced regional palaeodiversity (Fig. 17). Various taxa that are currently shown to end with the *B. ultimus ultimus* Zone may have to be added to the faunal list with further sampling. The records of *Pa. gracilis gonioclymeniae* in Alberti (1970), which have not been repeated by Kaiser (2005), can be taken as an example. On the other hand, the zonal index species is rare and partly lacking, for example in a fauna from

https://doi.org/10.1017/S0016756816000893 Published online by Cambridge University Press

Parawo. paradoxa nodules of El Atrous (UD VI-C2; Kaiser, 2005; Kaiser *et al.* 2013).

Since the *Wocklumeria* Zone (UD VI-D) is missing all over the Tafilalt (Kaiser *et al*. 2011), it is not possible to document regional effects of the Hangenberg Mass Extinction on conodonts, as discussed in Kaiser *et al*. (2009) and Kaiser, Aretz & Becker (2015). The associated long-lasting carbonate crisis (e.g. Becker *et al.* 2013*a*) led to the effect that only three uppermost Famennian conodont taxa reappear in the Lower Tournaisian of the Tafilalt (Kaiser, 2005): *M. strigosa*, *Neo. communis communis* and *B. aculeatus aculeatus*. The Lalla Mimouna conodont record of the northern Maider (Belka in Korn *et al*. 2004; Becker *et al*. 2013*c*) shows that there were more survivors or re-immigrants in the eastern Anti-Atlas.

Associated taxa. *Bispathodus bispathodus*, *B. jugosus*, *B. stabilis stabilis* (= *stabilis* Morphotype 2), *B. aculeatus aculeatus*, *B. aculeatus anteposicornis*, *B. costatus* (both morphotypes), *B. ultimus ultimus* (both morphotypes), *B. spinulicostatus*, *Br. inornata*, *Br. suprema*, *M. strigosa*, *Neo. communis communis*, *Pa. gracilis gracilis*, *Pa. gracilis sigmoidalis* and *Pa. gracilis expansa* occur. An icriodid from the last limestone at Ouidane Chebbi (Kaiser, 2005), a very rare genus in the pelagic uppermost Famennian, was not identified at the species level.

Conodont–ammonoid correlation. In the Tafilalt, there is currently no correlation of the base of the *S. (Eo.) praesulcata* Zone with the ammonoid zonation. The so far studied sections of Ouidane Chebbi and M'karig are rather poor in uppermost Famennian macrofauna. The Jebel Erfoud offers the best potential (Alberti, 1970). In the Rhenish Massif *S. (Eo.) praesulcata* (s.l.) enters above the oldest *Muess. bisulcata* (basal UD VI-A_2) and below the entry of *Effenbergia* (basal UD VI-B; Clausen *et al*. 1989: Muessenberg; Kürschner *et al*. 1993 and Becker, 1996: Hasselbachtal; Schindewolf, 1937 and Kürschner *et al*. 1993: Oberrödinghausen; Becker *et al.* 1993 and H. Nowak, unpub. B.Sc. thesis, Westfälische Wilhelms-Universität, 2008: Oese). There is complete agreement with data from the Carnic Alps (Kaiser *et al*. 2009: sections Großer Pal and Casera Malpasso).

5. Implications for the regional and international ammonoid zonation (Fig. 17)

The loose slabs and the new Jebel Ihrs West section give a clear age difference between *Gonioclymenia* (*B. costatus* Subzone) and *Kalloclymenia* (*B. ultimus ultimus* Zone with early *S. (Eosiphonodella)*) limestones. This is supported by the only other previous conodont dating of a Moroccan *Kalloclymenia* from M'karig (Kaiser, 2005: Bed 18; Fig. 14e, f). The record of *B. ziegleri* (= *B. ultimus ultimus* Morphotype 1) from the *Gonioclymenia* Limestone of Oum el Jerane by Ginter, Hairapetian & Klug (2002) is at odds with this distinction. Possibly, it can be explained by the inclusion of thin units encrusted on top of the true *Gonioclymenia* Limestone during the original sampling. Such units occur along strike in the Amessoui Syncline at El Atrous; there, they also contain many shark teeth and *B. ultimus ultimus*, but also Wocklumian (UD VI) ammonoids and trilobites (Kaiser, 2005; Kaiser *et al*. 2013).

The middle Dasbergian of the Tafilalt (UD V-B) is characterized by the onset of the spinose, relatively small-sized *Gonio. hoevelensis* (see Becker *et al*. 2002: pl. 6, figs 1–2; Bogoslovskiy, 1981: pl. 8, fig. 1a–b). In order to stabilize this important marker species, a lectotype is fixed below (Fig. 14a, b, see taxonomic notes). *Muessenbiaergia diversa* and *Post. camerata* can serve as alternative regional markers. As discussed in Becker *et al.* (2002), *Gonio. hoevelensis* enters in the Russian section Kiya-1 (Simakov *et al.* 1983; Nikolaeva & Bogoslovskiy, 2005) together with *Ornatoclymenia*, the marker of UD V-B in the Rhenish Massif (Korn, 1981). *Gonioclymenia speciosa* enters at Ouidane Chebbi Northwest just slightly later than *Muess. diversa* (Hartenfels & Becker, 2009; Hartenfels, 2011) and one nodule layer above the first *Gonio. hoevelensis* at the Ouidane Chebbi section of Kaiser (2005) and Kaiser *et al.* (2011). At Bou Tchrafine, *Gonio. hoevelensis*, *Gonio. speciosa*, *Post. camerata* and *Muess. diversa* occur jointly in the loose assemblage of 'Bed Za' (Becker & House, 2000). Similar faunas are known from much thicker nodular limestone units of the Maider (Becker *et al.* 2000).

In the Maider sections, *Gonioclymenia* disappears gradually in the upper part of the Dasbergian (UD V), well before the onset of *Kalloclymenia* and/or *Linguaclymenia*, the index clymeniids of the basal Wocklumian (UD VI-A_1, section Lambidia 1, Kaiser, 2005). This interval (beds 10c–11a) is characterized by the distinctive *Medio. aguelmousensis*, which occurs widely along the Aguelmous Syncline. In the Tafilalt it occurs in the same interval above *Gonioclymenia* at Ouidane Chebbi (Becker in Kaiser, 2005: '*Spheno. intermedia*' of Bed 10b), Hamar Laghdad East (Becker *et al*. 2000: '*Spheno. brevispina*' from the top of Bed X), Jebel Erfoud (Becker & House, 2000: 'relative of *Gonio. kiense*' from 'Bed Zb') and El Khraouia (Hartenfels *et al*. 2013). Consequently, Becker, El Hassani & Tahiri (2013) noted in their new stratigraphical chart for the Tafilalt a new *Medio. aguelmousensis* Zone (UD V-C). The different previous identications of the index species (see also the record as '*Sphenoclymenia* sp.' in Korn, 1999) stem from the time before *Medio. aguelmousensis* was established and separated from the closely related *Medio. intermedia* (Korn & Klug, 2002). Also, it was not known then that juveniles may have ventral groves and spines as in *Levi. kiensis* and *Spheno. brevispina*. The correlation of the Moroccan *Medio. aguelmousensis* Zone with the Rhenish *Piriclymenia piriformis* Zone (Korn, 1981; UD V-C) is currently tentative. But the recent discovery of very close relatives of *Medio. aguelmousensis* at Effenberg (Hartenfels & Becker, 2016), where the *Piriclymenia piriformis* level

https://doi.org/10.1017/S0016756816000893 Published online by Cambridge University Press

was noted by Korn & Luppold (1987), gives prospects for a future refined correlation. Based on the presence of *Medio. intermedia*, the Anti-Atlas *Mediocly*menia Zone can be correlated into the topmost Dasbergian of Thuringia (Bartzsch & Weyer, 2012: beds 18.2–20.1), where supposed last gonioclymeniids are associated (see discussion below). Unlike as in the Anti-Atlas, *Mediocly*menia is claimed to range into levels with the oldest *Kalloclymenia*.

Our new data reject an overlap of *Gonioclymenia* and *Kalloclymenia* in the Anti-Atlas as suggested by Becker *et al.* (2002), who emphasized that this was not found in the thicker, more complete basinal successions of the Maider. This refutes the idea that the regional *Kallo. subarmata* Zone falls in the top of the Dasbergian (UD V-C). *Kalloclymenia* can be re-installed as a widespread index genus for the base of the Wocklumian (UD VI), as proposed in the classical monograph on the German Wocklum Beds by Schindewolf (1937). At least *Kallo. subarmata* regains its old stratigraphical significance. The alleged overlap of *Kallo. bimpressa* (correctly = *Kallo. insignis*) and *Clymenia* in the Lower Petherwin Beds of Cornwall (Selwood, 1960) is based on faunas from the Gatepost Quarry and Oldwitt Farm. However, the *Cly. hoevelensis* record of both localities is not based on any modern description or illustration. Furthermore, the unit comprises more than one level/zone. Stewart (1981) found no conodonts in the calcareous sandstones of Gatepost Quarry but showed that the Cephalopod Limestone Member (= Lower Petherwin Beds) covers in general a long interval, up to the Middle *costatus* Zone (= *B. ultimus ultimus* to *S. (Eo.) praesulcata* zones, UD VI). Accordingly, Price & Korn (1989) noted that matrix from the holotype of *Kallo. insignis* yielded conodonts of the Middle *costatus* Zone (probably from the *B. ultimus ultimus* Zone).

The co-occurrence of *Gonio. corpulenta* and *Kallo. subarmata* in the Kiya-1 section of the southern Urals is also problematical. The section is condensed and *Gonio. corpulenta* was based on a single, large specimen (Bogoslovskiy, 1981). Nikolaeva (2007) and Gibshman & Nikolaeva (2011) commented on the rather provisional correlation of the regional *frechi-corpulenta* Zone, possibly partly with the *Piriclymenia piriformis* Zone and partly with the lower part of the '*Kalloclymenia-Wocklumeria* Genozone' (= UD VI). Simakov *et al.* (1983) showed the entry of two marker conodonts of the *B. ultimus ultimus* Zone, *Pa. gracilis gonioclymeniae* and *Ps. marburgensis trigonicus*, between *Ornatoclymenia* and *Kallo. frechi*, below the *subarmata–corpulenta* level. The Kiya record, therefore, is no evidence for *Kalloclymenia* ranging into the Dasbergian (UD V) but evidence of a possible last gonioclymeniid in the lower Famennian VI (Wocklumian). However, a critical look at the holotype of *Gonio. corpulenta* shows that it is not a typical *Gonioclymenia* at all. Median whorls have no ventral furrow and the presence of a shallow ventral depression on the last whorl is obscured by weathering and not convincingly documented. The wide, bell-shaped subumbilical lobe differs from all other members of the Gonioclymeniidae. The morphologically isolated species is better placed in the lower Wocklumian giant *'Kallo.' pachydiscus* Group, which requires a new generic name, and which occurs in Russia and the Rhenish Massif (Becker, 1988: UD VI-A_1; Hartenfels & Becker, 2016).

Price & Korn (1989) discussed the possible occurrences of two other *Kalloclymenia* species in Dasbergian (UD V) beds of the Rhenish Massif. The strongly spinose, early Dasbergian (UD V-A) *Kallo. crassa* does not possess the lanceolate adventitious lobe of the genus, has an unusually deep and narrow external lobe and, therefore, belongs to a different (new) genus. In the original description by Wedekind (1914) similarities with *Sellaclymenia torleyi* were emphasized. It has been generally overlooked that, despite its name, the type-specimen of *Kallo. dasbergensis* is not from the Dasberg of the Rhenish Massif, but from Dzikowiec (Ebersdorf), Silesia, where the pelagic ammonoid succession falls entirely in the lower/middle Wocklumian (Schindewolf, 1937; UD VI-A to C). The species was not only omitted from the faunal list in Schindewolf, but also in later accounts of the Dzikowiec fauna (Lewowicki, 1959; Dzik, 2006). Due to the lack of descriptions or illustrations, there is no evidence that the stratigraphically older Dasberg fragments mentioned by Wedekind (1914) belong to the same species. The *dasbergensis* holotype has higher whorls than in typical *Kalloclymenia*, with a whorl expansion rate of *c.* 2.1, and possibly *Gonioclymenia*-type adventitious flank lobes (Wedekind, 1914: pl. 5, fig. 6b). Therefore, it may be related to the *'Kallo.' pachydisca* Group. Because of similarities of its shell form with *Mediocly*menia, it is possible that Wedekind's Dasberg fragments belonged to that genus.

In summary, the occurrence of typical *Kalloclymenia* in beds with *Gonioclymenia* or *Clymenia* (Dasbergian, UD V) is not proven by any record. There is also no unequivocal range overlap in the lower Wocklumian (UD VI-A_1). Kononova & Weyer (2014) showed *Gonioclymenia* to range in Thuringia into the first beds with *B. ultimus ultimus* below the entry of *Kalloclymenia*. However, neither the last Thuringian gonioclymeniids nor the supposed first *B. ultimus ultimus* have been illustrated. This leaves doubts concerning their taxonomy, especially since *B. spinulicostatus* has not been separated from *B. ultimus*. Further research by D. Weyer is under way in order to solve the question.

6. Regional correlation of the *Gonioclymenia* Limestone (Fig. 10)

The trans-regressive couplet of the *Gonioclymenia* Limestone is recognizable in the higher Dasbergian of lateral, less condensed settings. At Bou Tchrafine (Becker & House, 2000), the lower part of the *Gonio. hoevelensis* Zone (Bed Za, UD V-B) is characterized by

https://doi.org/10.1017/S0016756816000893 Published online by Cambridge University Press

a change from solid limestone to marls with limestone nodules, indicating a slight deepening trend. Towards the east, at the eastern end of Hamar Laghdad (Becker *et al.* 2002), the same deepening phase is recorded above a solid *Cymaclymenia* limestone (UD V-A_1) by Bed X. Beyond, at Ouidane Chebbi Northwest (Hartenfels & Becker, 2009; Hartenfels, 2011), the *Gonio. hoevelensis* Zone commences during a short deepening episode, characterized by the deposition of a marl unit with limestone nodules, which is overlain by a regressive, solid limestone with *Gonio. speciosa* and others. Further east, in the Ouidane Chebbi sections of Belka *et al.* (1999), Kaiser (2005) and Kaiser *et al.* (2011), nodule levels with *Gonio. speciosa* are lithologically not distinct from under- and overlying beds. The same applies to the Jebel Erfoud sequence (Fig. 10, section log of Korn, 1999).

In the northern Tafilalt, the last recorded Famennian limestones fall in the *Gonio. subcarinata* Zone (UD V-A_2), despite a generally more basinal setting (Rheris Basin; Becker, 1993). The same is true for the Mfis and Hassi Nebech areas of the Tafilalt Basin to the south (Hartenfels, 2011; Kaiser *et al.* 2011). At Tazoult Nehra, there is obviously a gap between lower Dasbergian beds and shales with a goethitic fauna of the lower Wocklumian (UD VI-A/B), including *Kalloclymenia* and *Effenbergia* (T. Fischer, unpub. B.Sc. thesis, Westfälische Wilhelms-Universität, 2010). Further east, at Erg Kseir, Wocklumian shales continue with sideritic ammonoid preservation but, again, *Gonio. speciosa* or other species of the *Gonio. hoevelensis* Zone have not been found. On the western slope of the Tafilalt Basin, at El Khraouia (NE Amessoui Syncline), the upper/uppermost Famennian consists of poorly exposed marls/shales without a gap at the UD V/VI transition. This assumption is based on loose specimens of *Gonioclymenia* sp. and *Medio. aguelmousensis*, followed by a single *Muess. bisulcata* of UD VI-B.

In the Bou Maiz Syncline, at Ottara East, the *Gonio. subcarinata* Zone (UD V-A_2) consists of solid, iron-rich, reddish nodular limestone. *Postclymenia camerata*, one of the UD V-B markers, was found in overlying poorly fossiliferous red marl, which represents a deepening interval (see regional facies model of Hartenfels, 2011). *Gonioclymenia speciosa* enters in larger red limestone nodules right above. It is very difficult to trace the *Gonioclymenia* Transgression into the Maider Basin (Aguelmous Syncline), where *Gonio. speciosa* appears to be very rare or absent. The thick successions of shales with goethitic or calcareous faunas do not easily record sea-level changes.

The *Medio. aguelmousensis* Zone (UD V-C) is missing above the *Gonioclymenia* Limestone in the most condensed platform sections, such as Jebel Ihrs and all over the Amessoui Syncline in the southern Tafilalt. Therefore, the *Kalloclymenia* Limestone records a minor basal Wocklumian re-onset of sedimentation due to deepening. It is not recognizable in the rather uniform nodular limestones of Jebel Erfoud and the eastern Tafilalt (Ouidane Chebbi Northwest to M'Karig). In the Bou Maiz Syncline (Ottara) the Wocklumian may be represented by poorly exposed red shales with some cymaclymeniids. As noted above, a deepening trend is recorded by the onset of hypoxic, goniatite-rich shales of UD VI-A/B (T. Fischer, unpub. B.Sc. thesis, Westfälische Wilhelms-Universität, 2010) at Tazoult Nehra in the SE Tafilalt (Tafilalt Basin). In the northern Maider, crinoidal limestones of the *B. ultimus ultimus* Zone transgressed over an Ordovician seamount (Lalla Minouna; Becker *et al*. 2013*c*).

7. Eustatic aspects

Hartenfels & Becker (2009) and Hartenfels (2011) discussed upper/uppermost Famennian eustatic changes that were not recorded in previous global sea-level curves. They recognized the two transgressive Dasberg Event phases at the top of the *B. stabilis stabilis* (= top Lower *expansa*) Zone and at the base of the *B. aculeatus aculeatus* (= base Middle *expansa*) Zone. They justified the onset of Depophase IIf1 in the revised sea-level chart of Becker, Aboussalam & Hartenfels (2012). The Epinette Event on the Ardennes Shelf (Dreesen, Paproth & Thorez 1989) marks the initial phase of the 'Strunian Transgression' and the end of the Condroz Sandstone sedimentation (base of Depophase IIf2 in Becker, Aboussalam & Hartenfels, 2012). Originally, it was linked with the base of the Wocklumian ('Wocklum Event'), but it occurred earlier, still within the *B. aculeatus aculeatus* Zone. It is marked by the appearance of the globally distributed marker spore *Retispora lepidophyta lepidophyta* (e.g. Streel, 2009). A better correlation of the *Gonioclymenia* Transgression with the Epinette Event requires palynological data for the base of UD V-B, which are not yet at hand. As noted by Hartenfels & Becker (2009), *expansa* Zone transgressions of other regions are not dated with the necessary precision for reliable correlations. In general, there is some evidence for a eustatic deepening pulse higher in the *B. aculeatus aculeatus* Zone (*B. costatus* Subzone). The transgressive phase of the lower Wocklumian (UD VI-A) can be correlated with the main Strunian Transgression, which is a part of the eustatic Depophase IIf *sensu* Johnson, Klapper & Sandberg (1985) and the peak of transgression within Depophase IIf2 *sensu* Becker, Aboussalam & Hartenfels (2012).

8. Systematic palaeontology

8.a. Conodonts

8.a.1. Authorships and records

Bispathodus aculeatus aculeatus (Branson & Mehl, 1934*a*), Figure 18k–r; 470 specimens from Jebel Ihrs

https://doi.org/10.1017/S0016756816000893 Published online by Cambridge University Press

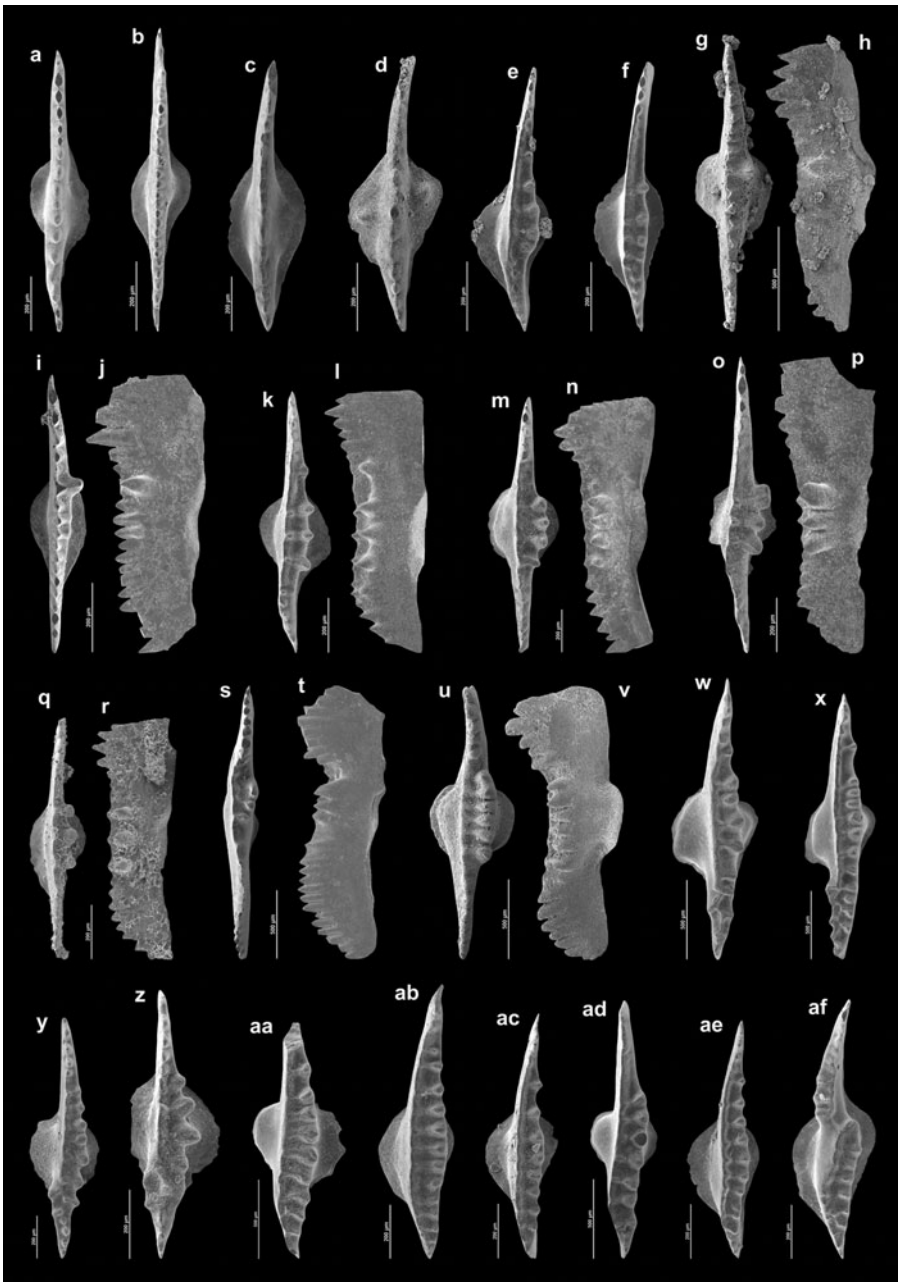

Figure 18. Bispathodids from the upper/uppermost Famennian of the Tafilalt. (a, b) *Bispathodus stabilis vulgaris* (Dzik, 2006), GMM B9A.4-1 (a, Jebel Ihrs West, Bed 2, lower *B. costatus* Subzone) and GMM B9A.4-2 (b, Jebel Ihrs West, loose slab with *Kalloclymenia* sp., *B. ultimus ultimus* Zone); (c) *Bispathodus stabilis stabilis* (Branson & Mehl, 1934*a*), GMM B9A.4-3, Jebel Ihrs West, Bed 2, lower *B. costatus* Subzone; (d) *Bispathodus stabilis bituberculatus* (Dzik, 2006), GMM B9A.4-4, Jebel Ihrs West, loose slab with *Gonio. subcarinata*, *B. costatus* Subzone; (e, f) *Bispathodus bispathodus* Ziegler, Sandberg & Austin, 1974, GMM B9A.4-5 (e, Jebel Ihrs West, loose slab with *Kalloclymenia* sp., *B. ultimus ultimus* Zone) and GMM B9A.4-6 (f, Jebel Ihrs West, Bed 5b, *B. ultimus ultimus* Zone); (g–j) *Bispathodus aculeatus anteposicornis* (Scott, 1961), GMM B9A.4-7 (g, h, Jebel Ihrs West, Bed 3, upper *B. costatus* Subzone) and GMM B9A.4-8 (i, j, Jebel Ihrs West, Bed 2, lower *B. costatus* Subzone, intermediate specimen between *B. aculeatus anteposicornis* and *B. aculeatus aculeatus*); (k–r) *Bispathodus aculeatus aculeatus* (Branson & Mehl, 1934*a*), GMM B9A.4-9 (k, l, Jebel Ihrs West, loose slab with *Kalloclymenia* sp., *B. ultimus ultimus* Zone), GMM B9A.4-10 (m, n, Jebel Ihrs West, loose slab with *Kallo. subarmata*, *B. ultimus ultimus* Zone), GMM B9A.4-11 (o, p, Takhbtit West, Bed 5, *B. costatus* Subzone), and GMM B9A.4-12 (q, r, Jebel Ouaoufilal, Bed 21b, *B. costatus* Subzone); (s–v) *Bispathodus aculeatus* aff. *aculeatus* (Branson & Mehl, 1934*a*), GMM B9A.4-13 (s, t) and GMM B9A.4-14 (u, v, both Jebel Ihrs West, Bed 3, upper *B. costatus* Subzone); (w–y) *Bispathodus spinulicostatus* (Branson, 1934) Morphotype 1, GMM B9A.4-15 (w) and GMM B9A.4-16 (x, both Jebel Ihrs West, loose slab with *Kalloclymenia* sp., *B. ultimus ultimus* Zone) and GMM B9A.4-17 (y, Jebel Ihrs West, loose slab with *Kallo. subarmata*, *B. ultimus ultimus* Zone); (z) *Bispathodus spinulicostatus* (Branson, 1934) Morphotype 2, GMM B9A.4-18, Jebel Ihrs West, Bed 2, lower *B. costatus* Subzone; (aa–ad) *Bispathodus costatus* (Branson, 1934) Morphotype 2, GMM B9A.4-19 (aa, Jebel Ihrs West, Bed 3, upper *B. costatus* Subzone), GMM B9A.4-20 (ab, Jebel Ihrs West, loose slab with *Kalloclymenia* sp., *B. ultimus ultimus* Zone), GMM B9A.4-21 (ac, Jebel Ihrs West, Bed 4b, *B. ultimus ultimus* Zone), and GMM B9A.4-22, Jebel Ihrs West, loose slab with *Kallo. subarmata*, *B. ultimus ultimus* Zone); (ae, af) *Bispathodus costatus* (Branson, 1934) Morphotype 1, GMM B9A.4-23 (ae) and GMM B9A.4-24 (af, both Jebel Ihrs West, loose slab with *Kalloclymenia* sp., *B. ultimus ultimus* Zone).

https://doi.org/10.1017/S0016756816000893 Published online by Cambridge University Press

West, Jebel Kfiroun South, Jebel Ouaoufilal, Oum el Jerane, Seheb el Rhassal and Takhbtit West.

Bispathodus bispathodus Ziegler, Sandberg & Austin, 1974, Figure 18e, f; ten specimens from Jebel Ihrs West.

Bispathodus costatus (Branson, 1934) Morphotype 2 (= typical morphotype *sensu* Ziegler, Sandberg & Austin, 1974), Figure 18aa–ad; 335 specimens from Jebel Ihrs West, Jebel Kfiroun South and Oum el Jerane.

Bispathodus stabilis stabilis (Branson & Mehl, 1934*a*), Figure 18c; 47 specimens from Hamar Laghdad, Jebel Ihrs West, Oum el Jerane and Seheb el Rhassal.

Bispathodus stabilis bituberculatus (Dzik, 2006), Figure 18d; two specimens from Jebel Ihrs West.

Bispathodus stabilis vulgaris (Dzik, 2006), Figure 18a, b; 232 specimens from Jebel Ihrs West, Jebel Kfiroun South, Oum el Jerane and Seheb el Rhassal.

Branmehla fissilis (Branson & Mehl, 1934*a*), Figure 19y–aa; 21 specimens from Jebel Ihrs West and Oum el Jerane.

Mehlina strigosa (Branson & Mehl, 1934*a*), Figure 19ab–ac; 87 specimens from Jebel Ihrs West, Jebel Kfiroun South, Oum el Jerane, Seheb el Rhassal and Takhbtit West.

Neopolygnathus communis communis (Branson & Mehl, 1934*b*), Figure 19p–r; 413 specimens from Jebel Ihrs West, Jebel Kfiroun South, Oum el Jerane, Seheb el Rhassal and Takhbtit West.

Palmatolepis gracilis gracilis Branson & Mehl, 1934*a*, Figure 19h–j; 876 specimens from Jebel Ihrs West, Jebel Kfiroun South, Ouidane Chebbi Northwest, Oum el Jerane, Seheb el Rhassal and Takhbtit West.

Palmatolepis gracilis expansa Sandberg & Ziegler, 1979 Morphotype 1 (= typical morphotype *sensu* Hartenfels, 2011), Figure 19k, l; 26 specimens from Jebel Ihrs West.

Palmatolepis gracilis sigmoidalis Ziegler, 1962; one specimen from Jebel Ihrs West.

Palmatolepis perlobata helmsi Ziegler, 1962, Figure 19m, n; one specimen from Jebel Ihrs West.

Palmatolepis perlobata schindewolfi Müller, 1956, Figure 19o; five specimens from Jebel Ihrs West and Oum el Jerane.

Polygnathus delicatulus Ulrich & Bassler, 1926, Figure 19v; 18 specimens from Jebel Ihrs West, Jebel Kfiroun South and Oum el Jerane.

Polygnathus semicostatus Branson & Mehl, 1934*a* (central morphotype *sensu* Dreesen & Orchard, 1974); one specimen from Jebel Kfiroun South.

Pseudopolygnathus controversus Sandberg & Ziegler, 1979 Morphotype 2 (*sensu* Sandberg & Ziegler, 1979), Figure 20aa; one specimen from Jebel Ihrs West.

N. Gen. 1 div. sp., Figure 21i–n; eight specimens from Jebel Ihrs West.
N. Gen. 2 div. sp., Figure 21o–z; 21 specimens from Jebel Ihrs West.
aff. N. Gen. 2 sp., Figure 21aa–ab; one specimen from Jebel Ihrs West.

Siphonodella (*Eosiphonodella*) sp. nov. B. (*sensu* Becker *et al.* 2013*c*), Figure 21ac–ad; four specimens from Jebel Ihrs West.

8.a.2. Descriptions and taxonomic notes

Bispathodus aculeatus aff. *aculeatus* (Branson & Mehl, 1934a)

Figure 18s–v

Material. Four specimens from Jebel Ihrs West and Oum el Jerane.

Description. In oral view, this form is elongate, nearly straight, or only slightly bowed laterally. Two or more (up to six) fused side denticles are developed on the right side of the blade in a central position more or less above the basal cavity and not extending to the posterior tip of the blade. The side denticles form a discrete platform-like bulk rather than splitting off from the main blade denticles. The latter are distinctively fused in the range of the basal cavity. Posterior, the denticles stand in close contact and show rounded cusps. Ideally, they are spiky and triangular. Anteriorly, the transition from the carina to the free blade is slightly discontinuous. The high free blade is an extension of the carina; in lateral view, it shows a tendency towards *Clydagnathus*. The denticles increase successively and reach the highest point just before the anterior margin. The oral profile posterior to the basal cavity is gently convex. The aboral outline is conspicuously straight, but slightly arched downwards behind the basal cavity. The latter is relatively small, symmetrical, and restricted to the central part. Aborally, a small median groove extends from the anterior to the posterior end.

Discussion. In typical *B. aculeatus aculeatus*, the lateral denticles are connected by transverse ridges with the carina and stand more or less isolated from each other. Ziegler, Sandberg & Austin (1974) pointed out that in some specimens the side denticles split off from the main blade. According to Ziegler, Sandberg & Austin (1974: pl. 2, fig. 1), the re-illustrated lectotype of *B. aculeatus aculeatus*, selected by Ziegler (1962), shows a tendency towards *B. aculeatus plumulus* (= *Clyd. plumulus*) in the development of a high anterior free blade. This is also true for *B. aculeatus* aff. *aculeatus*. However, the typical plume-like *Clydagnathus* blade (Rhodes, Austin & Druce, 1969), with denticles which are highest in the posterior part and markedly recurved backwards, are not developed. In *Clyd. plumulus*, the free blade does not continue the platform carina. *Bispathodus aculeatus* aff. *aculeatus* is distinguished from

https://doi.org/10.1017/S0016756816000893 Published online by Cambridge University Press

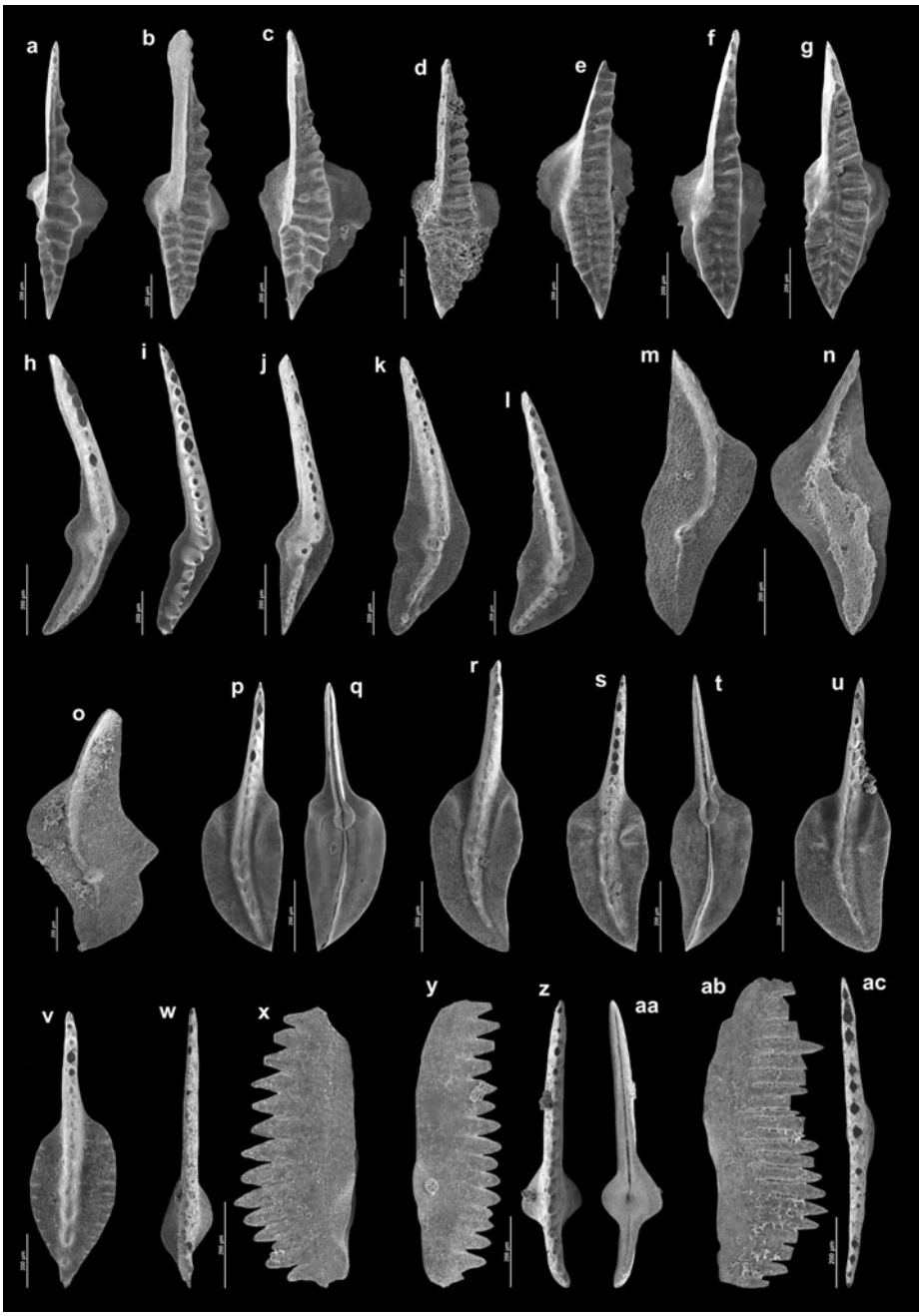

Figure 19. Various upper/uppermost Famennian conodonts of the Tafilalt. (a, b) *Bispathodus ultimus ultimus* (Bischoff, 1957), GMM B9A.4-25 (a, Jebel Ihrs West, Bed 5b, *B. ultimus ultimus* Zone, slightly transitional specimen from *B. spinulicostatus* Morphotype 1) and GMM B9A.4-26 (b, Jebel Ihrs West, loose slab with *Kalloclymenia* sp., *B. ultimus ultimus* Zone); (c–g) *Bispathodus ultimus ultimus* (Bischoff, 1957) Morphotype 1, GMM B9A.4-27 (c) and GMM B9A.4-28 (d, both Jebel Ihrs West, loose slab with *Kalloclymenia* sp., *B. ultimus ultimus* Zone) and GMM B9A.4-29 (e), GMM B9A.4-30 (f) and GMM B9A.4-31 (g, all Jebel Ihrs West, loose slab with *Kallo. subarmata*, *B. ultimus ultimus* Zone); (h, j) *Palmatolepis gracilis gracilis* Branson & Mehl, 1934*a*, GMM B9A.4-32 (h, Takhbtit West, Bed 5, *B. costatus* Subzone), GMM B9A.4-33 (i, Jebel Ihrs West, Bed 2, lower *B. costatus* Subzone), and GMM B9A.4-34 (j, Jebel Ihrs West, loose slab with *Gonio. subcarinata*, *B. costatus* Subzone); (k, l) *Palmatolepis gracilis expansa* Sandberg & Ziegler, 1979 Morphotype 1, GMM B9A.4-35 (k, Jebel Ihrs West, Bed 2, lower *B. costatus* Subzone) and GMM B9A.4-36 (l, Jebel Ihrs West, loose slab with *Gonio. subcarinata*, *B. costatus* Subzone); (m, n) *Palmatolepis perlobata helmsi* Ziegler, 1962, GMM B9A.4-37, Jebel Ihrs West, loose slab with *Gonio. subcarinata*, *B. costatus* Subzone); (o) *Palmatolepis perlobata schindewolfi* Müller, 1956, GMM B9A.4-38, Jebel Ihrs West, Bed 2, lower *B. costatus* Subzone); (p–r) *Neopolygnathus communis communis* (Branson & Mehl, 1934*b*), GMM B9A.4-39 (p, q, Jebel Ihrs West, Bed 2, lower *B. costatus* Subzone) and GMM B9A.4-40 (r, Jebel Ihrs West, Bed 3, upper *B. costatus* Subzone); (s–u) *Neopolygnathus fibula* sp. nov., holotype GMM B9A.4-41 (s, t, Jebel Ihrs West, loose slab with *Kallo. subarmata*, *B. ultimus ultimus* Zone) and paratype GMM B9A.4-42 (u, Jebel Ihrs West, Bed 2, lower *B. costatus* Subzone); (v) *Polygnathus delicatulus* Ulrich & Bassler, 1926, GMM B9A.4-43, Jebel Ihrs West, loose slab with *Gonio. subcarinata*, *B. costatus* Subzone; (w, x) *Branmehla inornata* (Branson & Mehl, 1934*a*), GMM B9A.4-44, Jebel Ihrs West, loose slab with *Kalloclymenia* sp., *B. ultimus ultimus* Zone); (y–aa) *Branmehla fissilis* (Branson & Mehl, 1934*a*), GMM B9A.4-45, Jebel Ihrs West, loose slab with *Gonio. subcarinata*, *B. costatus* Subzone; (ab, ac) *Mehlina strigosa* (Branson & Mehl, 1934*a*), GMM B9A.4-46, Takhbtit West, Bed 5, *B. costatus* Subzone.

https://doi.org/10.1017/S0016756816000893 Published online by Cambridge University Press

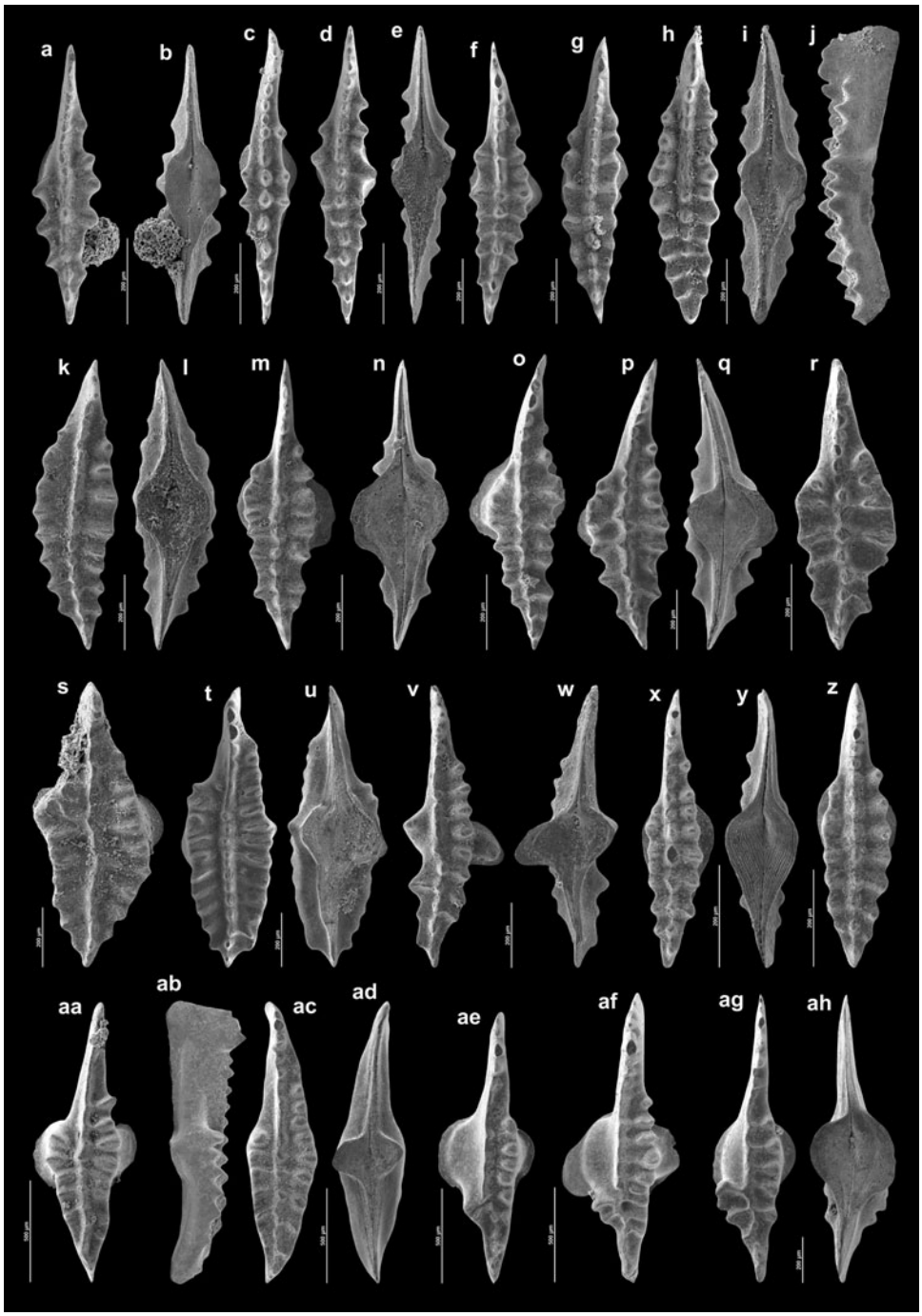

Figure 20. *Pseudopolygnathus* and *Bispathodus* from the upper/uppermost Famennian of the Tafilalt. (a–l) *Pseudopolygnathus primus tafilensis* ssp. nov., paratypes GMM B9A.4-47 (a, b), GMM B9A.4-50 (f), and GMM B9A.4-53 (k, l, all Jebel Ihrs West, Bed 2, lower *B. costatus* Subzone), paratypes GMM B9A.4-48 (c), GMM B9A.4-49 (d, e), GMM B9A.4-51 (g) and holotype GMM B9A.4-52 (h–j, all Jebel Ihrs West, Bed 3, upper *B. costatus* Subzone); (m–u) *Pseudopolygnathus primus primus* Branson & Mehl, 1934*b* Morphotype 3, GMM B9A.4-54 (m, n), GMM B9A.4-55 (o) and GMM B9A.4-58 (s, all Jebel Ihrs West, Bed 3, upper *B. costatus* Subzone), GMM B9A.4-56 (p, q) and GMM B9A.4-57 (r, both Jebel Ihrs West, Bed 2, lower *B. costatus* Subzone) and GMM B9A.4-59 (t, u, Jebel Ihrs West, loose slab with *Gonio. subcarinata*, *B. costatus* Subzone); (v, w) *?Bispathodus* aff. *spinulicostatus* (Branson, 1934), GMM B9A.4-60, Jebel Ihrs West, Bed 3, upper *B. costatus* Subzone; (x–z) *Psedopolygnathus primus* aff. *tafilensis* ssp. nov., GMM B9A.4-61 (x, y, Jebel Ihrs West, Bed 2, lower *B. costatus* Subzone) and GMM B9A.4-62 (z, Jebel Ihrs West, Bed 3, upper *B. costatus* Subzone); (aa) *Pseudopolygnathus controversus* Sandberg & Ziegler, 1979 Morphotype 2, GMM B9A.4-63, Jebel Ihrs West, loose slab with *Kallo. subarmata*, *B. ultimus ultimus* Zone; (ab–ad) *Pseudopolygnathus primus* aff. *primus* Branson & Mehl, 1934b, GMM B9A.4-64, Jebel Ihrs West, loose slab with *Kallo. subarmata*, *B. ultimus ultimus* Zone; (ae–ah) *Bispathodus spinulicostatus* (Branson, 1934) Morphotype 3, GMM B9A.4-65 (ae), GMM B9A.4-66 (af) and GMM B9A.4-67 (ag, ah, all Jebel Ihrs West, loose slab with *Kallo. subarmata*, *B. ultimus ultimus* Zone).

https://doi.org/10.1017/S0016756816000893 Published online by Cambridge University Press

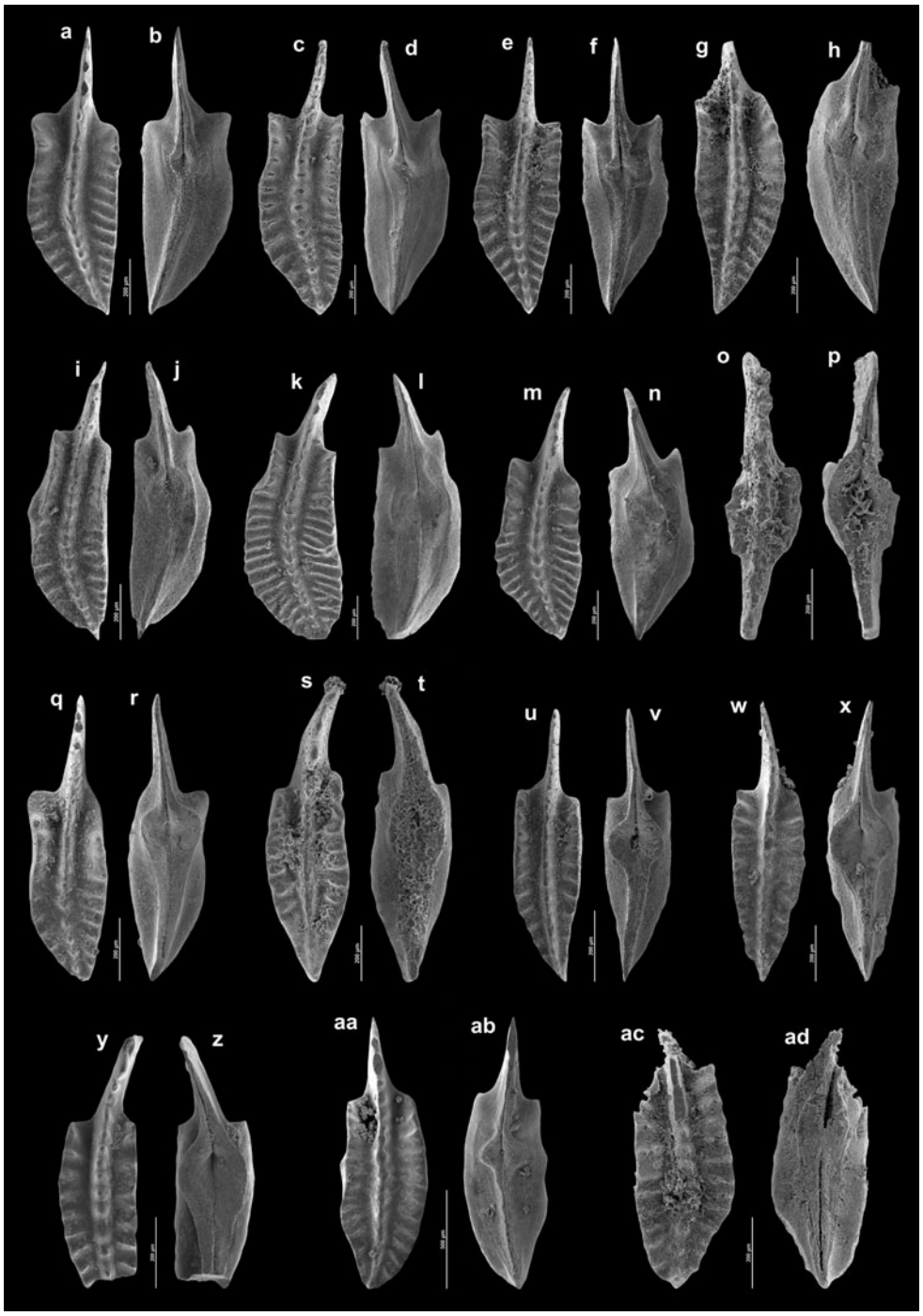

Figure 21. 'Siphonodelloids', early *S. (Eosiphonodella)* and transitional forms from *'Polygnathus'* from the *B. ultimus ultimus* Zone at Jebel Ihrs West. (a–h) '*Polygnathus*' sp. transitional to N. Gen. 1 *sensu* Becker *et al.* 2013*c*, GMM B9A.4-68 (a, b), GMM B9A.4-69 (c, d) and GMM B9A.4-70 (e, f, all loose slab with *Kalloclymenia* sp.) and GMM B9A.4-71 (g, h, loose slab with *Kallo. subarmata*); (i–n) N. Gen. 1 sp., GMM B9A.4-72 (i, j), GMM B9A.4-73 (k, l), and GMM B9A.4-74 (m, n, all loose slab with *Kalloclymenia* sp.); (o–z) N. Gen. 2 sp., GMM B9A.4-75 (o, p, Bed 4b), GMM B9A.4-76 (q, r) and GMM B9A.4-79 (w, x, both loose slab with *Kallo. subarmata*), GMM B9A.4-77 (s, t) and GMM B9A.4-80 (y, z, both Bed 5b) and GMM B9A.4-78 (u, v, loose slab with *Kalloclymenia* sp.); (aa, ab) aff. N. Gen. 2 sp., GMM B9A.4-81, loose slab with *Kallo. subarmata*; (ac, ad) *Siphonodella* (*Eosiphonodella*) n. sp. B *sensu* Becker *et al.* 2013*c*, GMM B9A.4-82, Bed 5b.

Clyd. tragelehni both by the dense arrangement of the right denticles and the absence of a plume-like free blade (see Hartenfels, 2011). In the latter, there is also a break between the carina and anterior free blade. *Bispathodus bispathodus* differs by having a basal cavity that extends to or close to the posterior tip. Again, the side denticles show a somewhat wider arrangement.

Geographical distribution. Tafilalt.

https://doi.org/10.1017/S0016756816000893 Published online by Cambridge University Press

Stratigraphic range. *Gonioclymenia* Limestone (*B. costatus* Subzone).

Bispathodus aculeatus anteposicornis (Scott, 1961)
Figure 18g–j

1961 *Spathognathodus anteposicornis* sp. nov.; Scott, pp. 1224–5, fig. 2H–K.
2011 *Bispathodus aculeatus anteposicornis* (Scott); Hartenfels, p. 217, pl. 33, fig. 1 [further remarks and synonymy].

2013 *Bispathodus aculeatus anteposicornis* (Scott); Kononova & Weyer, p. 32, pl. 3, figs 14–15.

Material. 18 specimens from Jebel Ihrs West, Jebel Kfiroun South and Oum el Jerane.

Discussion. One of the illustrated specimens (Fig. 18i, j) is intermediate between *B. aculeatus anteposicornis* and *B. aculeatus aculeatus*. A large denticle is present above the anterior margin of the basal cavity on the right side of the blade. In addition, two extremely weak right-side denticles split off from the carina just above the central basal cavity. This specimen is included as a variant within *B. aculeatus anteposicornis*.

Bispathodus costatus (Branson, 1934) Morphotype 1 (*sensu* Ziegler, Sandberg & Austin, 1974)
Figure 18ae–af

1974 *Bispathodus costatus* (Branson) Morphotype 1; Ziegler, Sandberg & Austin, pp. 102–3, pl. 2, fig. 13.

2011 *Bispathodus costatus* (Branson) Morphotype 1; Hartenfels, p. 219, pl. 34, figs 3–4 [further remarks and synonymy].

2013 *Bispathodus costatus* (Branson) Morphotype 1; Kononova & Weyer, p. 33, pl. 4, figs 9–10, 12, 14.

Material. 41 specimens from Jebel Ihrs West.

Description. As noted by Hartenfels (2011) and Kononova & Weyer (2014), the holotype of *B. bischoffi* Rhodes, Austin & Druce, 1969 falls in this morphotype and would be available as a subspecies name. However, because of identical stratigraphic ranges and intergradation we do not support a subspecies distinction of the two *costatus* morphotypes.

The loose *Kalloclymenia* sp. sample yielded an aberrant adult specimen of *B. costatus* (Fig. 18af). The large, rather flat basal cavity extends close to the posterior tip. Thus, the specimen falls in Morphotype 1 *sensu* Ziegler, Sandberg & Austin (1974). Above the anterior margin of the basal cavity, the main blade is interrupted and offset to the left. The side denticles are connected by weak ridges with the main blade. But curiously, in the anterior part the ornamentation is developed on the left, not on the usual right side.

Bispathodus spinulicostatus (Branson, 1934), Morphotype 1 (= typical morphotype *sensu* the holotype)
Figure 18w–y

1934 *Spathodus spinulicostatus* n. sp., Branson, pp. 305–6, pl. 27, fig. 19

2011 *Bispathodus spinulicostatus* (Branson) Morphotype 1; Hartenfels, p. 221, fig. 59, pl. 32, figs 5–6 [further remarks and synonymy].

e.p. 2013 *Bispathodus ziegleri* (Rhodes, Austin & Druce) Morphotype 1; Kononova & Weyer, pp. 35–6, pl. 5, fig. 3 [slightly transitional towards *ultimus*], pl. 7, fig. 3 [only].

e.p. 2013 *Bispathodus ziegleri* (Rhodes, Austin & Druce) Morphotype 2; Kononova & Weyer, pp. 35–6, pl. 7, figs 1, 7 [only].

2013 *Bispathodus costatus* (Branson) Morphotype 2; Kononova & Weyer, pp. 32–3, pl. 5, fig. 6 [only].

e.p. 2014 *Bispathodus spinulicostatus* (Branson); Malec, fig. 4E, G.

Material. 160 specimens from Jebel Ihrs West and Seheb el Rhassal.

Discussion. Morphotype 1 is characterized by a small basal cavity. It includes several specimens assigned by Kononova & Weyer (2014) either to *B. costatus* or *B. ziegleri*.

Bispathodus spinulicostatus (Branson, 1934) Morphotype 2 (*sensu* Hartenfels, 2011)
Figure 18z

e.p. 1999 *Bispathodus ultimus* (Bischoff); García-López, Sanz-López & Padro Alonso, fig. 3, pl. 3, fig. 13 [only].

2011 *Bispathodus spinulicostatus* (Branson) Morphotype 2; Hartenfels, pp. 221–2, fig. 60, pl. 32, figs 5–6 [further remarks and synonymy].

e.p. 2013 *Bispathodus ziegleri* (Rhodes, Austin & Druce) Morphotype 1; Kononova & Weyer, pp. 35–6, pl. 5, fig. 3 [slightly transitional towards *ultimus*], pl. 7, figs 2, 5 [only].

e.p. 2013 *Bispathodus* aff. *ziegleri* (Rhodes, Austin & Druce); Kononova & Weyer, pp. 35–6, pl. 5, fig. 5 [transitional towards Morphotype 3], pl. 5, fig. 7 [only].

e.p. 2014 *Bispathodus spinulicostatus* (Branson); Malec, fig. 4F, ?S.

Material. 36 specimens from Jebel Ihrs West.

Description. Morphotype 2 is distinguished from the typical Morphotype 1 by having a large, shallow basal cavity that extends to or close to the posterior tip. The

https://doi.org/10.1017/S0016756816000893 Published online by Cambridge University Press

anterior margin of the cavity is more or less rounded and it tapers towards the posterior end of the element. The arrangement of the lateral denticles resembles the typical morphotype. In addition to a row of lateral denticles on the right side of the blade, a row of lateral denticles occurs in the posterior third on the left side. Both rows extend close to the posterior tip. Right and left side denticles are connected by transverse ridges with the main blade and alternate. These ridges are absent or only slightly developed in juveniles, which, however, show the typical proportions of the basal cavity. *Bispathodus spinulicostatus* Morphotype 2 differs from *B. ultimus ultimus* Morphotype 1 in the form and arrangement of the ornament, but transitional forms without alternating rows occur.

Discussion. Since Alberti (1970) and Kaiser (2005) did not illustrate their *B. spinulicostatus* specimens, these first records of the species from the Tafilalt cannot be assigned to the morphotypes established by Hartenfels (2011).

Bispathodus spinulicostatus (Branson, 1934) Morphotype 3 (new)

Figure 20ae–ah

1979 *Bispathodus* aff. *spinulicostatus* (Branson); Kononova, pl. 2, fig. 1.

Material. Six specimens from Jebel Ihrs West.

Description. This new morphotype of *B. spinulicostatus* shows a row of lateral denticles on the right side of the blade. In some specimens (Fig. 20ae), the minor side denticles anterior to the basal cavity split off (only slightly) from the blade. Towards the posterior end, the denticles are connected with the main blade variably by weak or strong transverse ridges (Fig. 20af–ag); they extend close to the posterior tip. A single transverse ridge or a second row of transverse ridges is developed on the left side of the main blade. They start above the posterior margin of the basal cavity or slightly behind this position and extend close to the posterior tip, too. Their arrangement seems to be irregular, without any specified scheme. If there is more than one transverse ridge, these build a very robust posterior platform. Since their terminal cusps reach beyond the platform, a serrate morphology is generated. In the posterior two-thirds, the denticles of the main blade are commonly fused and transformed into a ridge. The basal cavity is restricted to the central part of the element and does not reach the posterior tip, similar to *B. spinulicostatus* Morphotype 1. On the left side of the main blade, the basal cavity shows a distinctive bulge, that forms a smooth, platform-like structure. In aboral view, the basal cavity is flat and a weak median groove reaches from the anterior to the posterior tip (Fig. 20ah). Juveniles are not yet known.

Discussion. Within *Bispathodus*, several species/subspecies show a bulge-like basal cavity on the left side of the main blade. This has been illustrated for *B. aculeatus aculeatus* (Wang & Yin in Yu, 1988: pl. 24, fig. 9), *B. aculeatus anteposicornis* (Bardasheva *et al.* 2004: pl. 13, fig. 4), *B. costatus* Morphotype 2 (Luppold, Hahn & Korn, 1984: pl. 4, fig. 5; Wang & Yin in Yu 1988: pl. 24, fig. 14; García-López, Sanz-López & Padro Alonso, 1999: pl. 2, fig. 12) and *B. spinulicostatus* Morphotype 1 (Corradini, 2003: pl. 1, fig. 10). Similar features are illustrated here for *B. aculeatus aculeatus* (Fig. 18m), *B. costatus* Morphotype 2 (Fig. 18ad) and *B. spinulicostatus* Morphotype 1 (Fig. 18w, x). *Bispathodus* aff. *spinulicostatus sensu* Kononova (1979) agrees with our concept of *B. spinulicostatus* Morphotype 3. As in our specimen illustrated in Figure 20ae, both characteristic features are developed in her material, an initial platform-bulk as well as a single strong transverse ridge on the left side of the main blade.

Morphotype 3 differs from Morphotype 1 in two features on the left side of the main blade, the distinctive bulge above the basal cavity and the strong transverse ridges, which cause a robust posterior platform. In contrast, Morphotype 2 has a large *B. bispathodus*-like basal cavity that extends to or close to the posterior tip. *Bispathodus ultimus ultimus* Morphotype 2 differs in the denticle arrangement on the left side of the main blade, which is much more regular, extending generally above the basal cavity. *Bispathodus ultimus ultimus* Morphotype 1 is additionally distinguished by its larger basal cavity that reaches to or close to the posterior tip. Both morphotypes of *B. costatus* differ in the absence of a second row of ornamentation posterior to the basal cavity.

A somewhat similar specimen was illustrated as *Ps. dentilineatus* by Wang & Yin (in Yu 1988: pl. 24, fig. 12) from Sample 29 of the Nanbiancun section IV (Guangxi, south China), which falls in the Lower Carboniferous. However, this specimen develops a right platform with a significant extension to the anterior tip.

Geographic distribution. Tafilalt (Jebel Ihrs) and southern Urals (Sikaza River section 2).

Stratigraphic range. *Gonioclymenia* and *Kalloclymenia* limestones, *B. costatus* Subzone to *B. ultimus ultimus* Zone with the oldest *S. (Eosiphonodella)*. The specimen of Kononova (1979) is from the Lytvin horizon and Upper *expansa* Zone (= *B. ultimus ultimus* Zone).

?Bispathodus aff. *spinulicostatus* (Branson, 1934)

Figure 20v, w

Material. One specimen from Jebel Ihrs West.

Description. The two platforms halves of the adult specimen differ considerably. On the right side, the denticulation consists of regularly arranged, mostly isolated, elongated nodes of the platform margin. They extend much further anteriorly than on the left side.

https://doi.org/10.1017/S0016756816000893 Published online by Cambridge University Press

Thereby, the right platform forms a gentle, convex arch that gradually approaches the free blade. The last posterior node is linked with the carina. On the left side, the platform ornament consists of two isolated, widely spaced nodes and a thin ridge connected with the carina. These produce a serrate margin. An additional node is situated above the protruding basal cavity, almost at the same level as the posterior platform nodes. There is also a small node on the opposite right basal cavity extension. The carina is low and extends to the posterior tip. In the anterior part, its denticles are merged into a nodose ridge. The free blade consists of five laterally compressed and fused denticles, showing free tips. An adcarinal groove is restricted on the right side of the platform to the anterior half. In side view, the free blade is highest at mid-length. Towards the posterior tip, the platform is slightly bent downwards. In aboral view, there is a central, broad, constricted and strongly asymmetric basal cavity that tapers towards the posterior end. The lower left side forms a prominent side lobe that, in oral view, protrudes widely below the platform.

Discussion. The specimen may represent a new, rare taxon. It is distinguished from *B. spinulicostatus* Morphotype 1 by its laterally widened basal cavity with nodes on the upper surface and by the serrate posterior left margin. There are possibly distant relationships with *B. ostrovkensis* (Dzik, 2006), which type-series seems to include both some *Ps. primus primus* (his fig. 113A, E) and bispathodids (the holotype, his fig. 113F). In *B. muessenbergensis* Luppold in Luppold, Hahn & Korn, 1984 the basal cavity is similar to that in *B.* aff. *spinulicostatus*, but the very different carina ends in the holotype above it.

Geographic distribution. Tafilalt.

Stratigraphic range. *Bispathodus costatus* Subzone.

Bispathodus ultimus ultimus (Bischoff, 1957) Morphotype 1 (*sensu* Ziegler & Sandberg, 1984)

Figure 19c–g

1957 *Spathognathodus spinulicostatus ultimus* Bischoff; Ziegler (in Flügel & Ziegler), pl. 1, figs 10, 16–17.

1959 *Spathognathodus spinulicostatus ultimus* Bischoff; Helms, pl. 3, figs 6, 9.

e.p. 1962 *Spathognathodus costatus spinulicostatus* (Branson); Ziegler, pp. 108–9, pl. 14, fig. 11 [only].

1962 *Spathognathodus costatus ultimus* Bischoff; Ziegler, p. 109, pl. 14, figs 19–20.

1967 *Spathognathodus costatus ultimus* Bischoff; van Adrichem Boogaert, p. 187, pl. 3, fig. 25.

e.p. 1969 *Spathognathodus ziegleri* sp. nov.; Rhodes, Austin & Druce, pp. 238–9, pl. 4, fig. 8 [holotype only].
e.p. 1973 *Spathognathodus costatus spinulicostatus* (Branson); Szulczewski, p. 53, pl. 2, fig. 5 [only].

1974 *Bispathodus ultimus* (Bischoff); Ziegler, Sandberg & Austin, p. 104, pl. 2, fig. 12.

1975 *Bispathodus ultimus* (Bischoff); Ziegler, pp. 53–4, *Bispathodus*, pl. 3, fig. 9.

1984 *Bispathodus ultimus* (Bischoff) Morphotype 1; Ziegler & Sandberg, pp. 186–7.
2009 *Bispathodus ultimus* (Bischoff) Morphotype 1; Kaiser, Becker, Spalletta & Steuber, p. 130.

2013 *Bispathodus ultimus* (Bischoff); Girard *et al.* fig. 3q.

e.p. 2013 *Bispathodus ultimus ultimus* (Bischoff); Kononova & Weyer, p. 34, pl. 5, figs 9–11, pl. 6, figs 6–8, pl. 7, figs 11, 14.

e.p. 2013 *Bispathodus ziegleri* (Rhodes, Austin & Druce) Morphotype 1; Kononova & Weyer, pp. 35–6, pl. 5, fig. 8, pl. 6, figs 1, 4, pl. 7, fig. 6 [only].

? 2013 *Bispathodus ziegleri* (Rhodes, Austin & Druce) Morphotype 1; Kononova & Weyer, pp. 35–6, pl. 6, figs 2–3, pl. 7, fig. 4 [only, transitional from *B. spinulicostatus*]

e.p. 2014 *Bispathodus ultimus* (Bischoff); Malec, fig. 4A–B.

Material. 84 specimens from Jebel Ihrs West.

Discussion: Because of past taxonomic uncertainties and discrepancies, we supply here a new synonymy list for Morphotype 1. The holotype of *B. ziegleri* Rhodes, Austin & Druce, 1969 (their pl. 4, fig. 8) clearly has a broad basal cavity of *bispathodus* type, which tapers to the posterior tip. This fact has already been mentioned by Ziegler (1975, p. 55: 'In the majority of specimens, the basal cavity, although *aculeatus*-like in shape, is distinctly larger than in *B. aculeatus*. There are few specimens including the holotype that have a *bispathodus* basal cavity'). Therefore, we re-assign the *ziegleri* holotype to *B. ultimus ultimus* Morphotype 1 (see synonymy list above), which corrects the wrong assignment to Morphotype 2 in the synonymy list of Ziegler & Sandberg (1984). Since the *ultimus* holotype represents Morphotype 2, it would be possible to separate both taxa at subspecies level. However, due to the identical stratigraphical range and complete intergradation between both types, we do not support such a taxonomic treatment. Kononova & Weyer (2014) used differences of the posterior ornamentation to separate both forms as species but in fact these are very subtle and there are intermediates that suggest ornament variability within one species. More important are intermediates from *B. spinulicostatus* Morphotype 2 in which the left posterior ornament consists partly still of nodes, not yet only of transverse ridges, but these do not alternate with the right-side ridges. Such specimens are assigned here with a query to *B. ultimus ultimus* Morphotype 1.

https://doi.org/10.1017/S0016756816000893 Published online by Cambridge University Press

Bispathodus ziegleri muessenbergensis Luppold, Hahn & Korn, 1984 is characterized by lateral extensions of the basal cavity that bear distinctive small to large denticles. Such forms fall outside the variability range of Moroccan or Thuringian *B. ultimus* populations and are, therefore, recognized here as a separate species.

***Bispathodus ultimus ultimus* (Bischoff, 1957)**
Morphotype 2 (= typical morphotype *sensu* the holotype)
Figure 19b

1957 *Spathognathodus ultimus* sp. nov.; Bischoff, pp. 57–8, pl. 4, figs 24 (holotype)–26.

1959 *Spathognathodus* cf. *costatus* (Branson); Voges, p. 299, pl. 34, fig. 47.

e.p. 1962 *Spathognathodus costatus spinulicostatus* (Branson); Ziegler, pp. 108–9, pl. 14, figs 12–18 [only].

1967 *Spathognathodus costatus spinulicostatus* (Branson); van Adrichem Boogaert, p. 187, pl. 3, figs 23–4.

e.p. 1967 *Spathognathodus costatus spinulicostatus* (Branson); Wolska, p. 427, pl. 19, figs 15–16 [only].

e.p. 1969 *Spathognathodus ziegleri* sp. nov.; Rhodes, Austin & Druce, pp. 238–9, pl. 4, figs ?5, 6–7 [only, non fig. 8 = holotype].

e.p. 1973 *Spathognathodus costatus spinulicostatus* (Branson); Szulczewski, p. 53, pl. 2, figs 1–2 [only].

1974 *Bispathodus ziegleri* (Rhodes, Austin & Druce); Ziegler, Sandberg & Austin, p. 104, pl. 2, fig. 16.

1975 *Bispathodus ziegleri* (Rhodes, Austin & Druce); Ziegler, pp. 55–6, *Bispathodus*-pl. 3, fig. 10.

1980 *'Bispathodus* cf. *B. ultimus'* (Bischoff); van den Boogaard & Schermerhorn, pp. 3–4, pl. 1, figs A–B.

1980 *'Bispathodus ziegleri'* (Rhodes, Austin & Druce); van den Boogaard & Schermerhorn, p. 7, pl. 1, figs C–D.

e.p. 1984 *Bispathodus ultimus* (Bischoff) Morphotype 2; Ziegler & Sandberg, pp. 186–7, pl. 2, figs 3–5, 7 [only].

e.p. 1999 *Bispathodus ultimus* (Bischoff); García-López, Sanz-López & Padro Alonso, fig. 3, pl. 2, fig. 14 [only].

2009 *Bispathodus ultimus* (Bischoff) Morphotype 2; Kaiser, Becker, Spalletta & Steuber, p. 130.

e.p. 2013 *Bispathodus ultimus ultimus* (Bischoff); Kononova & Weyer, p. 34, pl. 6, fig. 5 [only].

?e.p. 2013 *Bispathodus ziegleri* (Rhodes, Austin & Druce) Morphotype 1; Kononova & Weyer, pp. 35–6, pl. 5, fig. 2, pl. 7, fig. 9 [only, still transitional from *B. spinulicostatus*].

?e.p. 2013 *Bispathodus ziegleri* (Rhodes, Austin & Druce) Morphotype 2; Kononova & Weyer, pp. 35–6, pl. 5, fig. 12 [only, still transitional from *B. spinulicostatus*].

e.p. 2014 *Bispathodus ultimus* (Bischoff); Malec, fig. 4C–D.

2015 *Bispathodus ultimus* (Bischoff); Mossoni, Carta, Corradini & Spalletta, fig. 7g.

Material. 14 specimens from Jebel Ihrs West.

Discussion. The concept of *B. ultimus ultimus* in the sense of the holotype, Morphotype 2 *sensu* Ziegler & Sandberg (1984), is based on a centrally situated, *B. aculeatus aculeatus*-like basal cavity, which does not form a right angle with the main blade. According to Ziegler & Sandberg (1984), *Spathognathodus costatus ultimus sensu* Ziegler (1962) does not conform to the holotype of *B. ultimus*. Its basal cavity is broader and extends to or close to the posterior tip, as in *B. ultimus ultimus* Morphotype 1. Kaiser (2005) and Kaiser *et al.* (2009) added that *B. ultimus* Morphotype 2 has a small, almost symmetrical basal cavity, whereas Morphotype 1 has a large, asymmetrical one.

Kononova & Weyer (2014) questioned the morphotype concept of Ziegler & Sandberg (1984) and did not accept the published synonymies. Based on minor ornament differences, as discussed above, Kononova & Weyer (2014) kept *B. ultimus ultimus* separate from *B. ziegleri*. They distinguished two morphotypes of *B. ziegleri*: Morphotype 1 with large, *bispathodus*-type and Morphotype 2 with smaller, *aculeatus*-type basal cavity located in mid-position of the platform. All their figured specimens of *B. ziegleri* Morphotype 2 are obviously *B. spinulicostatus* Morphotype 1 (their pl. 7, figs 1, 7) or questionable transitional forms towards *B. ultimus ultimus* Morphotype 2 (their pl. 5, fig. 12).

A form that is slightly transitional from *B. spinulicostatus* Morphotype 1 is illustrated in Figure 19a. Its basal cavity is short, more or less restricted to the central platform and the posterior left ridges are very short and denticle-like.

We accept *B. ultimus bartzschi* Kononova & Weyer, 2014 as a valid subspecies of *B. ultimus*.

***Branmehla inornata* (Branson & Mehl, 1934*a*)**
Figure 19w, x

1934*a* *Spathodus inornatus* sp. nov.; Branson & Mehl, p. 185, pl. 17, fig. 23.

2011 *Branmehla inornata* (Branson & Mehl); Hartenfels, pp. 230–1, pl. 36, figs 4–6 [further remarks and synonymy].

Material. 305 specimens from Jebel Ihrs West, Jebel Kfiroun South, Oum el Jerane, Seheb el Rhassal and Takhbtit West.

Discussion. Nine specimens from the *B. ultimus ultimus* Zone of Jebel Ihrs West represent transitional

https://doi.org/10.1017/S0016756816000893 Published online by Cambridge University Press

forms between *Br. inornata* and *Br. suprema*. In contrast to typical *Br. inornata*, the basal cavity is more elongated but not so strongly asymmetric as in typical *Br. suprema*. They are also distinguished from *Br. suprema* by their posterior blade that is only slightly curved side- and downwards. We keep such intermediates as advanced variants of *Br. inornata*. Previously, similar specimens were noted from the Carnic Alps by Kaiser (2005) and Kaiser *et al.* (2009) and from Thuringia by Hartenfels (2011).

Neopolygnathus fibula sp. nov.

Figure 19s–u

? 1966 *Polygnathus communis* Branson & Mehl; Klapper, p. 21, pl. 6, figs 6, 11.

Types. Holotype GMM B9A.4-41, Figure 19s, t, paratype GMM B9A.4-42, Figure 19u, 16 more paratypes from the type locality.

Derivation of name. From the Latin *fibula*, due to the cramp shape of the anterior platform ornamentation.

Type locality and level. *Gonioclymenia* trench at Jebel Ihrs West, loose limestone slab with *Kallo. subarmata* (Bed 4b), *B. ultimus ultimus* Zone with the oldest *S. (Eosiphonodella)*, UD VI-A.

Diagnosis. A species of *Neopolygnathus* with an asymmetric, lanceolate, slightly ovate platform bearing a single, isolated, cramp-shaped node on each side of the anterior platform. The remaining platform is smooth; the curved carina consists of fused denticles and ends just before the posterior tip. The free blade is moderately long (*c.* 40 % of the total length), the basal pit small and positioned under the anterior platform end. Posterior to the basal pit, a large, shallow depression is developed.

Description. The slightly ovate platform of the new species is widest in the anterior third. The outer margin is broadly curved, the inner margin is anteriorly convex, then slightly concave. On both platform sides a single cramp-shaped node is developed, which runs vertical or moderately diagonal towards the carina. The remaining platform is smooth. The carina is separated on each side and over its whole length by a trough, which shallows to the posterior tip. The carina is generally low, but higher in the anterior part, weakly curved, and consists of fused nodes that become very small near the posterior tip. The free blade is shorter than the platform and consists of 9–11 laterally compressed, fused denticles of equal height and with free tips.

In lateral view, the platform is weakly bent downwards towards the posterior end. Aborally, a small, rounded to ovate basal pit lies at the anterior margin of the platform, right at the junction to the free blade. Anteriorly, it extends along the blade as a narrow groove. Immediately posterior to the basal pit, a large, shallow depression is developed, as typical for the genus. From there, a strong and sharp keel increases in height towards the posterior tip.

Discussion. All morphotypes of *Neo. communis communis*, *Neo. communis ozbakensis* Weddige, 1984, and *Neo. klapperianus* (Ashouri, 2006), which is only known from a juvenile, lack central platform nodes. In our samples there is no intergradation with the much more common *Neo. communis communis*. All other lower/middle Famennian species have different platform shapes and transverse costae, at least posteriorly. Among the upper/uppermost Famennian taxa, *Neo. communis hanensis* (Savage, 2013) and *Neo. communis phaphaensis* (Savage, 2013) have smooth platforms, *Neo. namdipensis* (Savage, 2013), here elevated to species level, a more leaf-shaped, subsymmetric platform with many marginal nodes reaching the posterior tip. *Neopolygnathus renatae* Corradini & Spalletta in Corradini, Barca & Spalletta (2003) is characterized by a large node or ridge at the margins of the anterior platform, *Neo. margaretae* Kononova & Weyer, 2014 by longer ridges and a very peculiar, guitar-shaped, constricted platform. *Neopolygnathus collinsoni* (Druce, 1969) differs from *Neo. fibula* sp. nov. in its nodose rostra on the anteriorly strongly constricted platform. In *Neo. mugodzaricus* (Gagiev, Kononova & Pazukhin, 1987), excluding stratigraphically older material (two morphotypes from Iran; Gholamalian, 2005), there are anterior rostra with few nodes and the unconstricted platform is smooth, with very deep adcarinal troughs. In the very different *Neo. shangmiaobeiensis* Qin, Zhao & Ji, 1988 there are two longitudinal ridges on each platform side. In an upper Famennian *communis* specimen from Wyoming figured in Klapper (1966) both platforms halves show a node and anteriorly a collar-forming thickening, which gives an ornament reminiscent of our new species. Its adcarinal furrows appear to be deeper.

Neopolygnathus carina s. str., originally from the Upper Tournaisian, is defined by the presence of an oblique, noded ridge on each side of the anterior platform. *Neopolygnathus fibula* sp. nov. can easily be distinguished by its different, large, cramp-like nodes. Many authors, such as Sandberg (1976), Sandberg & Ziegler (1979), Raven (1983), Weddige (1984), Dreesen, Sandberg & Ziegler (1986), Kalvoda & Kukal (1987), Matyja (1987), Ji & Ziegler (1993), Voronzova (1996) and Kaiser *et al.* (2006), have described or listed supposed Famennian *Neo. carina*. In most cases, there are no illustrations to prove the identification. Ziegler & Sandberg (1984) suggested that the species started in the upper Famennian *B. stabilis stabilis* Zone (= roughly Lower *expansa* Zone). However, the few figured Famennian (pre-Hangenberg extinction) specimens differ from both *Neo. carina* s. str. and *Neo. fibula* sp. nov. in their arrangement and type of the anterior ornament. As pointed out by Carman (1987), the specimens of Sandberg & Ziegler (1979) are rejected from *Neo. carina* because their anterior ridges

https://doi.org/10.1017/S0016756816000893 Published online by Cambridge University Press

parallel the carina (cf. Xia & Chen, 2004). They represent a new form, which is additionally characterized by deep and very narrow adcarinal furrows. The even older (*rhomboidea* Zone) Iranian specimen of Weddige (1984) possesses a short parallel ridge on the anterior left side, whereas the anterior right side has at least four nodose transverse ridges. The published evidence does not support the view that *Neo. carina* s. str. occurs in Famennian strata below the Hangenberg Event. Even the oldest post-Hangenberg Event forms, from the *Protognathodus kockeli* (= Upper *praesulcata*) Zone of south China (Ji *et al.* 1989) and the Russian Far East (Gagiev & Kononova, 1990), are not typical.

Among the numerous Carboniferous *Neopolygnathus* taxa there are no similar forms. The serrate, upturned anterior platform margins of *Neo. dentatus* (Druce, 1969) are rostra-like. In *Neo. lectus* (Kononova in Bushmina & Kononova, 1981) there are also short anterior, longitudinal rostra and the adcarinal furrows fade out on the posterior platform. The rostra of *Neo. carmanae* Xia & Chen, 2004 form a peculiar collar and there are many platform margin nodes, also near the posterior tip. Numerous nodes on wider anterior platforms characterize *Neo. tschatkalicus* Nigmadzhanov, 1986, *Neo*. aff. *tschatkalicus* in Bardasheva *et al*. (2004), *Neo*. aff. *stylensis* in Bardasheva *et al*. (2004), and *Neo. longanensis* (Qie *et al.* 2004). Other forms have distinctive longitudinal ridges on the platform, such as *Neo. porcatus* (Ni, 1984), *Neo. communis quadratus* (Wang, 1989), an invalid junior homonym (Becker, 2012), and *Neo. gancaohuensis* (Xia & Chen, 2004).

Geographic distribution. Tafilalt and Franconia, possibly Wyoming.

Stratigraphic range. In the Tafilalt, *Neo. fibula* sp. nov. ranges from the *B. costatus* Subzone to the top of the *B. ultimus ultimus* Zone. This agrees with unpublished data from Köstenhof (= Schübelhammer, Franconia, Tragelehn & Hartenfels). The questionable specimen figured in Klapper (1966) falls in the Lower *costatus* Zone *sensu* Ziegler (1962, = *B. aculeatus aculeatus* Zone).

'*Polygnathus*' div. sp. (transitional to N. Gen. 1 *sensu* Becker *et al*. 2013*c*)
Figure 21a–h

Discussion. There are 35 specimens from Jebel Ihrs West, Bed 4b (*Kalloclymenia* Limestone), that are transitional between the *Po. inornatus* Group (s.l.) and 'siphonodellids' with respect to the transformation of a small polygnathid pit into a wider, flat, poorly delimited basal body attachment area as in N. Gen. 1 *sensu* Becker *et al*. (2013*c*; cf. Tragelehn, 2010, and Fig. 21i–n) or in *'Po.' spicatus* Branson, 1934. Such forms will be treated in more detail in a publication by H. Tragelehn.

***Pseudopolygnathus primus primus* Branson & Mehl, 1934*b* Morphotypes 1–3**
Figures 20m–u, 22

1934*b* *Pseudopolygnathus prima* sp. nov.; Branson & Mehl, p. 298, pl. 24, figs 24–5 [Morphotype 1].

1934 *Pseudopolygnathus irregularis* sp. nov.; Branson, p. 316, pl. 26, figs 25–6 [Morphotype 2].
1934 *Pseudopolygnathus lobata* sp. nov.; Branson, p. 316, pl. 26, figs 1–2 [Morphotype 2 with side lobe].

1934 *Pseudopolygnathus unispinosa* sp. nov.; Branson, p. 316, pl. 26, fig. 24 [Morphotype unclear].

1934 *Pseudopolygnathus corrugata* sp. nov.; Branson, p. 317, pl. 26, fig. 23 [Morphotype unclear].

1934 *Pseudopolygnathus dentilineata* sp. nov.; Branson, p. 317, pl. 26, fig. 22 [Morphotype 2].

1934 *Pseudopolygnathus costata* sp. nov.; Branson, pp. 317–18, pl. 26, fig. 21 [Morphotype 2].

1934 *Pseudopolygnathus varicostata* sp. nov.; Branson, p. 318, pl. 26, figs 19–20 [Morphotype 2].

1934 *Pseudopolygnathus subrugosa* sp. nov.; Branson, pp. 318, pl. 26, fig. 18 [possibly Morphotype 2].

1934 *Pseudopolygnathus projecta* sp. nov.; Branson, p. 320, pl. 26, figs 10–11 [Morphotype 2].

1934 *Pseudopolygnathus inequicostata* sp. nov.; Branson, p. 321, pl. 26, fig. 6 [Morphotype unclear].

1934 *Pseudopolygnathus crenulata* sp. nov.; Branson, p. 321, pl. 26, figs 4–5, 7–8 [Morphotype 2].

1934 *Pseudopolygnathus brevimarginata* sp. nov.; Branson, p. 322, pl. 26, fig. 3 [Morphotype 2].

1949 *Pseudopolygnathus carinata* sp. nov.; Youngquist & Patterson, p. 68, pl. 16, fig. 4 [Morphotype 1 with incipient right side lobe].

1949 *Pseudopolygnathus constrictiterminata* sp. nov.; Thomas, p. 428, pl. 4, fig. 16 [Morphotype unclear].

1949 *Pseudopolygnathus* cf. *Ps. crenulata* Branson; Thomas, pl. 4, fig. 18 [Morphotype unclear].

1957 *Pseudopolygnathus irregularis* Branson; Bischoff, p. 51, pl. 6, figs 12–13 [Morphotype 1 with small side lobe].

1959 *Pseudopolygnathus asymmetrica* Branson; Hass, pl. 49, fig. 14 [Morphotype unclear].

1959 *Pseudopolygnathus prima* Branson & Mehl; Hass, pl. 49, fig. 27 [Morphotype unclear].

1959 *Pseudopolygnathus dentilineata* Branson; Voges, pp. 300–1, fig. 5/II-l [Morphotype 1], fig. 5/II-r

https://doi.org/10.1017/S0016756816000893 Published online by Cambridge University Press

[Morphotype 2], pl. 34, figs 49–50 [Morphotype unclear].

1966 *Pseudopolygnathus prima* Branson & Mehl; Klapper, p. 14, pl. 4, fig. 8 [Morphotype unclear].

1966 *Pseudopolygnathus dentilineata* Branson; Klapper, pp. 14–15, pl. 5, figs 10–11 [Morphotype 2].

1968 *Pseudopolygnathus dentilineata* Branson; Canis, p. 546, pl. 73, figs 10, 29 [Morphotype unclear], figs 30–1 [Morphotype 1].
1968 *Pseudopolygnathus prima* Branson & Mehl; Canis, p. 547, pl. 73, figs 12, 17, 32 [Morphotype 1].

1969 *Pseudopolygnathus expansus* sp. nov.; Rhodes, Austin & Druce, pp. 209–10, pl. 5, fig. 2 [Morphotype 2 with incipient right side lobe], fig. 4 [trend towards Morphotype 3].

1969 *Pseudopolygnathus vogesi* sp. nov.; Rhodes, Austin & Druce, pp. 216–17, pl. 5, figs 1, 3, 5–8 [Morphotype 2].

1969 *Pseudopolygnathus prima* Branson & Mehl; Schönlaub, p. 340, pl. 1, figs 23–4 [Morphotype 1].

1971 *Pseudopolygnathus primus* Branson & Mehl; Rhodes & Austin, pl. 1, fig. 2 [Morphotype 2].

1971 *Pseudopolygnathus dentilineatus* Branson; Rhodes & Austin, pl. 2, fig. 20 [Morphotype 2].

1973 *Pseudopolygnathus dentilineatus* Branson; Szulczewski, pp. 44–5, pl. 5, figs 5, ?6 [Morphotype unclear].

e.p. 1973 *Pseudopolygnathus primus* Branson & Mehl; Szulczewski, pp. 46–7, pl. 4, fig. 7 [Morphotype unclear], fig. 8 [Morphotype 1] [only].

1973 *Pseudopolygnathus dentilineatus* Branson; Matthews & Naylor, p. 365, pl. 38, figs 14–15 [?Morphotype 3].

1973 *Pseudopolygnathus primus* Branson & Mehl; Matthews & Naylor, p. 365, pl. 38, figs 5–6, 21–3 [Morphotype 1].

e.p. 1976 *Pseudopolygnathus vogesi* Rhodes, Austin & Druce; Dreesen, Dusar & Groessens, pl. 4, figs 1–2, pl. 13, fig. 3 [Morphotype 2] [only].

? 1979 *Pseudopolygnathus* cf. *dentilineatus* Branson; Sandberg & Ziegler, pp. 183–4, pl. 3, fig. 19 [non figs 18, 20–21 = relatives of *Ps. koestenhofensis*/*Ps. inordinatus*].

e.p. 1981 *Pseudopolygnathus primus* Branson & Mehl; Klapper (in Ziegler), pp. 401–8, *Pseudopolygnathus*-pl. 3, fig. 3, pl. 4, figs 1, 6–7, pl. 5, figs 2–3, ?4, 5 [only] [further remarks and synonymy].

1983 *Pseudopolygnathus primus* Branson & Mehl; Raven, pl. 5, fig. 4 [Morphotype unclear].

e.p. 1985 *Pseudopolygnathus* aff. *dentilineatus* Branson; Bartzsch & Weyer, pp. 21–3, pl. 5, figs 1, 4 [Morphotype 1], fig. 6 [Morphotype unclear] [only].

? 1986 *Pseudopolygnathus primus* Branson & Mehl; Buggisch, Rabien & Hühner, Tab. 1 [no illustration].

1987 *Pseudopolygnathus primus* Branson & Mehl; Korn & Luppold, pp. 213–14, pl. 2, figs 4, 9, 11 [Morphotype unclear], figs 8, 10 [Morphotype 3].

1987 *Pseudopolygnathus primus* Branson & Mehl; Kalvoda & Kukal, pl. 5, figs 11–12 [Morphotype unclear].

1989 *Pseudopolygnathus primus* Branson & Mehl; Ji, Wang & Luo, p. 93, pl. 22, fig. 9 [Morphotype 1].

? 1990 *Pseudopolygnathus primus* Branson & Mehl; Gagiev & Bogus, fig. 2b [no illustration].

1992 *Pseudopolygnathus primus* Branson & Mehl; Nemirovskaya, Chermnykh, Kononova & Pazukhin, pl. 3, fig. 2 [Morphotype 2], fig. 3 [Morphotype unclear], fig. 4 [slightly advanced Morphotype 3].

1997 *Pseudopolygnathus primus* Branson & Mehl; Molloy, Talent & Mawson, pl. 9, figs 4–8 [Morphotype 2].

1999 *Pseudopolygnathus dentilineatus* Branson; Sanz-López, García-López, Montesinos & Arbizu, pl. 2, fig. 6 [Morphotype unclear].

1999 *Pseudopolygnathus primus* Branson & Mehl; Sanz-López, García-López, Montesinos & Arbizu, pl. 2, figs 7–8 [Morphotype unclear].

2000 *Pseudopolygnathus primus* Branson & Mehl; Matyja, Turnau & Żbikowska, fig. 4.1 [Morphotype 3], fig. 4.2 [morphotype unclear].

non 2002 *Pseudopolygnathus primus* Branson & Mehl; Draganits *et al.* p. 17, tab. 1, pl. 2, figs 17–19, pl. 3, figs 13, 15 [different subspecies].

e.p. 2003 *Pseudopolygnathus primus* Branson & Mehl; Corradini, Barca & Spalletta, p. 240, pl. 5, fig. 5 [Morphotype 2] [only].

2004*b* *Pseudopolygnathus primus* Branson & Mehl; Piecha, pp. 259–60, pl. 2, figs 1–8 [Morphotype 3, including forms with incipient right side lobe].

2004 *Pseudopolygnathus primus* Branson & Mehl; Gereke, pl. 2, figs 26–7 [?Morphotype 2].

2007 *Pseudopolygnathus dentilineatus* Branson; Boncheva *et al.* p. 343, pl. 3, fig. 6 [Morphotype unclear].

2007 *Pseudopolygnathus primus* Branson & Mehl; Boncheva *et al.* p. 343, pl. 3, fig. 11 [Morphotype 2], figs 12–13 [Morphotype unclear].

2008 *Pseudopolygnathus primus* Branson & Mehl; Habibi, Corradini & Yazdi, p. 774, fig. 4.7 [Morphotype 1].

2009 *Pseudopolygnathus primus* Branson & Mehl; Gholamalian, Ghorbani & Sajadi, pl. 5, figs 20–1 [Morphotype unclear].

2011 *Pseudopolygnathus* cf. *primus* Branson & Mehl; Hartenfels, pp. 317–18, pl. 64, figs 9–12 [Morphotype 3].
non 2011 *Pseudopolygnathus* cf. *dentilineatus* Branson; Hartenfels, pp. 310–11, pl. 65, figs 1–3 [*Ps. koestenhofensis*/*Ps. inordinatus*].

2013 *Pseudopolygnathus primus* Branson & Mehl; Mossoni, Corradini & Spalletta, fig. 3.18 [morphotype unclear].

e.p. 2013 *Pseudopolygnathus primus* Branson & Mehl; Kononova & Weyer, pp. 44–5, pl. 8, figs 8–10 [Morphotype 2] [only, pl. 8, figs 11–12 = 'siphonodelloids'].

Material. 59 specimens from Jebel Ihrs West, Jebel Kfiroun South, Oum el Jerane and Seheb el Rhassal (all Morphotype 3).

Description. Specimens from the *Gonioclymenia* Limestone, here assigned to *Ps. primus primus* Morphotype 3 (Fig. 20m–u), are nearly straight or slightly bowed, with the flexion point at mid-length. The two anterior margins do not face each other; the right platform extends much further anteriorly and gradually approaches the free blade. The left platform ends with a distinctive, rounded shoulder. The free blade and carina consist of low, laterally compressed, and more or less fused denticles with free tips. The platform bears coarse, slightly elongate nodes or transverse ridges that are commonly connected with the carina; the ornamentation is always somewhat irregular. In the posterior third of the platform, the elongated nodes or ridges stretch above the platform and generate a serrate margin. Aborally, a wide, central basal cavity is slightly constricted at both ends and tapers to or close to the posterior tip without forming a keel. A weak median groove reaches from the anterior to the posterior end. In lateral view, the basal cavity is separated from the platform by a distinctive constriction.

Discussion. The synonymy list of Ziegler (1981), here updated, suggests a large variability within *Ps. primus*, especially in the Tournaisian. According to Klapper (in Ziegler, 1981), there is a complete gradation between forms with a wide basal cavity of the '*dentilineatus*' type and a smaller, more restricted basal cavity of the '*primus*' type. Consequently, *Ps. dentilineatus* was included in the synonymy of *Ps. primus* by Klapper (in Ziegler, 1981). Piecha (2004*b*) postulated that the Devonian specimens have a large '*dentilineatus*' pit, whereas the Carboniferous elements are characterized by a small '*primus*' pit. This is contradicted by early variants with '*primus*' type basal cavity from the *B. aculeatus aculeatus* Subzone of section Kahlleite East (Thuringia), which are illustrated here (Fig. 22a, b).

As noted by Klapper (in Ziegler, 1981) and Corradini, Barca & Spalletta (2003), *Ps. primus primus* shows a large variation of platform outline and ornament. Generally, the platform is thick, slightly or strongly asymmetric, and the left margin forms a distinctive projection (e.g. *Ps. primus* type material, *Ps. crenulatus* Branson, 1934, *Ps. asymmetricus* Branson, 1934, *Ps. sulciferus* Branson, 1934) or at least a rounded corner before it joins the free blade/carina. In typical specimens the right platform extends farther anteriorly. There are elements with either a pointed or more rounded posterior platform end. The ornament varies from strong transversal ridge (running across the whole platform width and partly fused with the carina) to somewhat oblique ridges or large nodes (sometimes elongated) that are restricted to the platform margins.

We recognize three morphotypes, which can be distinguished based on the size and shape of the basal cavity and on the presence or absence of a posterior keel. Morphotype 1 equals the '*primus*' Morphotype *sensu* Klapper (in Ziegler, 1981). The small basal cavity is restricted to the anterior third or the central part of the platform. Posteriorly, a sharp keel reaches the posterior tip (Fig. 22b, cf. Fig. 22d). The '*dentilineatus*' Morphotype *sensu* Klapper (in Ziegler, 1981), Morphotype 2, has a bilobate, laterally more expanded basal cavity than Morphotype 1, which is often more extended posteriorly. Again, a strong keel runs to the posterior end. In Morphotype 3 there is a large, shallow basal cavity, which is slightly constricted and tapers to the posterior tip (Fig. 20n, q). The posterior part of the basal cavity forms a narrow, flat ridge, instead of a keel. All our new Moroccan material belongs to the new *Ps. primus primus* Morphotype 3, which links *Ps. primus primus* with the more weakly ornamented *Ps. controversus*. We are aware that one could place our new morphotype alternatively as a distinctive morphotype within the latter species.

It may be argued to separate other morphological extremes as additional *primus* morphotypes, for example forms with shortened right platform, resulting in a longer free blade. Forms with an incipient right side lobe are not taxonomically relevant; they developed within Morphotype 1 (*Ps. carinatus* Youngquist & Patterson, 1949; *Ps. irregularis* in Bischoff, 1957), Morphotype 2 (Tournaisian *Ps. lobatus* Branson, 1934, and *Ps. expansus* Rhodes, Austin & Druce, 1969) and Morphotype 3 (see upper Famennian examples in Piecha, 2004*b* and Hartenfels, 2011: pl. 64, fig. 9), and also in the Tournaisian *Ps. constrictiterminatus* Thomas, 1949. But there is no evidence for Famennian specimens with a large, anteriorly directed

https://doi.org/10.1017/S0016756816000893 Published online by Cambridge University Press

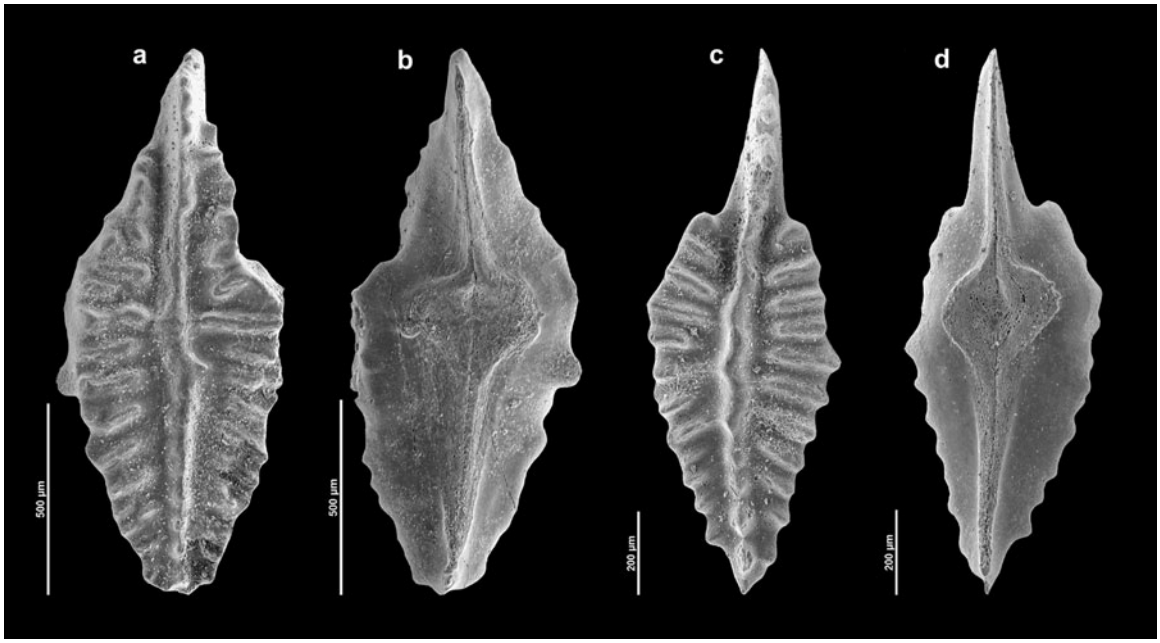

Figure 22. Upper Famennian *Pseudopolygnathus primus primus* Branson & Mehl, 1934*b*, early variant of Morphotype 1 (= '*primus*' Morphotype *sensu* Klapper, in Ziegler, 1981) with a small basal cavity converting into a keel, which reaches the posterior tip, Kahlleite East, Thuringia, Bed 36, *B. aculeatus aculeatus* Zone. (a, b) GMM B9A.4-83; (c, d) GMM B9A.4-84, slightly transitional from Morphotype 3.

side-lobe or an 'ear-like process', as in *Ps. foliaceus* Branson, 1934, *Ps. apetodus* Cooper, 1939, or, especially, in *Ps. auritus* Youngquist & Patterson, 1949.

Stratigraphic range. As pointed out by Piecha (2004*b*), the main occurrence of the species is in the Lower Carboniferous. However, there is evidence of upper to uppermost Famennian specimens in the literature. Piecha (2004*b*, Refrath 1 Borehole, Rhenish Massif) and Hartenfels (2011, Kahlleite East, Thuringia; Oum el Jerane, Tafilalt) described Morphotype 3 specimens from the *B. aculeatus aculeatus* Zone (= Middle *expansa* Zone). This may also apply to the record of Buggisch, Rabien & Hühner (1986, Beuerbach, southern Rhenish Massif, without illustration). Korn & Luppold (1987) illustrated Morphotype 3 from the *B. costatus* Subzone of Effenberg, Rhenish Massif. The two specimens figured by Gholamalian, Ghorbani & Sajadi (2009) from the *B. aculeatus aculeatus* to *B. ultimus ultimus* Zone interval (= roughly Middle/Upper *expansa* Zone) of Kal-e-Sadar, east-central Iran, and the specimen from Sardinia figured by Mossoni, Corradini & Spalletta (2013) cannot be re-assigned to a morphotype. The possible oldest Morphotype 2 representatives are from the *B. aculeatus aculeatus* Zone of the Ardennes (Dreesen, Dusar & Groessens, 1976;Yves-Gomezée Road Section), *B. costatus* Subzone of Thuringia (Kononova & Weyer, 2014: pl. 8, figs 8, 10), and from the last limestone nodules below the Hangenberg Black Shale at Kahlleite East, Thuringia (Gereke, 2004). Our samples show Tafilalt occurrences of Morphotype 3 in the *B. aculeatus aculeatus* and *B. ultimus ultimus* zones.

There are alleged older records without illustrations from the *Ps. granulosus* Zone of Beringhauser Tunnel, Rhenish Massif (= Upper *trachytera* Zone; oral comm. of I. Schülcke, noted in Piecha, 2004*b*), from the Upper *styriacus* Zone in Sardinia (Corradini, Barca & Spalletta, 2003), and from the *B. stabilis stabilis* (= Lower *expansa*) Zone of the Russian Far East (Gagiev & Bogus, 1990: Prikolymsky Anticline); these cannot be accepted without revision or further documentation. Older specimens with shorter platforms, a much longer free blade and very large basal cavity, described by Hartenfels (2011) as *Ps.* cf. *dentilineatus* from the Tafilalt, Holy Cross Mountains, and Germany (see also specimens of Sandberg & Ziegler, 1979), are closely related to *Ps. koestenhofensis* Tragelehn & Hartenfels, 2011, and *Ps. inordinatus* Tragelehn & Hartenfels, 2012.

In summary, upper/uppermost Famennian beds are dominated by Morphotype 3, which ranges from the *B. aculeatus aculeatus* Zone to the *B. ultimus ultimus* Zone. However, from the *B. aculeatus aculeatus* Zone on, there are also isolated occurrences of the two other morphotypes, which dominate after the Hangenberg Event and which range into the Middle Tournaisian.

Pseudopolygnathus primus tafilensis ssp. nov.

Figure 20a–l

e.p. 1985 *Pseudopolygnathus* aff. *dentilineatus* Branson; Bartzsch & Weyer, pp. 21–3, pl. 5, figs 2–3, 5 [only].

e.p. 2013 *Pseudopolygnathus dentilineatus* Branson; Kononova & Weyer, p. 44, pl. 8, ?fig. 4 [broken and

https://doi.org/10.1017/S0016756816000893 Published online by Cambridge University Press

encrusted], figs 5–7, pl. 9, figs 1, 3 [only; pl. 9, fig. 2 ?pathological].

Types. Holotype GMM B9A.4-52, Figure 20h–j, paratypes GMM B9A.4-47, Figure 20a, b, GMM B9A.4-48, Figure 20c, GMM B9A.4-49, Figure 20d, e, GMM B9A.4-50, Figure 20f, GMM B9A.4-51, Figure 20g, GMM B9A.4-53, Figure 20k, l.

Derivation of name. After the type region.

Type locality and level. *Gonioclymenia* trench at Jebel Ihrs West, Bed 3, *Gonioclymenia* Limestone, *B. costatus* Subzone, UD V-B.

Diagnosis. A subspecies of *Ps. primus* with a slender, elongate and weakly curved platform, which lacks a rounded shoulder/corner at the anterior left margin. In medium stages the ornament consists of distinctive, irregularly arranged, partly elongate nodes of platform margins. On the right side, the denticulation extends much farther anteriorly than on the left side and gradually approaches the short free blade. In adult specimens the platform is slightly wider and bears large, closely spaced, partly elongated nodes. Both the right and left sides of the platform meet the blade at about the same position. The central, wide and shallow basal cavity of adults is slightly constricted and tapers to or close to the anterior and posterior tips.

Description. The new subspecies is characterized by its distinctively elongate and weakly curved platform, which is widest near mid-length. In typical specimens, the platform is 4.1–4.7 times as long as wide, but there are specimens with lower (Fig. 20k, l: 3.5) and much higher values (Fig. 20c: 6.0). Both right and left curved specimens are common. In medium stages (Fig. 20a–e) the marginal denticles are isolated, partly elongated and irregularly arranged. The carina comprises a row of discrete nodes, which are somewhat fused at the anterior end. Two adcarinal grooves parallel the carina. The denticulation extends much further anteriorly on the right than on the left side.

In adult forms (Fig. 20f–j) the platform margins bear large, closely spaced, partly elongated nodes. Thus, the ornament becomes less irregular, and the margin serration weakens. Furthermore, the left platform margin is built more anteriorwards. Therefore, the right and left platform sides meet the blade at about the same position. The carina is low and extends to the posterior tip. In the anterior part the nodes are commonly fused to a ridge. Adcarinal grooves are restricted to the anterior two-thirds. Posteriorly, the side nodes are incipiently connected with the carina. In the transition to the free blade, the carina rises slightly; the short free blade is highest in mid-position and consists of four or five laterally compressed, fused denticles with free tips. Throughout ontogeny there is no distinctive or rounded shoulder/corner of the anterior left margin.

In lateral view, the platform is weakly bent downward towards the posterior tip. The central basal cavity is separated from the platform by a constriction. Aboral, in adult forms it is slightly constricted and tapers to or close to the anterior and posterior tips. A weak median groove reaches from the anterior to the posterior end. There is no posterior keel.

Discussion. The new subspecies differs from all three morphotypes of *Ps. primus primus* in its different platform outline, especially of the left side. This distinction can also be applied to slender forms of *Ps. primus primus* (e.g. Matyja, Turnau & Żbikowska, 2000, fig. 4.2). Our new form has previously been described from Thuringia as *Ps*. aff. *dentilineatus* by Bartzsch & Weyer (1985), who recognized two different forms. Their specimens (their pl. 5, figs 1, 4, 6), in which the anterior margins are not directly opposite and with an anterior left platform corner are here re-assigned to *Ps. primus primus*. Other lanceolate elements (their pl. 5, figs 2–3, 5) show the diagnostic features of *Ps. primus tafilensis* ssp. nov., which was supported more recently by Kononova & Weyer (2014).

The majority of Famennian pseudopolygnathids have very different platforms and longer free blades (e.g. Bischoff & Ziegler, 1956; Bouckaert & Groessens, 1976; Korn & Luppold, 1987; Hartenfels, 2011; Tragelehn & Hartenfels, 2011; Mossoni *et al*. 2015). Among Carboniferous pseudopolygnathids, the similarly slender *Ps. nodosus* Wang & Wang, 2005 has a much weaker ornament and different carina. *Pseudopolygnathus primus tafilensis* ssp. nov. is slightly similar in oral view to *Ps. multistriatus* (or rather, its younger synonym *Ps. lanceolatus* Hass, 1959). But the latter consistently has a much more restricted basal cavity, especially in large specimens (see distinction of *Ps. multistriatus* from the '*dentilineatus*' morphotype of *Ps. primus* by Klapper in Ziegler, 1981). *Pseudopolygnathus altaicus* Kononova, 1984 records from the Carboniferous at Kozhim (Polar Urals), figured in Nemirovskaya *et al.* (1992), differs also in the position, shape and morphology of the basal cavity; the basal cavity is situated more anteriorly, not in a central position. The distinction of *Ps. primus tafilensis* ssp. nov. as an early subspecies is underlined by the fact that no similar Carboniferous specimen was recorded by the various authors who described or named the many Tournaisian *primus*/*dentilineatus* variants (see synonym list).

Geographic distribution. Tafilalt, Franconia, Thuringia.

Stratigraphic range. In the Tafilalt *Ps. primus tafilensis* ssp. nov. ranges from the *B. costatus* Subzone to the *B. ultimus ultimus* Zone. In Thuringia, Bartzsch & Weyer (1985) illustrated it from nodular interbeds of the Hauptquarzit (*B. aculeatus aculeatus* Subzone), Kononova & Weyer (2014) from the *B. costatus* Subzone. Unpublished collections from Köstenhof (= Schübelhammer, Franconia, Tragelehn & Hartenfels, in prep.) include specimens from the middle part of the *B. aculeatus aculeatus* Zone.

https://doi.org/10.1017/S0016756816000893 Published online by Cambridge University Press

***Pseudopolygnathus primus* aff. *tafilensis* ssp. nov.**
Figure 20x–z

e.p. 2013 *Pseudopolygnathus dentilineatus* Branson; Kononova & Weyer, pp. 44, pl. 8, fig. 3 [Morphotype 2] [only].

Material. Four specimens from Jebel Ihrs West.

Discussion. The specimens represent a slightly wider variant of *Ps. primus tafilensis* sp. nov. with straight platform and without posterior constriction of the basal cavity. The anteriormost node on the right side is separated from the others. This form is somewhat transitional towards the typical subspecies with respect to the presence of an incipient left platform shoulder. In contrast to adult *Ps. primus tafilensis* ssp. nov., the rounded left side nodes end with the anterior margin of the basal cavity. We include a similar specimen from Thuringia figured by Kononova & Weyer (2014).

Draganits *et al.* (2002) illustrated poorly preserved, partly fragmentary pseudopolygnathids from just below and above a supposed Hangenberg Black Shale equivalent of Spiti, NW India, unfortunately without views of the basal cavity. Two of the more complete specimens lack a left platform shoulder, as in *Ps. primus tafilensis* ssp. nov., but there are only a few left platform nodes. The Himalayan form, therefore, differs from both *Ps. primus* subspecies recognized here.

Geographic distribution. Tafilalt, Thuringia.

Stratigraphic range. *Bispathodus costatus* Subzone (*Costaclymenia* and *Gonioclymenia* beds at Jebel Ihrs West).

Pseudopolygnathus primus* aff. *primus* Branson & Mehl, 1934*b
Figure 20ab–ad

Material. Two specimens from Jebel Ihrs West.

Discussion. The elongate specimens differ from typical *Ps. primus primus* Morphotype 1 in the lack of a distinctive left platform shoulder (Fig. 20ac). The left platform continues anteriorly from the basal cavity area as a very narrow, smooth area and both platform sides meet in same position close to the anterior tip. Therefore, there is only a very short free blade with three fused denticles that are higher than the carina (Fig. 20ab); the highest point of the free blade is at the central or posterior denticle. The main distinction from *Ps. primus tafilensis* ssp. nov., including the aff. specimens, is the wide but much shorter, strongly constricted basal cavity, which converts into a marked posterior keel.

No similar specimen has been previously described. With respect to the limited material, we keep open nomenclature but leave the option to establish a future second new subspecies or *Ps. primus primus* morphotype.

Geographic distribution. Tafilalt (Jebel Ihrs West).

Stratigraphic range. *Bispathodus costatus* Subzone (limestone slab with *Gonio. subcarinata*) to *B. ultimus ultimus* Zone (slab with *Kallo. subarmata*).

8.b. Ammonoids

***Gonioclymenia hoevelensis* Wedekind, 1914**
Figure 14a–d

Type. In order to stabilize the nomenclature of the species, the original of Wedekind (1914: pl. VI, fig. 2a–b, Göttingen Collection, no. 388-54, re-illustrated in Fig. 14a, b), is here designated as lectotype. Only a part of the original specimen was available for re-examination but it shows the typical, marked ventrolateral spines of an inner whorl, up to *c.* 35 mm diameter, and strong, paired ribbing. On the subsequent whorl (up to 18 mm whorl height and *c.* 11.5 mm whorl width), the spines turn into elongated ventrolateral nodes of approximately every second rib and there is a very deep median furrow on the venter. Sutures possess a very shallow, rounded outer flank lobe (second adventitious lobe), a deep, V-shaped, first adventitious mid-flank lobe and a subangular, moderately deep lobe on the umbilical edge. In the second, more complete syntype (Göttingen Collection, no. 588-53, original of pl. V, fig. 7), now paralectotype (Fig. 14c, d), the inner whorls with their distinctive spines are not preserved and there are no sutures. Up to *c.* 55 mm diameter, each rib pair produces a marginal node. This specimen is more difficult to separate from *Gonio. subcarinata*, which lacks pronounced spines and strong subumbilical ribbing at small size (cf. Moroccan and Russian representatives of both taxa illustrated in Bogoslovskiy, 1981 and Becker *et al.* 2002).

***Leviclymenia ramula* sp. nov.**
Figures 14g–j, 23

Types. Holotype GMM B6C.42-3.

Derivation of name. From the Latin *ramulus* = small spike or branch; due to the incipient subdivision of the ventral lobe by a small third adventitious lobe.

Type locality and level. Loose at Jebel Ouaoufilal, *Gonioclymenia* Limestone (UD V-B).

Diagnosis. Large-sized, moderately evolute (uw/dm = 0.39), strongly compressed (ww/wh = *c.* 0.50), bicarinate, with gently rounded flanks, ventrolateral edges and shallow ventral furrows until maturity, and with straight, low, rounded flank ribs. Sutures with deep, very narrow ventral lobe, moderately high, asymmetric and pointed ventral saddle subdivided by a small, rounded third adventitious lobe, moderately deep, asymmetrically pointed second A-lobe, high, narrowly rounded outer flank saddle, very deep, asymmetric, V-shaped first adventitious lobe on the mid-flanks, very high,

https://doi.org/10.1017/S0016756816000893 Published online by Cambridge University Press

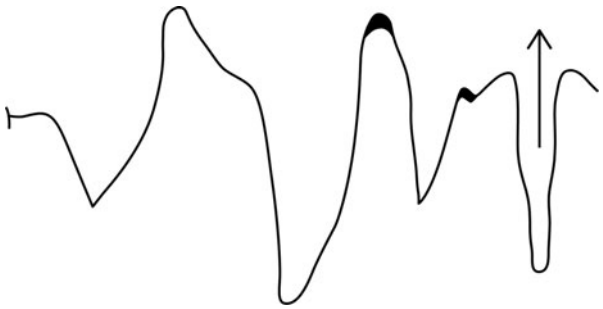

Figure 23. Complete outer suture of *Leviclymenia ramula* sp. nov., holotype GMM B6C.42-3, at 36 mm wh.

subangular lateral saddle with a concavity of the upper, outer limb, asymmetric, pointed, deep lobe on the inner flanks, and a low saddle subdivided by a wide, shallow lobe on the umbilical wall.

Description. The holotype is still septate at 120 mm diameter, which suggests an original size of up to 200 mm or more. The inner whorls are not preserved. Shell parameters are: preserved maximum diameter (dm) 130 mm, umbilical width 51 mm, whorl height (wh) 48 mm (wh/dm = 0.37), whorl width (ww) *c.* 25 mm (ww/dm = *c.* 0.19, extremely discoidal, ww/wh = *c.* 0.50), whorl expansion rate 2.30–2.35. A typical suture is illustrated in Figure 23. There are nine low ribs on the quarter of a whorl, which are not as wide as the interspaces. The upper side of the specimen was corroded during a long exposure on the sea-floor and settled by numerous cladochonid corals.

Discussion. In terms of shell form and ribbing, the new species resembles *Gonio. speciosa*, from which it is clearly separated by its additional adventitious lobe that characterizes *Leviclymenia* Korn & Klug, 2002. The type-species, *Levi. levis* (Bogoslovskiy, 1981) and *Levi. kiensis* (Bogoslovskiy, 1981), are both more evolute (uw/dm = 0.44–0.50 and 0.46–0.48, respectively). There are also suture differences, for example the shape of the saddle at the umbilical seam and of the lobe on the lower flanks.

Leviclymenia was a direct descendant of *Gonioclymenia* and, therefore, has been included by Korn & Klug (2002) in the Gonioclymeniidae. The recognition of very shallow ventral furrows in juveniles of *Medio. aguelmousensis* from both the Maider (Lambidia) and Tafilalt (Bou Tchrafine and Hamar Laghdad East) suggests that *Leviclymenia*, again, was the ancestor of *Medioclymenia*, currently the morphologically simplest member of the Sphenoclymeniidae. Bartzsch & Weyer (2012) proposed to distinguish the genus by its very small third A-lobes from the younger *'Spheno.' brevispina* Group with deeper, well-developed A_3, which is followed here. Ventral furrows are also present in *'Spheno.' plana* Bogoslovskiy, 1981, which represents a different genus with *Kalloclymenia*-type first and second adventitious lobes that may have rooted independently in *Leviclymenia*. With repect to this taxonomic and phylogenetic complexity it seems better to place all taxa with three A-lobes in a subfamily Sphenoclymeniinae, rather than placing the successive *Leviclymenia* and *Medioclymenia* in different families.

Geographic distribution. Restricted to the Tafilalt.

Stratigraphic range. Most likely exposed top of *Gonioclymenia* Limestone (top UD V-B).

9. Conclusions

1. The widespread and intensively mined *Gonioclymenia* Limestone of the Tafilalt falls in the *B. costatus* Subzone and represents a transgressive–regressive cycle of the middle Dasbergian (of German substage terminology, UD V-B, *Gonio. hoevelensis* Zone).

2. Apart from abundant, giant *Gonio. speciosa*, it also yielded *Levi. ramula sp. nov.*, the first member of the genus from outside the Urals, which is re-assigned to the Sphenoclymeniinae.

3. The *Kalloclymenia* Limestone falls in the next younger *B. ultimus ultimus* Zone and records a second, younger (lower Wocklumian, UD VI-A1) sea-level cycle.

4. In more complete sections of the Tafilalt and Maider, *Gonioclymenia* and *Kalloclymenia* levels are separated by a *Medio. aguelmousensis* Zone (UD V-C). A global review of supposed *Gonioclymenia* from UD V and *Kalloclymenia* from UD VI shows that there is so far no reliable evidence of overlapping ranges.

5. The *Gonioclymenia* Limestone deepening is tentatively correlated with the Ardennes Epinette Event, the very subtle *Kalloclymenia* Limestone deepening with the supposedly eustatic 'Strunian Transgression'.

6. Conodont faunas include a new *Neopolygnathus*, new subspecies and morphotypes of *Bispathodus* and *Pseudopolygnathus*, as well as new early siphonodellids and 'siphonodelloids' that are currently left in open nomenclature. The regional conodont zonation and the ranges of all Dasbergian/Wocklumian conodonts are summarized.

Acknowledgements. Over the several years involved, Dr Lahsen Baider (Casablanca), Dr Zhor Sarah Aboussalam (Münster), M.Sc. Tobias Fischer (Münster, now Heidelberg), M.Sc. Sören Stichling (Münster), Jürgen Bockwinkel (Leverkusen) and the late Dr Volker Ebbighausen took part in some of the field work. Work permits and fossil export licences were provided by Prof. Dr Ahmed El Hassani (Rabat), our principal Moroccan cooperation partner. Dr Harald Tragelehn (Wallenfels) and Dr Matthias Piecha (Krefeld) discussed conodont identifications and stratigraphy, based on largely unpublished huge collections from Franconia/Thuringia (Tragelehn) and the Rhenish Massif (Piecha). Gerd Schreiber and his team (Münster) prepared ammonoids and thin-sections. Traudel Fährenkämper (Münster) assisted with some of the illustrations. This research

https://doi.org/10.1017/S0016756816000893 Published online by Cambridge University Press

received no specific grant from any funding agency, commercial or not-for-profit sectors. We appreciate the helpful reviews.

References

ABOUSSALAM, Z. S., BECKER, R. T. & BULTYNCK, P. 2015. Emsian (Lower Devonian) conodont stratigraphy and correlation of the Anti-Atlas (Southern Morocco). *Bulletin of Geosciences* **90**(4), 893–980.

ALBERTI, H. 1970. Neue Trilobiten-Faunen aus dem Oberdevon Marokkos. *Göttinger Arbeiten zur Geologie und Paläontologie* **5**, 15–29.

ASHOURI, A. R. 2006. Middle Devonian–Early Carboniferous conodont faunas from the Khoshyeilagh Formation, Alborz Mountains, North Iran. *Journal of Sciences, Islamic Republic of Iran* **17**(1), 53–65.

BARDASHEVA, N. P., BARDASHEV, I. A., WEDDIGE, K. & ZIEGLER, W. 2004. Stratigraphy and conodonts of the Lower Carboniferous of the Shishkat section (southern Tien Shan, Tajikistan). *Senckenbergiana lethaea* **84**(1), 225–301.

BARTZSCH, K. & WEYER, D. 1985. Zur Stratigraphie der Oberdevon-Quarzite von Saalfeld im Thüringischen Schiefergebirge. *Freiberger Forschungshefte* **C 400**, 5–36.

BARTZSCH, K. & WEYER, D. 2012. Zur Stratigraphie des Breternitz-Members (Obere Clymenien-Schichten, Oberdevon) von Saalfeld (Schwarzburg-Antiklinorium, Thüringisches Schiefergebirge). *Freiberger Forschungshefte* **C 542**, 1–54.

BECKER, R. T. 1988. Ammonoids from the Devonian–Carboniferous Boundary in the Hasselbach Valley (Northern Rhenish Slate Mountains). *Courier Forschungsinstitut Senckenberg* **100**, 193–213.

BECKER, R. T. 1993. Stratigraphische Gliederung und Ammonoideen-Faunen im Nehdenium (Oberdevon II) von Europa und Nord-Afrika. *Courier Forschungsinstitut Senckenberg* **155**, 1–405.

BECKER, R. T. 1996. New faunal records and holostratigraphic correlation of the Hasselbachtal D/C-Boundary Auxiliary Stratotype (Germany). *Annales de la Société Géologique de Belgique* **117**(1), 19–45.

BECKER, R. T., ABOUSSALAM, Z. S. & HARTENFELS, S. 2012. The Devonian–Carboniferous boundary at Lalla Mimouna (Northern Maider, Anti-Atlas, SE Morocco) – preliminary new data. *SDS Newsletter* **27**, 31–7.

BECKER, R. T., ABOUSSALAM, Z. S., HARTENFELS, S., EL HASSANI, A. & BAIDDER, L. 2013*a*. The global carbonate crisis at the Devonian–Carboniferous transition in Morocco. In *Palaeobiology and Geobiology of Fossil Lagerstätten through Earth History* (eds J. Reiter, Q. Yang, Y. Wang & M. Reich), Universitätsdrucke Göttingen vol. 19.

BECKER, R. T., ABOUSSALAM, Z. S., HARTENFELS, S, EL HASSANI, A. & FISCHER, T. 2013*b*. The Givetian–Famennian at Oum el Jerane (Amessoui Syncline, southern Tafilalt). *Document de l'Institut Scientifique, Rabat* **27**, 61–76.

BECKER, R. T., BOCKWINKEL, J., EBBIGHAUSEN, V. & HOUSE, M. R. 2000. Jebel Mrakib, Anti-Atlas (Morocco), a potential Upper Famennian substage boundary stratotype section. *Notes et Mémoires du Service Géologique du Maroc* **399**, 75–86.

BECKER, R. T., EL HASSANI, A. & TAHIRI, A. (eds) 2013. International Field Symposium "The Lower Devonian and Lower Carboniferous of northern Gondwana". *Document de l'Institut Scientifique, Rabat* **27**, 150 pp.

BECKER, R. T., HARTENFELS, S., ABOUSSALAM, Z. S., TRAGELEHN, H., BRICE, D. & EL HASSANI, A. 2013*c*. The Devonian–Carboniferous boundary at Lalla Mimouna (Northern Maider) – a progress report. *Document de l'Institut Scientifique, Rabat* **27**, 109–20.

BECKER, R. T. & HOUSE, M. R. 2000. The Famennian ammonoid succession at Bou Tchrafine (Anti-Atlas, Southern Morocco). *Notes et Mémoires du Service Géologique Maroc* **399**, 37–42.

BECKER, R. T., HOUSE, M. R., BOCKWINKEL, J., EBBIGHAUSEN, V. & ABOUSSALAM, Z. R. 2002. Famennian ammonoid zones of the eastern Anti-Atlas (southern Morocco). *Münstersche Forschungen zur Geologie und Paläontologie* **93**, 159–205.

BECKER, R. T., KAISER, S. I. & ARETZ, M. 2016. Review of chrono-, litho- and biostratigraphy across the global Hangenberg Crisis and Devonian–Carboniferous Boundary. In *Devonian Climate, Sea Level and Evolutionary Events* (eds R. T. Becker, P. Königshof & C. E. Brett). Geological Society of London, Special Publication no. 423, published online. doi: 10.1144/SP423.10.

BECKER, R. T., KORN, D., PAPROTH, E. & STREEL, M. 1993. Beds near the Devonian–Carboniferous boundary in the Rhenish Massif, Germany. *Guidebook, International Union of Geological Sciences, Commission on Stratigraphy, Subcommission on Carboniferous Stratigraphy (SCCS)*. Liège: International Union of Geological Sciences, 86 pp.

BELKA, Z., KLUG, C., KAUFMANN, B., KORN, D., DÖRING, S., FEIST, R. & WENDT, J. 1999. Devonian conodont and ammonoid succession of the eastern Tafilalt (Ouidane Chebbi section), Anti-Atlas, Morocco. *Acta Geologica Polonica* **49**(1), 1–23.

BISCHOFF, G. 1957. Die Conodonten-Stratigraphie des rheno-herzynischen Unterkarbons mit Berücksichtigung der Wocklumeria-Stufe und der Devon/Karbon-Grenze. *Abhandlungen des Hessischen Landesamtes für Bodenforschung* **19**, 1–64.

BISCHOFF, G. & ZIEGLER, W. 1956. Das Alter der „Urfer Schichten" im Marburger Hinterland nach Conodonten. *Notizblatt des Hessischen Landesamtes für Bodenforschung* **84**, 138–69.

BOGOSLOVSKIY, B. I. 1981. Devonskie Ammonoidei III: Klimenii (Podotrad Gonioclymeniina). *Trudy Paleontologicheskogo Instuta Akademiya Nauk SSSR* **191**, 1–123.

BÖHM, F. & BRACHERT, T. C. 1993. Deep-water Stromatolites and *Frutexites* Maslov from the Early and Middle Jurassic of S-Germany and Austria. *Facies* **28**, 145–68.

BONCHEVA, I., BAHRAMI, A., YAZDI, M. & TORABY, H. 2007. Carboniferous conodont biostratigraphy and Late Palaeozoic depositional evolution in South Central Iran (Asadabad section – SE Isfahan). *Rivista Italiana di Paleontologia e Stratigrafia* **113**(3), 329–56.

BOUCKAERT, J. & GROESSENS, E. 1976. *Polygnathus paprothae*, *Pseudopolygnathus conili*, *Pseudopolygnathus graulichi*: espèces nouvelles a la limite Dévonien-Carbonifère. *Annales de la Société Géologique de Belgique* **99**, 587–99.

BRANSON, E. B. & MEHL, M. G. 1934*a*. Conodonts from the Grassy Creek Shale of Missouri. *The University of Missouri Studies* **8**(3), 171–259.

BRANSON, E. B. & MEHL, M. G. 1934*b*. Conodonts from the Bushberg Sandstone and equivalent formations of Missouri. *The University of Missouri Studies* **8**(4), 265–300.

BRANSON, E. R. 1934. Conodonts from the Hannibal Formation of Missouri. *The University of Missouri Studies* **8**(4), 301–43.

BUGGISCH, W., RABIEN, A. & HÜHNER, G. 1986. Stratigraphie und Fazies von Oberdevon/Unterkarbon-Profilen im Steinbruch „Beuerbach" bei Oberscheld (Conodonten- und Ostracoden-Biostratigraphie, Dillmulde, Rheinisches Schiefergebirge, Blatt 5216 Oberscheld). *Geologisches Jahrbuch Hessen* **114**, 5–60.

BUSHMINA, L. S. & KONONOVA, L. I. 1981. *Mikrofauna i biostratigrafija pogranisiych sloev Devona i Karbona*. Moscow: Akademija Nauk CCCP, 121 pp.

CANIS, W. F. 1968. Conodonts and biostratigraphy of the Lower Mississippian of Missouri. *Journal of Paleontology* **42**(2), 525–55.

CARMAN, M. R. 1987. Conodonts of the Lake Valley Formation (Kinderhookian-Osagean), Sacramento Mountains, New Mexico, U.S.A. *Courier Forschungsinstitut Senckenberg* **98**, 47–73.

CLAUSEN, C.-D., KORN, D., LUPPOLD, F. W. & STOPPEL, D. 1989. Untersuchungen zur Devon/Karbon-Grenze auf dem Müssenberg (nördliches Rheinisches Schiefergebirge). *Bulletin de la Société belge de Géologie* **98**(3/4), 353–69.

COOPER, C. L. 1939. Conodonts from a Bushberg-Hannibal horizon in Oklahoma. *Journal of Paleontology* **13**(4), 379–422.

CORRADINI, C. 2003. Late Devonian (Famennian) conodonts from the Corona Mizziu Sections near Villasalto (Sardinia, Italy). *Palaeontographia Italica* **89**, 65–116.

CORRADINI, C., BARCA, S. & SPALLETTA, C. 2003. Late Devonian–Early Carboniferous conodonts from the "Clymeniae Limestones" of SE Sardinia (Italy). *Courier Forschungsinstitut Senckenberg* **245**, 227–53.

DRAGANITS, E., MAWSON, R., TALENT, J. A. & KRYSTYN, L. 2002. Lithostratigraphy, conodont biostratigraphy and depositional environment of the Middle Devonian (Givetian) to Early Carboniferous (Tournaisian) Lipak Formation in the Pin Valley of Spiti (NW India). *Rivista Italiana di Paleontologia e Stratigrafia* **108**(1), 7–35.

DREESEN, R., DUSAR, M. & GROESSENS, E. 1976. Biostratigraphy of the Yves-Gomezée Road Section (uppermost Famennian). *Service Géologique de Belgique, Professional Paper* **6**, 1–20.

DREESEN, R. & ORCHARD, M. 1974. "Intraspecific" morphological variation within *Polygnathus semicostatus* Branson & Mehl. *Belgium Geological Survey, International Symposium on Belgian Micropaleontological Limits from Emsian to Viséan, Namur* **21**, 10 pp.

DREESEN, R., PAPROTH, E. & THOREZ, J. 1989. Events documented in Famennian sediments (Ardenne-Rhenish Massif, Late Devonian, NW Europe). In *Devonian of the World, Volume* **I***: Regional Syntheses* (eds N. J. McMillan, A. F. Embry & D. J. Glass), pp. 295–308. Canadian Society of Petroleum Geologists, Memoir no. 14(2).

DREESEN, R., SANDBERG, C. A. & ZIEGLER, W. 1986. Review of Late Devonian and Early Carboniferous conodont biostratigraphy and biofacies models as applied to the Ardenne Shelf. In *Late Devonian Events around the Old Red Continent* (eds M. J. M. Bless & M. Streel), pp. 97–103. Annales de la Société Géologique de Belgique no. 104.

DRUCE, E. C. 1969. Devonian and Carboniferous conodonts from the Bonaparte Gulf Basin, North Australia and their use in international correlation. *Bureau of Mineral Resources, Geology and Geophysics, Bulletin* **98**, 243 pp.

DZIK, J. 2006. The Famennian "Golden Age" of conodonts and ammonoids in the Polish part of the Variscan Sea. *Palaeontologica Polonica* **63**, 359 pp.

FLÜGEL, E. 2004. *Microfacies of Carbonate Rocks. Analysis, Interpretation and Application*. Berlin: Springer, 976 pp.

FLÜGEL, H. & ZIEGLER, W. 1957. Die Gliederung des Oberdevons und Unterkarbons am Steinberg westlich von Graz mit Conodonten. *Mitteilungen des Naturwissenschaftlichen Vereines für Steiermark* **87**, 25–60.

FOLK, R. L. 1959. Practical petrographic classification of limestones. *American Association of Petroleum Geologists, Bulletin* **43**(1), 1–38.

FOLK, R. L. 1974. The natural history of crystalline calcium carbonate: effect of magnesium content and salinity. *Journal of Sedimentary Petrology* **44**(1), 40–53.

GAGIEV, M. H. & BOGUS, O. I. 1990. Opornyj razrez Famensko-Turnejskih otloženij yugo-zapadnoj časti Prikkolymskogo podnâtiâ (Severo-Vostok CCCP). *Trudy Instituta Geologii i Geofiziki* **60**, 119–32.

GAGIEV, M. H. & KONONOVA, L. I. 1990. The Upper Devonian and Lower Carboniferous sequences in the Kamenka River Section (Kolyma River Basin, the Soviet North-East). Stratigraphic description. Conodonta. *Courier Forschungsinstitut Senckenberg* **118**, 81–103.

GAGIEV, M. K., KONONOVA, L. I. & PAZUKHIN, V. N. 1987. Conodonty. In *Fauna i Biostratigrafia Pogranicnyh Otlozenij Devona i Kabona Bercogura (Mugodzary)* (ed. V. A. Maslov), 120 pp. Moscow: Akademia Nauk CCCP.

GARCÍA-LÓPEZ, S., SANZ-LÓPEZ, J. & Padro Alonso, M. V. 1999. Conodontos (bioestratigrafía, biofacies y paleotemperaturas) de los Sinclinales de Almadén y Guadalmez (Devónico-Carbonífero Inferior), Zona Centroibérica Meridional, España. *Revista Española de Paleontología*, nº extr. Homenaje al Prof. J. Truyols, 161–72.

GEREKE, M. 2004. Das Profil Kahlleite Ost – die stratigraphische Entwicklung einer Tiefschwelle im Oberdevon des Bergaer Sattels (Thüringen). *Geologica et Palaeontologica* **38**, 1–31.

GHOLAMALIAN, H. 2005. New data on the Famennian conodonts from Esfahan Area, Central Iran. *Iranian International Journal of Science* **6**(1), 27–45.

GHOLAMALIAN, H., GHORBANI, M. & SAJADI, S.-H. 2009. Famennian conodonts from the Kal-e-Sardar section, Eastern Tabas, Central Iran. *Rivista Italiana di Paleontologia e Stratigrafia* **115**(2), 141–58.

GIBSHMAN, N. B. & NIKOLAEVA, S. V. 2011. Ammonoid and foraminiferal faunas in the Famennian of Western Kazakhstan: research summary and sedimentary settings. *SDS Newsletter* **26**, 58–64.

GINTER, M., HAIRAPETIAN, V. & KLUG, C. 2002. Famennian chondrichthyans from the shelves of North Gondwana. *Acta Geologica Polonica* **52**(2), 169–215.

GIRARD, C., CORNÉE, J.-J., CORRADINI, C., FRAVALO, A. & FEIST, R. 2013. Palaeoenvironmental changes at Col des Tribes (Montagne Noire, France), a reference section for the Famennian of north Gondwana-related areas. *Geological Magazine* **151**(5), 864–84.

HABIBI, T., CORRADINI, C. & YAZDI, M. 2008. Conodont biostratigraphy of the Upper Devonian–Lower Carboniferous Shahmirzad section, central Alborz, Iran. *Geobios* **41**, 763–77.

HARTENFELS, S. 2011. Die globalen *Annulata*-Events und die Dasberg-Krise (Famennium, Oberdevon) in Europa und Nord-Afrika – hochauflösende Conodonten-Stratigraphie, Karbonat-Mikrofazies, Paläoökologie

und Paläodiversität. *Münstersche Forschungen zur Geologie und Paläontologie* **105**, 17–527.

HARTENFELS, S. & BECKER, R. T. 2009. Timing of the global Dasberg Crisis – implications for Famennian eustasy and chronostratigraphy. In *Studies in Devonian Stratigraphy: Proceedings of the 2007 International Meeting of the Subcommission on Devonian Stratigraphy and IGCP 499* (ed. D. J. Over), pp. 71–97. Palaeontographica Americana no. 63.

HARTENFELS, S. & BECKER, R. T. 2016. Famennian sedimentation, faunas, and event stratigraphy at Effenberg Quarry (Remscheid-Altena Anticline, Rhenish Massive). In *Middle Devonian to Lower Carboniferous Stratigraphy, Facies, and Bioevents in the Rhenish Massive, Germany* (eds R. T. Becker, S. Hartenfels & P. Königshof). Münstersche Forschungen zur Geologie und Paläontologie **108**, 141–157.

HARTENFELS, S., BECKER, R. T., ABOUSSALAM, Z. S., EL HASSANI, A., BAIDER, L., FISCHER, T. & STICHLING, S. 2013. The Upper Devonian at El Khraouia (Southern Tafilalt). *Document de l'Institut Scientifique, Rabat* **27**, 41–50.

HASS, W. H. 1959. Conodonts from the Chappel Limestone of Texas. *U. S. Geological Survey Professional Paper* **294-J**, 365–99.

HELMS, J. 1959. Conodonten aus dem Saalfelder Oberdevon (Thüringen). *Geologie* **8**(6), 634–77.

HOLLARD, H. 1960. Une phase tectonique intra-famenniene dans le Tafilalt et le Maider (Maroc présaharien). *Compte Rendus Hebdomadaires des Séances de l'Académie des Sciences* **250**, 1303–5.

HOLLARD, H. 1967. Le Dévonien du Maroc et du Sahara nord-occidental. In *International Symposium on the Devonian System, Calgary, 1967, I* (ed. D. H. Oswald), pp. 203–44. Calgary: Alberta Society of Petroleum Geologists.

JAKUBOWICZ, M., BELKA, Z. & BERKOWSKI, B. 2014. *Frutexites* encrustions on rugose corals (Middle Devonian, southern Morocco): complex growth of microbial microstromatolites. *Facies* **60**(2), 631–50.

JI, Q., WANG, N. & LUO, X. 1989. Chapter 10, Systematic Palaeontology, 10.1. Conodonts. In *The Dapoushang Section – An Excellent Section for the Devonian-Carboniferous Boundary Stratotype in China* (eds Z. Li & X. Hu), pp. 80–103. Beijing: Science Press.

JI, Q., WANG, Z., SHENG, H., HOU, J., FENG, R., WIE, J., WANG, S., WANG, H., XIANG, L. & FU, G. 1989. *The Dapoushang section – An Excellent Section for the Devonian-Carboniferous Boundary Stratotype in China*. Beijing: Science Press, 165 pp.

JI, Q. & ZIEGLER, W. 1993. The Lali Section: an excellent reference section for Upper Devonian in South China. *Courier Forschungsinstitut Senckenberg* **157**, 183 pp.

JOHNSON, J. G., KLAPPER, G. & SANDBERG, C. A. 1985. Devonian eustatic fluctuations in Euramerica. *The Geological Society of America, Bulletin* **96**, 567–87.

KAISER, S. I. 2005. *Mass extinctions, climatic and oceanographic changes at the Devonian/Carboniferous boundary.* Ph.D. dissertation, Ruhr University Bochum, 156 pp.

KAISER, S. I., ARETZ, M. & BECKER, R. T. 2015. The global Hangenberg Crisis (Devonian-Carboniferous transition): review of a first-order mass extinction. In *Devonian Climate, Sea Level and Evolutionary Events* (eds R. T. Becker, P. Königshof & C. E. Brett). Geological Society of London, Special Publication no. 423, published online. doi: 10.1144/SP423.9.

KAISER, S. I., BECKER, R. T., HARTENFELS, S. & ABOUSSALAM, Z. S. 2013. Middle Famennian to Middle Tournaisian stratigraphy at El Atrous (Amessoui Syncline, southern Tafilalt). *Document de l'Institut Scientifique, Rabat* **27**, 77–86.

KAISER, S. I., BECKER, R. T., SPALLETTA, C. & STEUBER, T. 2009. High-resolution conodont stratigraphy, biofacies, and extinctions around the Hangenberg Event in pelagic successions from Austria, Italy, and France. In *Studies in Devonian Stratigraphy: Proceedings of the 2007 International Meeting of the Subcommission on Devonian Stratigraphy and IGCP 499* (ed. D. J. Over), pp. 99–143. Palaeontographica Americana no. 63.

KAISER, S. I., BECKER, R. T., STEUBER, T. & ABOUSSALAM, Z. S. 2011. Climate-controlled mass extinctions, facies, and sea-level changes around the Devonian-Carboniferous boundary in the eastern Anti-Atlas (SE Morocco). *Palaeogeography, Palaeoclimatology, Palaeoecology* **310**, 340–64.

KAISER, S. I. & CORRADINI, C. 2011. The early siphonodellids (Conodonta, Late Devonian–Early Carboniferous): overview and taxonomic state. *Neues Jahrbuch für Geologie und Paläontologie, Abhandlungen* **261**, 19–35.

KAISER, S. I., STEUBER, T., BECKER, R. T. & JOACHIMSKI, M. M. 2006. Geochemical evidence for major environmental change at the Devonian–Carboniferous boundary in the Carnic Alps and the Rhenish Massif. *Palaeogeography, Palaeoclimatology, Palaeoecology* **240**, 146–60.

KALVODA, J. & KUKAL, Z. 1987. Devonian–Carboniferous boundary in the Moravian Karst at Lesní Lom Quarry, Brno-Líšeň, Czechoslovakia. *Courier Forschungsinstitut Senckenberg* **98**, 95–117.

KLAPPER, G. 1966. Upper Devonian and Lower Mississippian conodont zones in Montana, Wyoming, and South Dakota. *The University of Kansas, Paleontological Contributions, Papers* **3**, 43 pp.

KONONOVA, L. I. 1979. Upper Frasnian, Famennian and Tournaisian conodonts of the Sikaza River section (southern Urals). *Service Géologique de Belgique, Professional Paper* **161**, 71–86.

KONONOVA, L. I. 1984. *Konodonty*. In *Mikrofauna i biostratigrafiya nizhnego karbona (yug Zapadnoy Sibiri* (eds L. S. Bushmina, O. I. Bogush & L. I. Kononova), pp.103–12. Trudy, Institut Geologii i Geofiziki, Sibirskoe Otdelenie, Akademiya Nauk CCCR, no. 599.

KONONOVA, L. I. & WEYER, D. 2014. Upper Famennian conodonts from the Breternitz Member (Upper Clymeniid Beds) of the Saalfeld region, Thuringia (Germany). *Freiberger Forschnungshefte* **C 545**, 15–97 [imprint 2013].

KOPTÍKOVÁ, L., BÁBEK, O., HLADIL, J., KALVODA, J. & SLAVÍK, L. 2010. Stratigraphic significance and resolution of spectral reflectance logs in Lower Devonian carbonates of the Barrandian area, Czech Republic; a correlation with magnetic susceptibility and gamma-ray logs. *Sedimentary Geology* **225**, 83–98.

KORN, D. 1981. *Cymaclymenia*, eine besonders langlebige Clymenien-Gattung (Ammonoidea, Cephalopoda). *Neues Jahrbuch für Geologie und Paläontologie, Abhandlungen* **161**(2), 172–208.

KORN, D. 1998. Ammonoid stratigraphy of late Famennian rocks in the Carnic Alps. In *Southern Alps Field Trip Guidebook. June 27–July 2, 1998. Ecos VII* (eds. M. C. Perri & C. Spalletta), pp. 123–4. Giornale di Geologia, Serie 3a, Special Issue no. 60.

KORN, D. 1999. Famennian ammonoid stratigraphy of the Ma'der and Tafilalt (Eastern Anti-Atlas, Morocco). *Abhandlungen der Geologischen Bundesanstalt* **54**, 147–79.

KORN, D., BELKA, Z., FRÖHLICH, S., RÜCKLIN, M. & WENDT, J. 2004. The youngest African clymeniids (Ammonoidea, Late Devonian) – failed survivors of the Hangenberg Event. *Lethaia* **37**, 307–15.

KORN, D. & KLUG, C. 2002. Ammoneae Devonicae. *Fossils Catalogus Animalia* **138**, 375 pp.

KORN, D., KLUG, C. & REISDORF, A. 2000. Middle Famennian ammonoid stratigraphy in the Amessoui Syncline (Late Devonian; eastern Anti-Atlas, Morocco). *Travaux de l'Institut Scientifique, Série Géologie & Géographie Physique* **20**, 69–77.

KORN, D. & LUPPOLD, F. W. 1987. Nach Clymenien und Conodonten gegliederte Profile des oberen Famennium im Rheinischen Schiefergebirge. *Courier Forschungsinstitut Senckenberg* **92**, 199–223.

KÜRSCHNER, W., BECKER, R. T., BUHL, D. & VEIZER, J. 1993. Strontium isotopes in conodonts: Devonian–Carboniferous transition, the northern Rhenish Slate Mountains, Germany. *Annales de la Société Géologique de Belgique* **115**(2), 595–621.

LEWOWICKI, S. 1959. Fauna wapieni Klimeniowych z Dzikowieca Kłodzkiego. *Biuletyn Instytutu Geologicznego* **146**, 73–118.

LONGMAN, M. W. 1977. Factors controlling the formation of microspar in the Bromide formation. *Journal of Sedimentary Petrology* **47**(1), 347–50.

LUBESEDER, S., RATH, J., RÜCKLIN, M. & MESSBACHER, R. 2010. Controls on Devonian hemipelagic limestone deposition analyzed on cephalopod ridge to slope sections, Eastern Anti-Atlas, Morocco. *Facies* **56**, 295–315.

LUPPOLD, F. W., HAHN, G. & KORN, D. 1984. Trilobiten-, Ammonoideen- und Conodonten-Stratigraphie des Devon/Karbon-Grenzprofiles auf dem Müssenberg (Rheinisches Schiefergebirge). *Courier Forschungsinstitut Senckenberg* **67**, 91–121.

MALEC, J. 2014. The Devonian/Carboniferous boundary in the Holy Cross Mountains (Poland). *Geological Quarterly* **58**(2), 217–34.

MATTHEWS, S. C. & NAYLOR, D. 1973. Lower Carboniferous conodont faunas from South-West Ireland. *Palaeontology* **16**(1), 335–80.

MATYJA, H. 1987. Conodont biofacies in the Famennian Stage of Pomerania, northwestern Poland. In *Conodonts: Investigative Techniques and Applications* (ed. R. L. Austin), pp. 363–81. Chichester: Ellis Horwood Limited for The British Micropalaeontological Society.

MATYJA, H., TURNAU, E. & ŻBIKOWSKA, B. 2000. Lower Carboniferous (Mississippian) stratigraphy of Northwestern Poland: conodont, miospore and ostracods zones compared. *Annales Societatis Geologorum Poloniae* **70**, 193–217.

MOLLOY, P. D., TALENT, J. A. & MAWSON, R. 1997. Late Devonian-Tournaisian conodonts from the Eastern Khyber region, North-West Pakistan. *Rivista Italiana di Paleontologia e Stratigraphia* **103**(2), 123–48.

MOSSONI, A., CARTA, N., CORRADINI, C. & SPALLETTA, C. 2015. Conodonts across the Devonian/Carboniferous boundary in SE Sardinia (Italy). *Bulletin of Geosciences* **90**(2), 371–88.

MOSSONI, A., CORRADINI, C. & SPALLETTA, C. 2013. Famennian-Tournaisian conodonts from the Monte Taccu section (Sardinia, Italy). In *Conodonts from the Andes, 3rd International Conodont Symposium* (eds G. L. Albanesi & G. Ortega), pp. 85–90. Publicatión Especial no 13.

MÜLLER, K. J. 1956. Zur Kenntnis der Conodonten-Fauna des europäischen Devons, 1: Die Gattung *Palmatolepis*. *Abhandlungen der Senckenbergischen Naturforschenden Gesellschaft* **494**, 1–70.

MÜNSTER, G. GRAF Z.U. 1831. Sur le gisement géognostique des Ammonées en Allemagne. *Bulletin de la Societé géologique de France* **1**, 173–85.

MÜNSTER, G. GRAF Z.U. 1832. *Über die Planuliten und Goniatiten im Uebergangs-Kalk des Fichtelgebirges*. Bayreuth, 38 pp

NEMIROVSKAYA, T. I., CHERMNYKH, V. A., KONONOVA, L. I. & PAZUKHIN, V. N. 1992. Conodonts of the Devonian-Carboniferous boundary section Kozhim, Polar Urals, Russia. *Annales de la Société Géologique de Belgique* **115**(2), 629–47.

NI, S. 1984. Conodonts. In *Biostratigraphy of the Yangtze Gorge Area, 3, Late Palaeozoic Era* (eds S. Feng, S. Xu, J. Lin & D. Yang), pp. 278–93, 334–5, 402–5. Yichang: Ministry of Geology and Mineral Resources.

NIGMADZHANOV, I. M. 1986. Novye vidy roda *Polygnathus* (konodonty) iz nizhnego Karbona Sredinnogo Tyan'-Schanya. *Paleontological Journal* **1**, 135–37.

NIKOLAEVA, S. V. 2007. New data on the Clymeniid Faunas of the Urals and Kazakhstan. In *Cephalopods, Present and Past: New Insights and Fresh Perspectives* (eds N. H. Landman, R. A. Davis & R. H. Mapes), pp. 317–343. Berlin: Springer.

NIKOLAEVA, S. V. & BOGOSLOVSKIY, B. I. 2005. Late Famennian Ammonoids from the Upper Part of the Kiya Formation of the South Urals. *Paleontological Journal, Supplement* **39**(5), S527–37.

PERRI, M. C. & SPALLETTA, C. 1991. Famennian conodonts from Cava Cantoniera and Malpasso sections, Carnic Alps, Italy. *Bollettino della Società Paleontologica Italiana* **30**(1), 47–78.

PERRI, M. C. & SPALLETTA, C. 1998. Late Famennian conodonts of the Malpasso section (Carnic Alps, Italy). In *Southern Alps Field Trip Guidebook. June 27–July 2, 1998. Ecos VII* (eds. M. C. Perri & C. Spalletta), pp. 220–27. Giornale di Geologia, Serie 3a, Special Issue no. 60.

PIECHA, M. 2004*a*. Late Famennian heterocorals from the Refrath 1 Borehole (Bergisch Gladbach-Paffrath Syncline; Ardennes-Rhenish Massif, Germany). *Courier Forschungsinstitut Senckenberg* **251**, 123–33.

PIECHA, M. 2004*b*. Late Famennian conodonts from the Refrath 1 Borehole (Bergisch Gladbach-Paffrath Syncline; Ardennes-Rhenish Massif, Germany). *Courier Forschungsinstitut Senckenberg* **251**, 253–65.

PRÉAT, A., EL HASSANI, A. & MAMET, B. 2008. Iron bacteria in Devonian carbonates (Tafilalt, Anti-Atlas, Morocco). *Facies* **54**, 107–20.

PRICE, J. D. & KORN, D. 1989. Stratigraphically important Clymeniids (Ammonoidea) from the Famennian (Late Devonian) of the Rhenish Massif, West Germany. *Courier Forschungsinstitut Senckenberg* **110**, 257–94.

QIE, W., ZHANG, X., DU, Y., YANG, B., JI, W. & LUO, G. 2004. Conodont biostratigraphy of Tournaisian shallow-water carbonates in central Guangxi, South China. *Geobios* **47**, 389–401.

QIN, G., ZHAO, R. & JI, Q. 1988. Late Devonian and Early Carboniferous conodonts from Northern Guangdong and their stratigraphic significance. *Acta Micropalaeontologica Sinica* **5**(1), 57–71.

RAVEN, J. G. M. 1983. Conodont biostratigraphy and depositional history of the Middle Devonian to Lower Carboniferous in the Cantabrian Zone (Cantabrian Mountains, Spain). *Leidse geologische Mededelingen* **52**(2), 265–339.

RHODES, F. H. T. & AUSTIN, R. L. 1971. Carboniferous conodont faunas of Europe. *Geological Society of America, Memoir* **127**, 317–52.

RHODES, F. H. T., AUSTIN, R. L. & DRUCE, E. C. 1969. British Avonian (Carboniferous) conodont faunas, and their value in local and intercontinental correlation. *Bulletin of the British Museum (Natural History) Geology, Supplement* **5**, 1–313.

SANDBERG, C. A. 1976. Conodont biofacies of the Late Devonian *Polygnathus styriacus* Zone in western United States. In *Conodont Paleoecology* (ed. C. R. Barnes), pp. 171–86. Geological Association of Canada, Special Paper no. 15.

SANDBERG, C. A. & ZIEGLER, W. 1979. Taxonomy and biofacies of important conodonts of Late Devonian *styriacus*-Zone, United States and Germany. *Geologica et Palaeontologica* **13**, 173–212.

SANZ-LÓPEZ, J., GARCÍA-LÓPEZ, S., MONTESINOS, J. R. & ARBIZU, M. 1999. Biostratigraphy and sedimentation of the Vidrieros Formation (middle Famennian-lower Tournaisian) in the Gildar-Montó unit (northwest Spain). *Bollettino della Società Paleontologica Italiana* **37**(2–3), 393–406.

SAVAGE, N. M. 2013. *Late Devonian conodonts from northwestern Thailand*. Eugene, OR: Bourland Printing, 48 pp.

SCHÄFER, W. 1976. Einige neue Conodonten aus dem höheren Oberdevon des Sauerlandes (Rheinisches Schiefergebirge). *Geologica et Palaeontologica* **10**, 141–52.

SCHINDEWOLF, O. H. 1937. Zur Stratigraphie und Paläontologie der Wocklumer Schichten (Oberdevon). *Abhandlungen der Preußischen Geologischen Landesanstalt, Neue Folge* **178**, 1–132.

SCHÖNLAUB, P. 1969. Conodonten aus dem Oberdevon und Unterkarbon des Kronhofgrabens (Karnische Alpen, Österreich). *Jahrbuch der Geologischen Bundesanstalt* **112**, 321–54.

SCOTT, A. J. 1961. Three new conodonts from the Louisiana Limestone (Upper Devonian) of Western Illinois. *Journal of Paleontology* **35**, 1223–7.

SELWOOD, E. B. 1960. Ammonoids and trilobites from the Upper Devonian and lowest Carboniferous of the Launceston area of Cornwall. *Palaeontology* **3**(2), 153–85.

SIMAKOV, K. V., BOGOSLOVSKIY, B. I., GAGIEV, M., KONONOVA, L. I., KOCHETKOVA, N. M., KUSINA, L. F., KULAGINA, E. I., ONOPRIENKO, U. I., PAZUKHIN, V. N., RADINOVA, E. P., RASINA, E. P., REITLINGER, E., SIMAKOVA, L. V. & YANOULATOVA, M. G. 1983. Biostratigrafiya pogranichnikh otlostzheniy Devona i Karbona. Kharakteristikye pogranichnikh otloszheniy Devona i Karbona Mugodzhar. *Akadademii Nauk Magadan* **51**

SPALLETTA, C., PERRI, M. C., CORRADINI, C. & OVER, J. D. 2015*a*. Proposal for a revised Famennian (Upper Devonian) standard conodont zonation. In *2nd International Congress on Stratigraphy. Strati 2015. Abstracts* (eds E. Gülli & W. E. Piller), p. 357. Berichte des Institutes für Erdwissenschaften Karl-Franzens-Universität Graz no. 21.

SPALLETTA, C., PERRI, M. C., CORRADINI, C. & OVER, J. D. 2015*b*. Proposed revision of the Famennian (Upper Devonian) standard conodont zonation. In *IGCP 596 – SDS Symposium. Climate Change and Biodiversity Patterns in the Mid-Palaeozoic. Abstracts* (eds B. Mottequin, J. Denayer, P. Königshof, C. Prestianni & S. Olive), pp. 135–6. Travaux de Géologie sédimentaire et Paléontologie, Série 1: communications no. 16.

SPALLETTA, C., PERRI, M. C. & PONDRELLI, M. 1998. Late Famennian conodonts from the Rio Boreado section (Carnic Alps, Italy). In *Southern Alps Field Trip Guidebook. June 27–July 2, 1998. ECOS VII* (eds M. C. Perri & C. Spalletta), pp. 214–19. Giornale di Geologia, Serie 3a, Special Issue no. 60.

STEWART, L. J. 1981. Late Devonian and Lower Carboniferous conodonts from north Cornwall and their stratigraphical significance. *Proceedings of the Ussher Society* **5**, 179–85.

STREEL, M. 2009. Upper Devonian miospore and conodont zone correlation in western Europe. In *Devonian Change: Case Studies in Palaeogeography and Palaeoecology* (ed. P. Königshof), pp. 163–76. The Geological Society, Special Publication no. 314.

SZULCZEWSKI, M. 1973. Famennian-Tournaisian Neptunian dykes and their conodont fauna from Dalnia in the Holy Cross Mts. *Acta Geologica Polonica* **23**(1), 15–59.

TEBBUTT, G. E., CONLEY, C. D. & BOYD, D. W. 1965. Lithogenesis of a carbonate rock fabric. *Contributions to Geology* **4**, 1–13.

THOMAS, L. A. 1949. Devonian-Mississippian formations of Southeast Iowa. *Bulletin of the Geological Society of America* **60**, 403–38.

TRAGELEHN, H. 2010. Short note on the origin of the conodont genus *Siphonodella* in the Uppermost Famennian. *SDS Newsletter* **25**, 41–3.

TRAGELEHN, H. & HARTENFELS, S. 2011. Neue Conodonten-Taxa aus dem höheren Famennium (Oberdevon) des Frankenwaldes. *Münstersche Forschungen zur Geologie und Paläontologie* **105**, 1–15.

TRAGELEHN, H. & HARTENFELS, S. 2012. *Pseudopolygnathus inordinatus* nov. nom. – homonym replacement for an upper Famennian (Upper Devonian) conodont species. *SDS Newsletter* **27**, 59–60.

ULRICH, E. O. & BASSLER, R. S. 1926. A classification of the toothlike fossils, conodonts, with descriptions of American Devonian and Mississippian species. *Proceedings of the United States National Museum* **68**(12), 1–63.

VAN ADRICHEM BOOGAERT, H. A. 1967. Devonian and Lower Carboniferous conodonts of the Cantabrian Mountains (Spain) and their stratigraphic application. *Leidse Geologische Mededelingen* **39**, 129–92.

VAN DEN BOOGAARD, M. & SCHERMERHORN, L. J. G. 1980. Conodont faunas from Portugal and southern Spain. Part 4. A Famennian conodont fauna near Nerva (Rio Tinto). *Scripta Geologica* **56**, 14 pp.

VOGES, A. 1959. Conodonten aus dem Untercarbon I und II (*Gattendorfia*- und *Pericyclus*-Stufe) des Sauerlandes. *Paläontologische Zeitschrift* **33**(4), 266–314.

VORONZOVA, T. N. 1996. The genus *Neopolygnathus* (Conodonta): phylogeny and some questions of systematics. *Palaeontological Journal* **1996**(2), 82–4.

WANG, C.-Y. 1989. Devonian conodonts of Guangxi. *Memoirs of Nanjing Institute of Geology and Palaeontology, Academia Sinica* **25**, 1–152 (in Chinese with English summary).

WANG, P. & WANG, C.-Y. 2005. Lower Carboniferous conodont faunas from the Jiehejie Formation of the Xiongjiashan in Fengxian County, Shaanxi, China. *Acta Palaeontologica Sinica* **44**(3), 258–375.

WEDDIGE, K. 1984. Zur Stratigraphie und Paläogeographie des Devons und Karbons von NE-Iran. *Senckenbergiana lethaea* **65**(1), 179–223.

WEDEKIND, R. 1914. Monographie der Clymenien des Rheinischen Gebirges. *Abhandlungen der Königlichen Gesellschaft der Wissenschaft zu Göttingen, Mathematisch-Physikalische Klasse, Neue Folge* **10**(1), 5–73.

WENDT, J. 1988*a*. Condensed carbonate sedimentation in the late Devonian of the eastern Anti-Atlas (Morocco). *Eclogae Geologicae Helvetiae* **81**(1), 155–73.

WENDT, J. 1988*b*. Facies pattern and paleogeography of the Middle and Upper Devonian in the eastern Anti-Atlas (Morocco). In *Devonian of the World, Volume I: Regional Syntheses* (eds N. J. McMillan, A. F. Embry & D. J. Glass), pp. 467–80. Canadian Society of Petroleum Geologists, Memoir no. 14(1).

WENDT, J., AIGNER, T. & NEUGEBAUER, J. 1984. Cephalopod limestone deposition on a shallow pelagic ridge: the Tafilalt Platform (upper Devonian, eastern Anti-Atlas, Morocco). *Sedimentology* **31**, 601–25.

WENDT, J. & BELKA, Z. 1991. Age and depositional environment of Upper Devonian (Early Frasnian to Early Famennian) black shales and limestones (Kellwasser Facies) in the Eastern Anti-Atlas, Morocco. *Facies* **25**, 51–90.

WEYANT, M. & PAREYN, C. 1975. Mise en évidence du caractère condensé de la série dinantienne de la bordure méridionale du Djebel Grouz (Sahara sud-oranais). *Bulletin de la Société géologique de France* **17**(7), 52–5.

WEYER, D. 1995. Heterocorallia aus Famenne-Cephalopodenkalken im Rheinischen Schiefergebirge und Tafilalt. *Abhandlungen und Berichte für Naturkunde* **18**, 103–35.

WEYER, D. 1997. News about Famennian Heterocorallia in Germany and Morocco. *Boletin de la Real Sociedad Española de Historia Natural, Sección Geológica* **91**, 145–51.

WOLF, K. H. 1965. Littoral environments, indicated by open-space structures in algal limestones. *Palaeogeography, Palaeoclimatology, Palaeoecology* **1**, 183–223.

WOLSKA, Z. 1967. Upper Devonian conodonts from the south-west region of the Holy Cross Mountains, Poland. *Acta Palaeontologica Polonica* **12**(4), 363–435 (in Polish).

XIA, F. & CHEN, Z. 2004. *Polygnathus communis gancaohuensis* subsp. nov. (Conodonta) from the Tournaisian–Viséan boundary beds of Xinjiang, NW China and the phylogeny of *Polygnathus communis* Branson et Mehl 1934. *Acta Micropalaeontologica Sinica* **21**(2), 136–47.

YOUNGQUIST, W. L. & PATTERSON, S. H. 1949. Conodonts from the Lower Mississippian Prospect Hill Sandstone of Iowa. *Journal of Paleontology* **23**(1), 57–73.

YU, C.-M. 1988. *Devonian–Carboniferous boundary in Nanbiancun, Guilin, China – aspects and records*. Beijing: Science Press, 379 pp.

ZIEGLER, W. 1962. Taxionomie und Phylogenie Oberdevonischer Conodonten und ihre stratigraphische Bedeutung. *Abhandlungen des Hessischen Landesamtes für Bodenforschung* **38**, 166 pp.

ZIEGLER, W. (ed.) 1975. *Catalogue of Conodonts. Volume 2*. Schweizerbart'sche Verlagsbuchhandlung, 404 pp.

ZIEGLER, W. (ed.) 1981. *Catalogue of Conodonts. Volume 4*. Schweizerbart'sche Verlagsbuchhandlung, 445 pp.

ZIEGLER, W. & SANDBERG, C. A. 1984. *Palmatolepis*-based revision of upper part of standard Late Devonian conodont zonation. *Geological Society of America, Special Papers* **196**, 179–94.

ZIEGLER, W. & SANDBERG, C. A. 1990. The Late Devonian standard conodont zonation. 1st International Senckenberg Conference and 5th European Conodont Symposium (ECOS V) Contributions V. *Courier Forschungsinstitut Senckenberg* **121**, 1–115.

ZIEGLER, W., SANDBERG, C. A. & AUSTIN, R. L. 1974. Revision of *Bispathodus* group (Conodonta) in the Upper Devonian and Lower Carboniferous. *Geologica et Palaeontologica* **8**, 97–112.